RÉPUBLIQUE ALGÉRIENNE DÉMOCRATIQUE ET POPULAIRE

Ministère de l'Enseignement Supérieur et de la Recherche Scientifique

Université Amar Telidji - Laghouat

Faculté de Technologie

THÈSE DE DOCTORAT EN TECHNOLOGIE

Spécialité : Analyse et contrôle

Présentée et soutenue publiquement
le 17/01/2017

BENMILOUD NOURELHOUDA

THEME

EFFET DU VIEILLISSEMENT SUR LA DEFORMATION MECANIQUE DE FILM EN POLYETHYLENE.

JURY :

Monsieur : BENHORMA AISSA	Président du jury	Professeur	UATL -Laghouat-
Monsieur : BEZZAZI BOUDJEMA	Examinateur	Professeur	UMBB –Boumerdes-
Monsieur : AZZAZ MOHAMMED	Examinateur	Professeur	USTHB –Alger-
Monsieur : RAHMANI MOHAMMED	Examinateur	Professeur	UATL –Laghouat-
Monsieur : CHABIRA S. FOUAD	Encadreur	Professeur	UATL –Laghouat-

PEOPLE'S DEMOCRATIC REPUBLIC OF ALGERIA

MINISTRY OF HIGHER EDUCATION AND SCIENTIFIC RESEARCH

Amar Telidji University -Laghouat-

Faculty Of Technology

DOCTORAL THESIS

Option : Analysis and control

Defended before a jury on:
January 17, 2017

BENMILOUD NOURELHOUDA

THEME

AGEING EFFECT ON THE MECHANICAL DEFORMATION OF POLYETHYLENE FILMS

JURY :

Monsieur : BENHORMA AISSA	President	Professor	UATL -Laghouat-
Monsieur : BEZZAZI BOUDJEMA	Examiner	Professor	UMBB –Boumerdes-
Monsieur : AZZAZ MOHAMMED	Examiner	Professor	USTHB –Alger-
Monsieur : RAHMANI MOHAMMED	Examiner	Professor	UATL –Laghouat-
Monsieur : CHABIRA S. FOUAD	Supervisor	Professor	UATL –Laghouat-

Abstract

Low density polyethylene (LDPE) films having semicrystalline morphology have been used to highlight the ageing effect on the relationship between LDPE film structure and its mechanical behavior. Four different subjects have been addressed are: 1) morphological analysis, 2) orientation dependence and controlled deformations, 3) creep-recovery behavior and loading effect, 4) ageing effects on the creep-recovery behavior.

For the first topic, the surface morphological changes due to exposure have been analyzed by AFM and FESEM, crystallinity has been calculated by DSC and XRD experiments. However DSC allowed the determination of lamellar thickness and its distribution which were affected by ageing. The three following topics, tensile tests, deformation under controlled deformation, and creep tests, were performed not only at different angles of the film plane with respect to the main directions machine direction (MD), but also at different ageing stages of exposure except the topic 5.0 which was the focus of the orientation and loading only.

In the structural and morphological study (chapter 2.0), DSC, XRD, AFM, and FESEM experiments were conducted for pristine and altered samples having different morphologies. it was shown that natural weathering leads to a complex photochemical mechanism by increasing crystalline concentration (calculated by XRD and DSC), either by the lamellar thickness or by nucleating new crystallite via a chemo-crystallization process, also it was found that crystallinity increase calculated with XRD agreed with DSC. AFM and FESEM were very efficient for the surface morphology analysis, the roughness and the height valley increase in reason of the increase of the surface crystalline zones, also it has been found that the peaks-spacing and R_{rms} which logically progress inversely, followed an evolution that obeys to linear mathematical relationships.

In the stress-strain deformation study (chapter 3.0), samples were stretched under controlled strain rates at 0°, 45°, and 90° angles of the film plan with respect to the original direction (MD). The relative elongation and true strain are strongly dependent on the deformations angles; the true strain is greater in the 45° stretch followed by 90° then 0°. Furthermore, planes delimited by the marks remain uniform during the whole deformation. The lateral contraction is significant in the 45° stretch.

Furthermore, ageing provokes a decrease in the true strain and lateral contraction. The Poisson's ratio was determined and found to be independent to orientation and ageing. In large stress-strain tests, samples are stretched in the two main directions (MD and TD), a contributive demonstration of several relationships between the microscopic deformation mechanisms and the induced morphological changes and macroscopic tensile properties. Stretching parallel to the MD results in lamellar separation, followed by break-up of the crystalline lamellae via chain slip. Stretching perpendicular to the MD causes the crystalline lamellae to break-up or rupture by chain pull-out. Furthermore, ageing decreases the properties at the break, the tensile behavior deformed with two strain rates for a given ageing state is different.

In loading and orientation effect on the creep-recovery behavior study (chapter 4.0), samples have been tested at the two main directions of the film plan (MD and TD). The creep deformation and creep rate is higher in TD. The creep resistance and the different creep-recovery deformations decreases with increasing applied stress, so the minimum strain rate increases. The linear-non-linear viscoelastic transition is around 7.6 MPa and lifetime of each deformation is determined. The recovered elastic portion decreased with increasing applied stress.

In the ageing effect on the creep-recovery behavior study (chapter 5.0), samples have been tested at different orientation, applied stress, and ageing stages. ATR-FTIR was very efficient to reveal each of the microstructural and morphological changes; crosslinking and chain scission reactions affect adversely the mechanical properties (tensile tests) leading to a global material stiffening, the increase in crystallinity calculated from ATR-FTIR agreed with those of DSC and XRD. The creep resistance increases with exposure time for both directions, however the minimum strain rate ($\dot{\varepsilon}_{min}$) is higher in the TD. The vinylidenes present a close relationship with viscous flow. The viscous character of the material is strongly lowered not only by crosslinking and chain scissions, but also by crystallinity. The instantaneous (ε_a) and the final recoveries (ε_b ,ε_c), diminish with increasing exposure time.

ACKNOWLEDGMENTS

At the beginning of thesis writing, I heard that the acknowledgments are the hardest part. I never would have believed it. And yet, I can confirm it now. Its often represent the most read part of a thesis, or at least the part that a reader naturally looks first.

It is therefore to find the right words for everyone, while not forgetting someone. I will begin by thanking everyone that I could have unfortunately forgotten thereafter.

Contrary to the received information, a dissertation is not the result of a purely personal work. Beyond being an amazing scientific experience is also an unforgettable human adventure that allowed me to meet and integrate with amazing people who have contributed, in one way or another, to the achievement of this work.

So naturally and sincerity that I thank now all the persons who surrounded me during these four ... five years!

First, I would like to thank the two persons who have supported me the most during this period of my life. My supervisor and my leader team: ***Mr.Chabira Salem Fouad*** *and* ***Mr.Sebaa Mohamed****.*

Mr.Chabira*, I owe you a lot in the success of this thesis. Thank you for your unfailing support throughout these five years, for your availability day and night but , also for the various discussions we had, that allowed me to build a scientific reasoning and awaken my curiosity in different domains. promiss I will not you send you emails on weekend and holidays.*
Mr.Sebaa*, Thank you to initiate me to a domain that was completely unknown to me in the beginning: the mechanical behavior of polymers. Thank you for the explanations and patience during our long discussions on this subject. And "last, but not least," thank you for your advices as being a grandfather.*

Also, I would like to thank all the jury members for the time they have given to reviewing the manuscript. I especially thank ***Mr.Benhorma Aissa*** *for being the president,* ***Mr.Azzaz Mohamed, Mr.Bezzazi Boudjema, and Mr.Rahmani Mohamed*** *with their experience.*

My deepest thanks are offered to the laboratory director (lme), ***Mr.Benchatti Ahmed****, where I spent the most time during these five years, thank you to opening doors to me and put between my hands any kind of equipment.*

I can't forget ***Mr.Benalia mokhtar*** *for being the founder of Analysis and control option, which motivate us research field.*

I would like to thank my colleagues and friends, those who know who they are, for making the past four and half year a valuable time in my life…

I will finish these acknowledgments with dearest persons: ***My family.***

Nassima, Djaouida, Samira, *and* ***Aicha****; being their sister is a source of inspiration, pride and example for the youngest one. Even we don't saying that to each other, thank you all for your support and comprehension during my absence in familiar precious moment.*

Finally, I will close by thanking those who are dearest to me: ***my parents.*** *Thank you for all the love that you gave to me since my childhood. I am truly grateful for everything you brought to me and what are you still bringing to me every day. The exemplary education you gave to me and the moral values instilled in me are a lot in the person I am today.*

You are a model for me and I am proud to be your daughter. Words fail me to express what I feel towards you ...

TABLE OF CONTENTS

LIST OF FIGURES

LIST OF TABLES

INTRODUCTION

Since several decades, polymer materials know a growing use in various areas. Applications related to greenhouse plastic films PE showed a significant progress. Indeed, ease of processing, low production cost and their various mechanical properties are all assets that led to favor this type of material. Algeria is a wide agricultural land and particularly in the south where the greenhouses made of transparent LDPE films provide better environmental conditions for plant growth and productivity. A general problem with polyethylene is the short shelf-life, especially in harsh weather conditions such as high temperature, high solar intensity, and dust, all of which are common in arid regions. In such conditions, mechanical resistance and light transmission may deteriorate rapidly.

At the microscopic scale, the only succeptibles chemical mechanisms affecting the mechanical properties are those that modify the backbone molecular chains. Detailed investigations on the nature of the oxidation mechanisms, the thermal and photochemical stability of final photoproducts as well as their effect on the mechanical properties have been the focus of previous dissertation studies [1, 2].

The main objective of this dissertation is to investigate the orientation dependence of mechanical properties, including large strain tensile properties, plans deformation, lateral contraction, and creep behavior, of the pristine and weathered LDPE films. All the above-mentioned mechanical tests were carried out at different angles with respect to the original MD of the extruded films. The morphological changes induced by ageing were investigated by wide angle X-ray scattering (WAXS), atomic force microscopy (AFM) and Field Emission Scanning Electron Microscopy (FESEM). In addition, LDPE films being semi-crystalline (i.e. constituted by alternative amorphous and crystalline phases), their morphological structure has been checked by different techniques including X-ray diffraction, Fourier Transform Infrared Spectroscopy (FTIR) and differential scanning calorimetry (DSC). The advantage of the DSC technique is to allow the crystalline lamellae thickness determination and their distribution and highlights how they are impacted by ageing. This dissertation is documented in the following format: It begins with chapter 1.0 that presents a general overview of the literature in the area of crystalline morphology and mechanical properties for semicrystalline polymers. Its objectives are to help the reader build some fundamentals related to the studies undertaken by the author. Different techniques of characterization are then introduced in

chapter 2.0, allowed the following of the microstructural and morphological changes of the material during their exposure. Tensile, plans deformation and lateral contraction are presented in chapter 3.0. Chapters 4.0 and 5.0 will focus upon the creep behavior studies. A synthesis of the complete dissertation is given in chapter 6.0. Since, chapters 3.0 ~ 5.0 have been written as manuscripts for publications in different scientific journals (one of them is already published in *Journal of Applied Polymer Science*). This manuscript has been expanded with more results to constitute chapter 5. Hence, the corresponding chapters are essentially "manuscript-based". Therefore, some materials may be repeated as common techniques for the different chapters, their relative references are given at the end of each chapter.

References

[1] Sebaa Mohamed, *Ph.D. Dissertation*, Vieillissement naturel et artificiel de films en polyéthylène basse densité (PEbd) utilisés comme couvertures de serres agricoles, university of Bordeaux I (France), 1992.

[2] Chabira Salem Fouad, *Ph.D. Dissertation*, Vieillissement naturel et thermique de films en polyéthylène et étude de l'évolution des propriétés viscoélastiques et du caractère d'anisotropie du matériau polyéthylène, Univerity of Setif (Algeria), 2004.

CHAPTER 1.0

LITERATURE REVIEW

1. GENERAL LITERATURE BACKGROUND

1.1.Material for greenhouses covering

In 2014, the global plastic production was around 311 million metric tons. The PE itself was a quarter of this production in reason of its low manufacturing cost and its physical and mechanical properties which are compatible with many applications in daily life [1]. In 2013 Algeria, produce 6 788 809 metric tons of vegetables in greenhouses [2]. Greenhouses provide better environmental conditions for plant growth and productivity. The important environmental factors affecting plant growth are temperature, relative humidity, light level, and carbon dioxide [3]. Greenhouses are covered with transparent material that transmits visible light (400–700 nm), which is the main source of energy for photosynthesis. Lozano et al. emphasized the importance of good light permeability in increasing greenhouse crop production [4]. Polyethylene has similar permeability as glass to short wave transmission but much higher permeability to long wave radiation. In addition, polyethylene covers are easy to handle and are the cheapest greenhouse covers. A general problem with polyethylene is the short shelf life, especially in harsh weather conditions such as high temperature, high solar intensity, and dust, all of which are common in arid regions. In such conditions, mechanical resistance and light transmission may deteriorate rapidly.

Low density polyethylene films contain significant concentrations of branches hindering the crystallization process, resulting in relatively low densities. The ramifications are mainly composed of ethyl groups and butyl groups as well as some long chain branching which may be branched at their turns. It is the reason of the high-pressure polymerization process used in production of low density polyethylene (Fig.1.1). It is a semicrystalline polymeric material with crystalline and amorphous phases. The crystalline lamellae provide polyethylene with structural integrity, while the amorphous parts provide polyethylene with its elastic properties [5]. The semicrystalline nature of polyethylene allowed it to become one of the most widely used polymers worldwide. The characteristic branches of LDPE hinder the crystallization of macromolecules, lowering thereby the material density (0.90~ 0.94 g/cm^3).

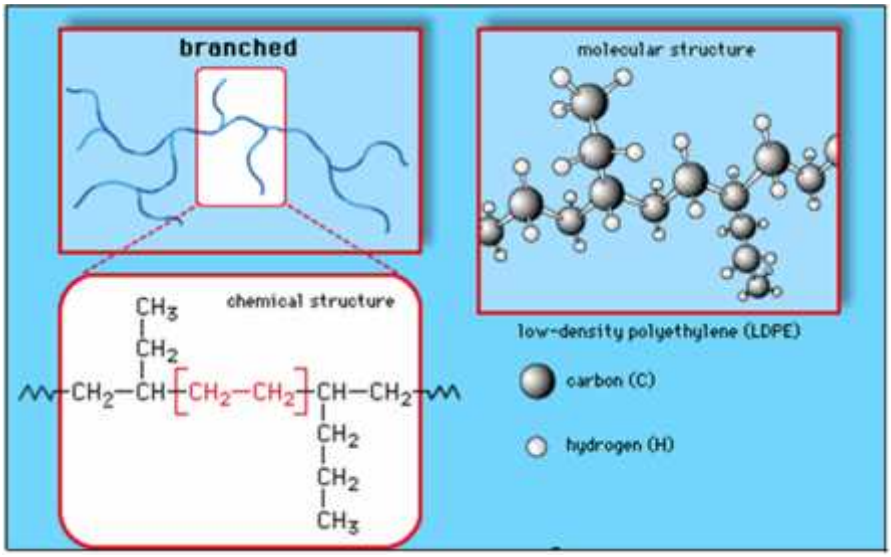

Fig.1.1: Different representation of LDPE [6].

Furthermore, polyethylene crystallinity is closely related to its density: more the PE is dense, more it is crystalline. The crystallinity is about 40% for LDPE. This structure gives the HDPE good elastic mechanical properties due to very high moduli (for example Young modulus E or shearing G,) and that is why it is mainly used for the manufacture of rigid products (e.g. tubes, bottles). Meanwhile, LDPE has other applications, such as flexible products (films, bags ...).

1.2.Structure and morphology of polyethylene

The semi-crystalline nature of polyethylene gives it a very particular morphology, which must be analyzed on different scales.

1.2.1. From macromolecular chains to spherolites

Figure 1.2 shows the three different scales describing the semi-crystalline structure of polyethylene:

- The crystallographic structure of the crystalline phase at the Angstrom scale,
- Lamellar structure of the crystallites at the nanoscale,
- And finally the superstructure of lamellae to spherolite at the microscopic scale.

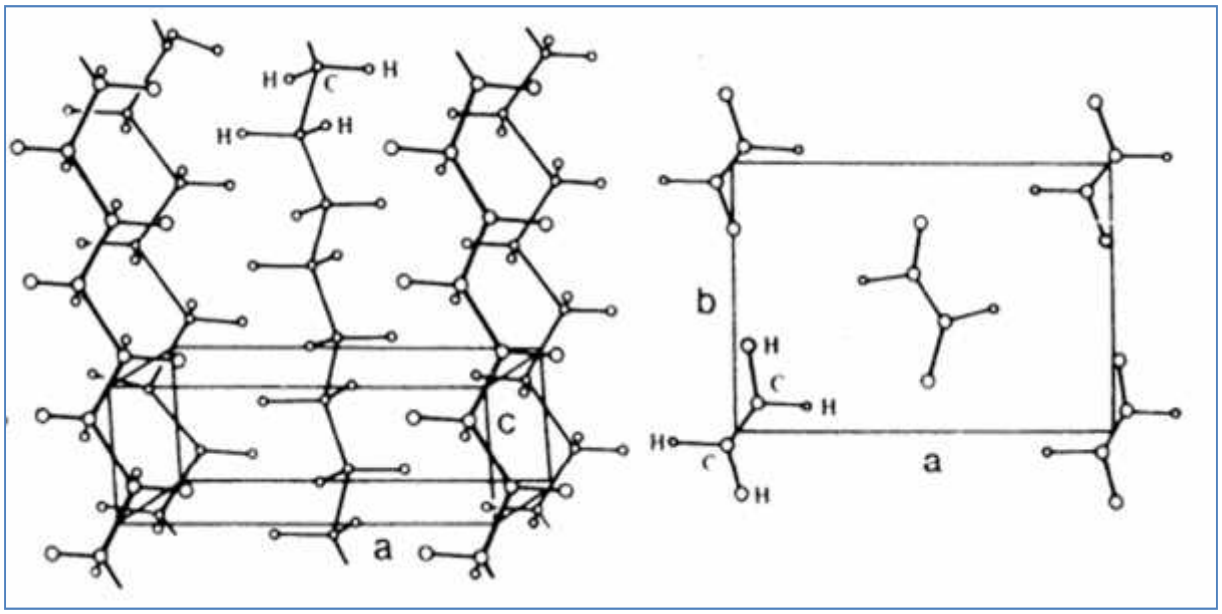

(a)

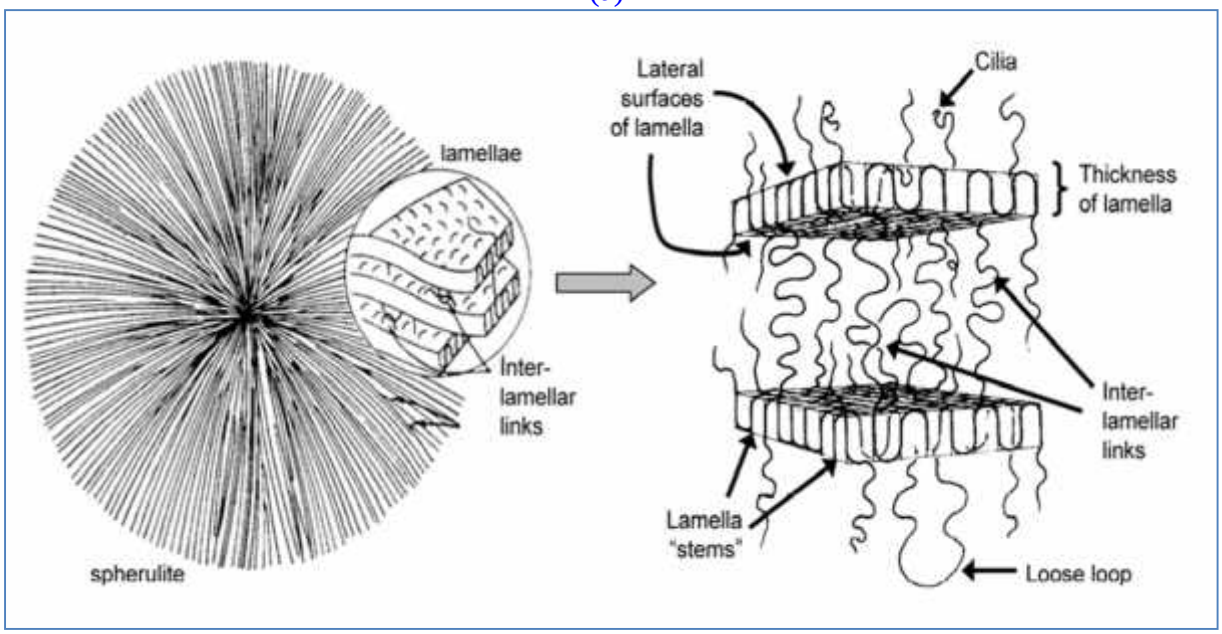

(b)

Fig.1.2: Schematic illustration of the three description scales of the PE structure: (a) crystallographic structure, (b) lamellar structure of the crystallites (left), superstructure spherolitic (right) [7, 8].

1.2.1.1.Crystallographic structure

Under certain conditions (slow cooling and structural regularity for example), the cooling of a semi-crystalline polymer from the liquid state causes crystallization of its macromolecular chains. They arrange themselves parallel to each other to form a stable

structure (Fig.1.2.a) The most stable structure of PE corresponds to an orthorhombic crystal lattice, the lattice parameters (a = 0.740 nm, b = 0.493 nm and c = 0.253 nm) were measured by Bunn in 1939.

1.2.1.2.Lamellar structure

During crystallization, the macromolecular chains are organized in a multiple folding process of the same chain to equal length segments to form crystalline lamellae. The thickness and regularity of these lamellae are dependent on crystallization conditions but also on the rigidity of chain, branching and entanglement defects [9]. The lamellae are linked by pieces of macromolecular chains belonging to other lamellae: these bridging are called chain links. The bridging can also be provided by the network entanglements pushed back into the amorphous phase during crystallization. Indeed, the lamellae are separated by an inter-lamellar amorphous phase composed of links chains, free chains, chain ends and everything that could not crystallize (additives, contaminants, etc ...) [10]. A detailed diagram of the layered arrangement is given in Figure 1.2.b.

1.2.1.3 Spherulitic structure

During their increasing phase, the lamellae are organized between themselves to form spherulites. A spherulite is a polycrystalline arrangement consists of a set of radial crystallites separated by the amorphous phase that grow from a center to occupy all the available space [10]. Spherulites are generally spherical in shape, the size; usually dependent on the cooling conditions can vary from micrometer to a millimeter. Spherulites rather have a spherical shape during their growth stage, until they meet other spherulites (end of crystallization) where their contour shows rather a polygonal aspect [11] (Fig.1.2.b).

1.2.2. General physical properties

1.2.2.1 Morphology

In semi-crystalline polymers, it is important to know the weight (X_{cw}) or volume (X_{cv}) fraction of the crystalline phase because it directly influences the mechanical properties. The method of polymerization of these materials leads to different crystallization rates. They are particularly difficult to crystallize the long chains (high M_n or M_w) having short branches [12-15]. Indeed, they hinder the macromolecular arrangement.

Figure 1.3 shows the effect of the rate and nature of short branches and effect of long branches rate on the PE density. It is noted a decrease in the density of the material when the

short branch increases. Moreover, for the same index of SCB, there was a decrease in density when the length of the side chains increases [12].

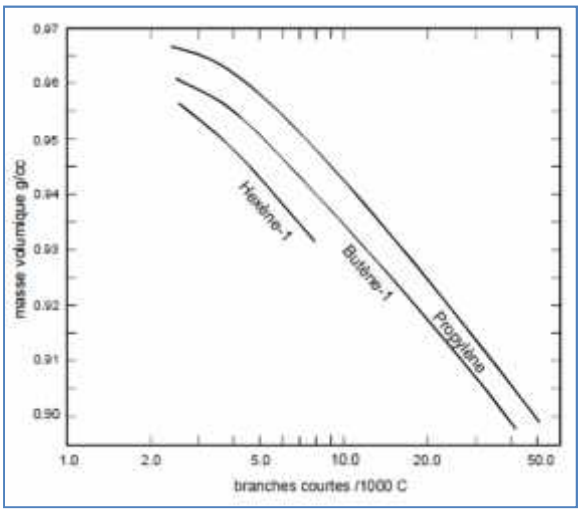

Fig.1.3: Variation of density functions of rate and nature of SCB [12].

Norton et Keller (1984) during their study on three types of PE (Fig.1.4.a): i) LDPE containing short and long branches, ii) linear HDPE containing low and short branches iii) a mixture of these two polymers, founds that the average melting temperature increases when passing from branched material to less branched one. We deduce that lamellae thickness increases when number of branching decreases. This phenomenon is due in same time to the SCB quantity and LSB rate [16].

Indeed, according to Yan et al. the size of crystal lamellae decreases with increasing LC index. Furthermore, the crystallinity is not affected by LC [17] (Fig.1.4.b).

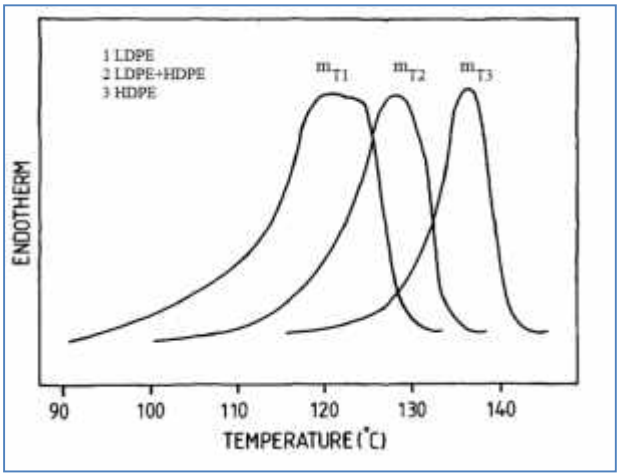

(a)

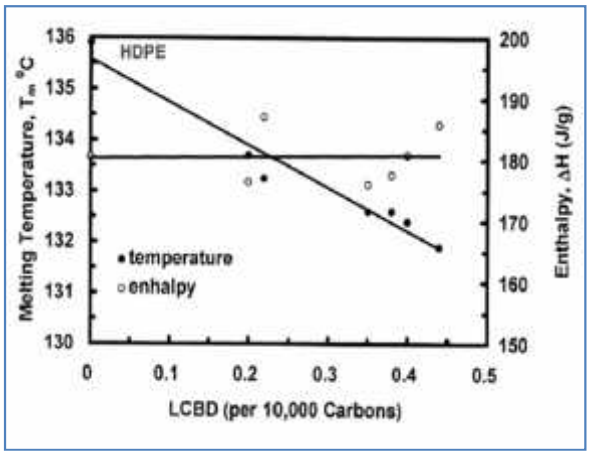

(b)

Figure 1.4**:** (a) DSC endotherms of three different macromolecular architecture PE [Norton et Keller (1984)), (b) Effect of LCB rate on the temperature and enthalpy of fusion of HDPE [17].

1.3. Mechanical behavior of semicrystalline polyethylene

Mechanical properties are one of the primary criteria to meet for engineering applications. The desired properties can be achieved by a variety of approaches, such as designing new chemistry, making polymer blends, and applying unique processing techniques. A better understanding of structure-property relationships can service as a guide to manipulate mechanical properties by these approaches. In what follows, a brief literature survey is provided to highlight some fundamentals of structure-property relationships, with a focus on semicrystalline polymers again using PE as an example. More detailed information dealing with specific topics that are covered in this dissertation will be given in the introduction sections of chapters 3.0 ~ 6.0.

Like any viscoelasic behavior of semicrystalline PE, below the glass transition temperature, the amorphous phase is rigid. Therefore, the plastic deformation is achieved by the formation and propagation of shear bands in the glassy amorphous state [1, 18-20], and shearing lamellae [21]. Above the α relaxation temperature, the amorphous phase has a rubbery behavior while the lamella sliding is eased because the nucleation and propagation process of dislocations are thermally activated [22- 24].

Our study focuses on the mechanical behavior of polyethylene at temperatures above T_g where the material has rubbery regime. We'll detail the microscopic and macroscopic processes that take place in this range.

1.3.1 Deformation micromechanisms

1.3.1.1 Amorphous phase deformation

The amorphous phase of the material is characterized by a free part containing entanglements and a related part to the crystalline lamellae. The mechanical role of this phase is the stress transmission from crystallite to another via link molecules. These interlamellar networks are physical crosslinking points which give the amorphous phase a certain mechanical resistance. Furthermore, the chains sliding at entangles is a source of irreversible deformation.

There are two modes of deformation of the amorphous phase involving the molecules link and the stacks lamellae: the interlamellar slippage and interlamellar separation. The lamellar slip corresponds to the parallel shear of two crystalline lamellae one over the other under the shear stress effect (Figure 1.5.b) [10]. Interlamellar separation results in a variation of the distance between two lamellae when applying a perpendicular stress (Figure 1.5.c) [10, 25, 26]. This deformation results in a density decrease of the amorphous phase and a creation of voides, both mechanisms cause the deformation of amorphous phase only [20, 25, 27, and 28].

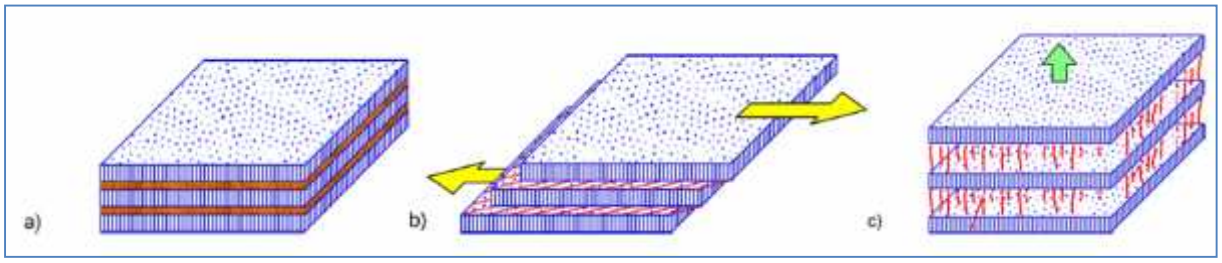

Fig1.5: Interlamellar mechanism deformation, a) non-deformed state, b) interlamellar Sliding, c) interlamellar separation [10].

1.3.1.2 Crystalline phase deformation

In a metal crystal, the slip involves moving crystalline block along a defined dense atomic plane. This latter is called the slip plane, while the direction of this process is called a sliding direction. In reality, the slip does not occur in block but progressively, step by step, through the dislocation motion.

Polymer crystallites also deform by a slip mechanism. However, unlike metals, are only the active slip systems whose plane contains the chains axis. This restriction is due to the presence of covalent bonds along the chains. Thus, in a crystal polymer, the slip plane must contain the macromolecules direction [29]. Critics' scissions resolved from slip systems in crystals of polymers depend on the van Waals bonds between the macromolecular chains [30].

If the direction of the macromolecules is [001], the slip planes have as Miller indices (hk0) and slip directions have two possible orientations: i) parallel to the chains axis <001> and ii) perpendicular to chains axis <uv0> (Figure 1.6). A slip system {hk0}<001> is called "chain slip", while a sliding system of the type {hk0}<uv0> is called "transverse slip". In polyethylene, parallel sliding systems channels are (100) [001], (010) [001] and {110} [001] while the slip systems perpendicular to the chains direction (100) [010], (010)[100] and {110}<110> (Figure 1.7) [30-32].

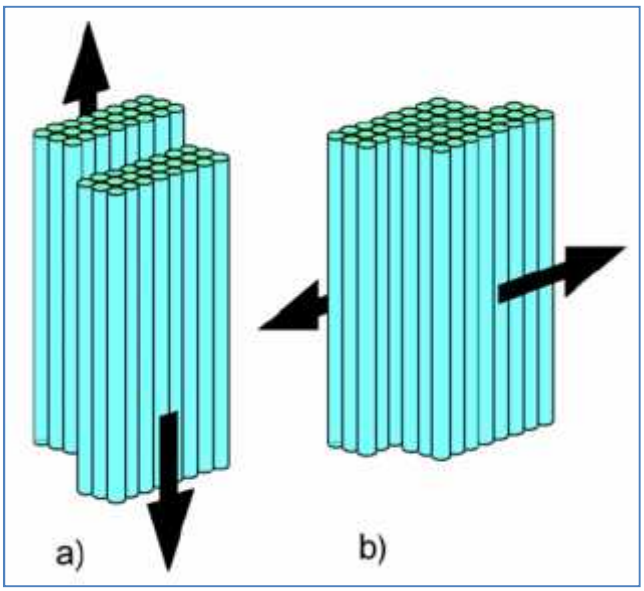

Fig1.6: Sliding processes a) parallel and b) perpendicular to crystalline lamellae chains [31, 32].

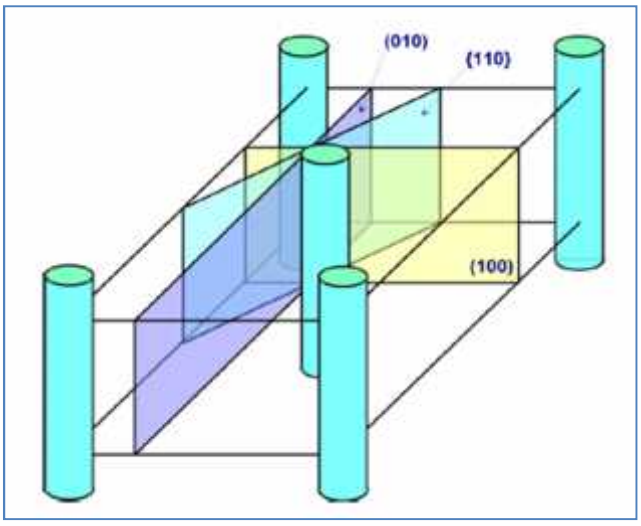

Fig.1.7: Slip system perpendicular to crystallites chains [31].

1.3.1.3. Fragmentation of crystalline lamellae

During stretching, the crystalline lamellae and the amorphous zones are subjected to tensile, shear, bending or compression depending to their orientation within spherulite [25, 27, 29, 33, 34, 35, and 36]. Deformation mechanisms of the amorphous and the crystalline phases interact during the destruction of the semi-crystalline morphology.

Among these local deformation modes, the shear action on the "Sandwich" structure (lamellae/ amorphous layers) leads to destruction of the crystalline order by fragmentation of the crystalline phase (Figure 1.8). According to Friedrich, Schultz, and Haudin, the shearing mechanism is preceded by separation and interlamellar slip (Figures 1.8.b and 1.8.I) resulting in the formation of voids between the lamellae [27, 33, and 37]. When the amorphous chains are fully extended, the shear occurs at the crystallite, favoring slip systems in parallel to chains. This gives an orientation of the crystal chains to the tensile direction.

Meanwhile, cavitation phenomena are amplified during the processing where the density and size of the voids increases (Fig 1.8.II). Under the combined effect of interlamellar separation and intracrystalline slip, the deformation leads to structure fragmentation (Figures 1.8.c and 1.8.II), followed by unfolding of some chain segments belonging to lamellae. This results in microfibrillar structure containing cavities oriented parallel to the loading axis (Figs 1.8.d and 1.8.III). According Fond and G'Sell, this crystallite destruction mechanism by tensile and shear is amplified by a lateral compression effect of the lamellae [36].

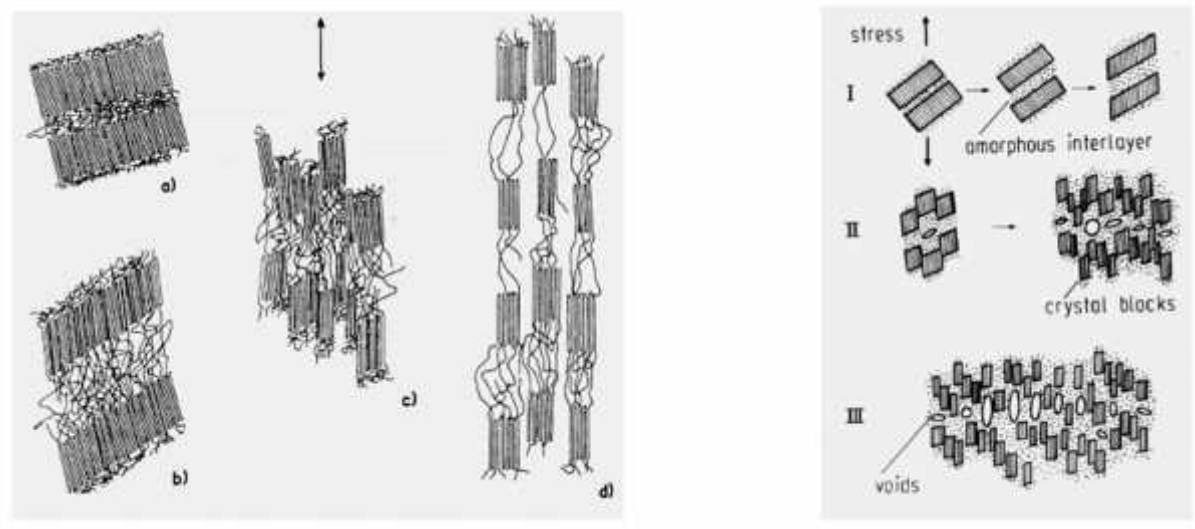

Figure 1.8: fragmentation mechanisms of crystalline lamellae: Schultz Models (1974) without cavitation and Friedrich (1983) with cavitation

Nitta and Takayanagi propose a model of crystallites fragmentation when the crystalline lamellae have an orientation that does not promote the crystallographic type of deformation mechanisms [34, 35].

1.3.1.4. Spherulites deformation

Inside the spherulites, the lamellae deformation depends on the orientation of the crystallized chains relative to the loading axis. According Aboulfaraj et al. and Haudin and G'Sell, three regions are distinguishable [38, 10]:

- *Equatorial region:*

The chains direction is parallel to the pulling axis (Fig.1.9.a). In this region, the plastic deformation by intracrystalline sliding is very difficult. The most active mechanism is the interlamellar separation which can lead to the formation of voids under certain conditions, followed by a fragmentation mechanism by bending the lamellae [20, 27, 34, 35, and 38].

- *Diagonal region:*

This region is characterized by an oblique orientation of the lamellae with respect to the pulling direction (Fig.1.9.b and Fig1.9.d). In this zone, the lamellae are subjected to a shear causing interlamellar sliding then interlamellar separation and finally there is a plastic deformation of the lamellae leading to their fragmentation.

- *Polar region:*

The direction of the chains is orthogonal to the pulling axis. In this zone, the lateral compression due to deformation of the diagonal areas causes early fragmentation of the crystals (Fig.1.9.c).

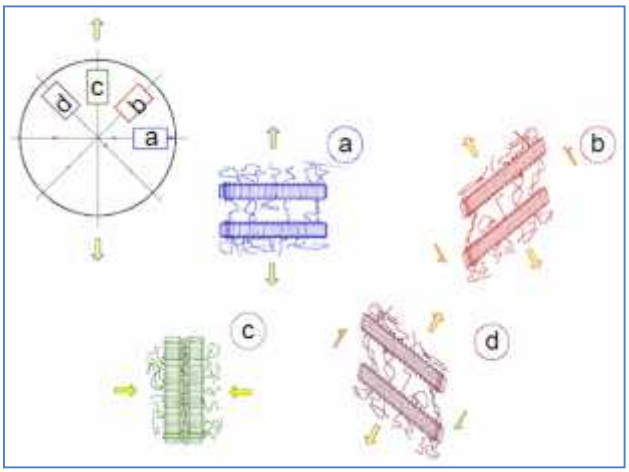

Fig.1.9: Deformation of a) Equatorial, b) and d) Diagonal, and c): Polar regions of spherulite.

1.3.2 Macroscopic plastic behavior

1.3.2.1. Tensile tests

The first studies of plastic behavior of semi-crystalline polymers were based on nominal laws that do not include plastic instabilities (necking) occurring during the deformation [22, 25, 39-43]. The following studies have sought to establish the true plastic behavior of the material and characterize the micro-mechanisms that control the deformation [44, 32, 45, 46, 47, 7, and 48].

Representative tensile curves of the true behavior of HDPE are shown in Figure 1.10. This latter shows the influence of strain rate on the evolution of the true stress - true strain obtained by tensile.

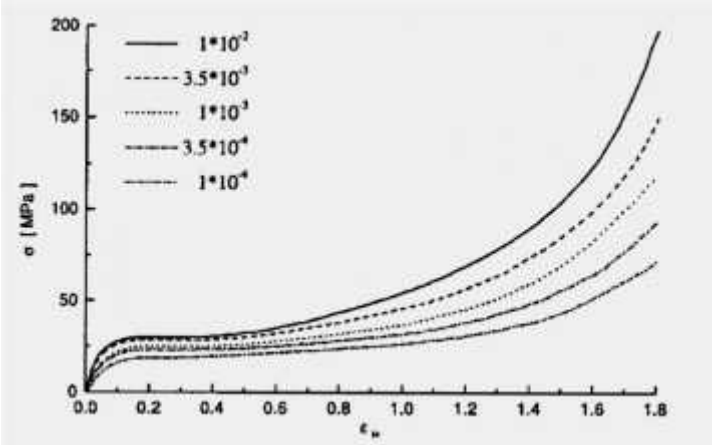

Fig.1.10: True stress-true strain curves of HDPE [46].

When the strain rate decreases or the temperature increases, the yield drops and the plastic hardening phenomenon decreases in intensity [46]. Indeed, if the temperature increases, the viscosity of the amorphous chains thus decreases the rearrangement of the amorphous texture is facilitated. In addition, the intralamellar sliding requires less energy because the process of formation and propagation of dislocations are thermally activated. When the strain rate decreases, the friction resulting from the sliding mechanisms between the amorphous and crystalline chains are lower. Consequently, the deformation of the amorphous phase and polymer crystals requires less energy.

LDPE knows many applications; its integration in all industrial and domestic products makes it a basic material of industry and households. One of the most important applications directly

related our food industry is the use of LDPE films for agricultural greenhouses. The harsh climatic conditions of our sub-Saharan region characterized by long and strong sunshine makes it very vulnerable material which rarely exceeds a season for its stabilized grade. So it becomes important to understand the PE degradation mechanisms in order to develop remedies that can extend their life time. This has a double impact from an economic standpoint but also from an environmental view point.

The design of this material should take into account the indiscernible damages of its physical, chemical and / or photochemical properties. The LDPE degradation should be understood and controlled since the photo-aging is its main cause; in order to better recognize the difficulty of this type of problem we describe some degradation aspects in next section.

2. AGEING OF POLYETHYLENE

The development of polymers as an important engineering material was inhibited at first time by the premature failure of these versatile compounds in many applications. The deterioration of the significant properties of both natural and synthetic polymers is the result of irreversible changes in composition and structure of polymer molecules. The term polymer degradation is used to denote changes in physical properties caused by chemical reactions involving bond scission in the backbone of the macromolecule. The most appropriate way to distinguish between different modes of polymer degradation is to subdivide this broad field according to its various mode of initiation. These comprise photochemical, thermal, radiation, mechanical, chemical and biological degradation of polymeric materials.

2.1.Natural weathering

Degradation of polyethylene films during their outdoor exposure is influenced to varying degrees by all natural meteorological phenomena. Heat, radiation (unltraviolet and infrared), rain, humidity, atmospheric contaminants, thermal cycling, and oxygen content of air all contribute to the degradation of PE subjected to outdoor exposure.

The photodegradation is the most important aspect of natural weathering, which was the subject of large number of publications [49-54].

The solar spectrum (Fig.1.11) contains 2 to 7% of UV radiations, which transport enough energy to excite some chemical groups having a selective absorption in this spectral range.

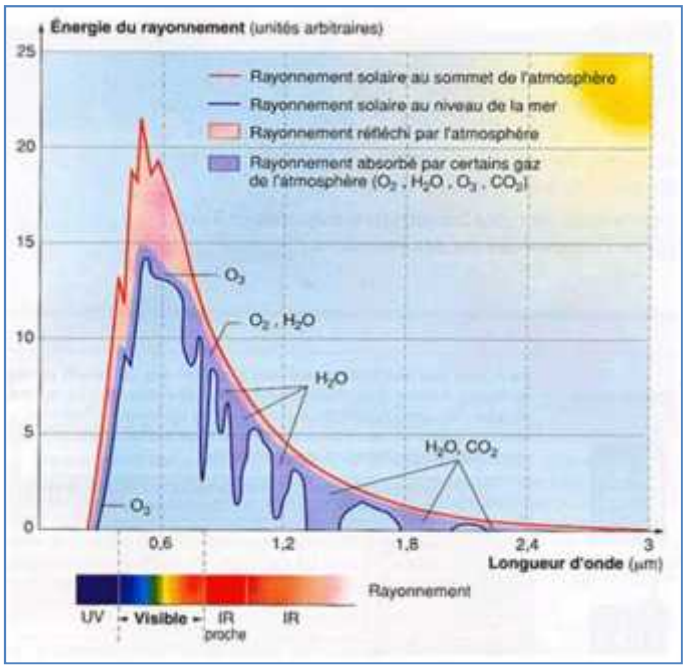

Fig1.11: A typical midday solar spectrum.

The industrial polyethylene is transparent to UV. The photo-sensibility of this polymer is attributed to cetonic groups, hydroperoxydes and to catalytic residues present during their transformation. Functional groups present in PE, able to absorb energy and could cause the breaking of carbon-carbon bond are [55, 56]: carbonyls ($270 \leq \lambda \leq 360$ nm), vinyls ($\lambda \geq 250$ nm), and hydroperoxydes ($\lambda \approx 320$ nm).

The role of heat in the outdoor degradation of PE films is an accelerating process. It is a well-experienced fact that deterioration rats of polymers in the tropics far exceed those in temperate zones. Simulated weathering experiments have shown that the oxidation rates of polyethylene exposed to 300 nm radiation increase fourfold from 10 to 50°C [57].

2.2. Ageing effect on the mechanical properties

The effect of natural weathering on the mechanical properties of LDPE has been widely studied. Chabira and Sebaa on their studies on LDPE samples exposed in Laghouat, Algeria, observed that there is an initial increase in strain at break due to cross-linking followed by a steady decrease until the sample becomes very brittle, the Young's modulus also tends to increase [58]. The tensile strength and elongation at break of the polyethylene samples, exposed in natural weather of Palmero, Italy, were studied by LaMantia and Severini et al. [59]. Qualitative property/structure correlations are proposed by LaMantia, taking into account previos structural results for the same samples. Severini et al.concluded that during the eathering macromolecules of polyethylene undergo, simultaniously, processes of photooxidation and chain breaking, which cause the decay of the mechanical properties.

It has been observed that photochemical degradation of polyethylene does not occur uniformly across the thickness of the material and a gradient of degraded material seem to exist. The damage is localized within a few micrometers of the surface and quickly decreases with depth. Such a gradient give rise to internal stresses. In addition the spherulitic boundaries characterized by high concentration of surface irregularities (including chromophores) result in the weak center formation. These defects eventually lead to stress concentration and microcracks [59].

3. Creep-recovery behavior of LDPE

Creep is the time-dependent strain (elongation) for a material under constant stress. For polymers, creep deformation is an important and powerful experimental method to study many physical properties such as viscoelastic behavior, physical aging, etc. On the other hand, creep is also a common phenomenon for engineering applications, namely LDPE films used in greenhouses covering, during their service are subjected to specific loadings, and the film's service life is a major concern. Therefore it is also critical to understand the origin of creep deformation and to be able to predict the long time creep behavior for a given polymeric material under specific conditions.

The creep behavior of polyethylene has extensively been studied in literature [60-66], three different approaches have been attempted to describe the time-dependent creep behavior of polymers [67]: engineering approaches, rheological approaches and molecular approaches. In an engineering approach, the goal is set to predict the creep behavior (usually creep strain) for a particular loading situation based on a low number of experiments, and empirical relationships are then proposed. Different relations such as a power law equation have been found to be valuable to describe creep strain for certain polymers under specific loading conditions.

For the rheological approach, attempts are directed to extend the linear viscoelastic relations, e.g. Boltzmann superposition principle, to a non-linear regime. One way of doing this is to preserve the separability of stress, strain and time in their functional representations, and this leads to the sophisticated form of single integral representations developed by Leaderman [68], Bernstein, Kearsley and Zapas [69], Valanis and Landel [70], and Schapery [71]. Another method is to use multiple integral representations [72], which has led to considerable mathematical complexity. An excellent introduction on this subject can be obtained in reference [73]. The rheological approach is the focus of Chapter 5.0.

The molecular approach is aimed at incorporating a molecular model that describes the molecular event of creep deformation to a physical property that can be measured experimentally. This approach has the attraction of possible identification of the molecular mechanisms and structural origins responsible for creep. The disadvantages of this approach are the lack of precise mathematical treatment/description as compared with the rheological method. However, this drawback is somewhat balanced by the built-in merit of non-linearity and temperature dependence [67]. The molecular approach was the research subject of Zhou et al on HDPE [74].

Many models have been proposed to describe the creep behavior of polymers [75], neither the simple Maxwell nor Voigt model accurately predicts the behavior of real polymeric materials. Various combinations of these two models may more appropriately simulate real material behavior. The four-parameter model is reported in Figure 1.12.a, which is a series combination of the Maxwell and Voigt models. Under creep, the total strain will be due to the instantaneous elastic deformation of the spring of modulus E, and irrecoverable viscous flow due to the dashpot of viscosity η_2, and the recoverable retarded elastic deformation due to the Voigt element with a spring of modulus E_3 and dashpot of viscosity η_3. Thus, the total strain is the sum of these three elements. That is,

$$\varepsilon(t)= \varepsilon_1+\varepsilon_2+\varepsilon_3 \qquad (1.1)$$

$$\varepsilon\ t\ = \frac{\sigma_0}{E_1} + \frac{\sigma_0 t}{\eta_2} + \frac{\sigma_0}{E_3}[1 - exp^{-t\ \tau_3}] \qquad (1.2)$$

Where σ_0 is the imposed constant stress and τ_3 equals η_3/E_3 and is referred to as the retardation time. In creep recovery, say, the load is removed at time t_1; the deformation, σ_0/E_1, due to the spring of modulus E_1 is recovered instantaneously. This will be followed by the retarded elastic creep recovery due to the Voigt element given by ε_3 or

$$\varepsilon_3 = \frac{\sigma_0}{E_3}[1 - exp^{-t_i\ \tau_3}] \qquad (1.3)$$

Only the deformation due to the dashpot of viscosity η_2 is retained as a permanent set. The creep and creep recovery curve of this model is shown in Figure 1.12.b.

The four-parameter model provides a crude qualitative representation of the phenomena generally observed with viscoelasic materials: instantaneous elastic strain, retarded elastic strain, viscous flow, instantaneous elastic recovery, retarded elastic recovery, and plastic deformation (permanent set). Also, the model parameters can be associated with various

molecular mechanisms responsible for the viscoelasic behavior of linear amorphous polymers under creep conditions. The analogies to the molecular mechanism can be made as follows.

1. The instantaneous elastic deformation is due to the Maxwell element spring, E_1. The primary valence bonds in polymer chains have equilibrium bond angles and lengths. Deformation from these equilibrium values is resisted, and this resistance is accompanied by an instantaneous elastic deformation.
2. Recoverable retarded elastic deformation is associated with the Voigt element. This arises from the resistance of polymer chains to coiling and uncoiling caused by the transformation of a given equilibrium conformation into a biased conformation with elongated and oriented structures. The process of coiling and uncoiling requires the cooperative motion of many chain segments, and this can only occur in a retarded manner.
3. Irrecoverable viscous flow is due to the Maxwell element dashpot η_3. This is associated with slippage of polymer chains or chain segments past one another.

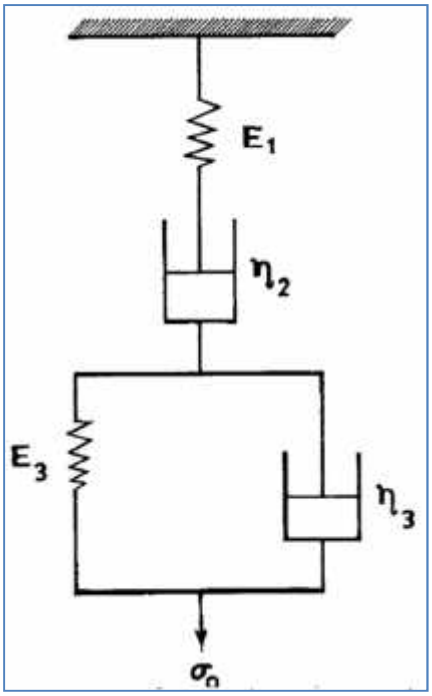

Fig.1.12.a: Schematic of the four parameter model.

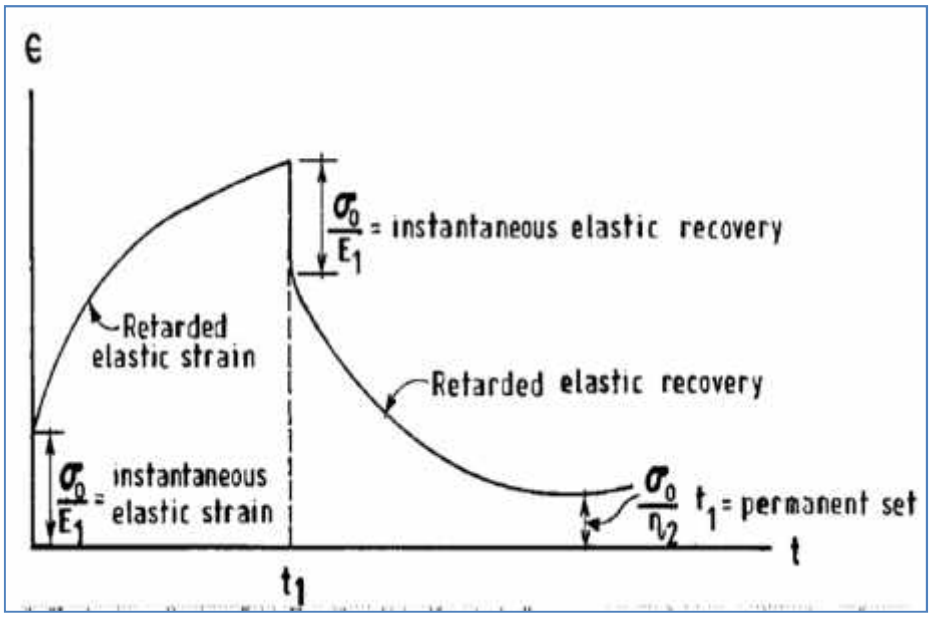

Fig.1.12.b: Creep response of the four parameter model [75].

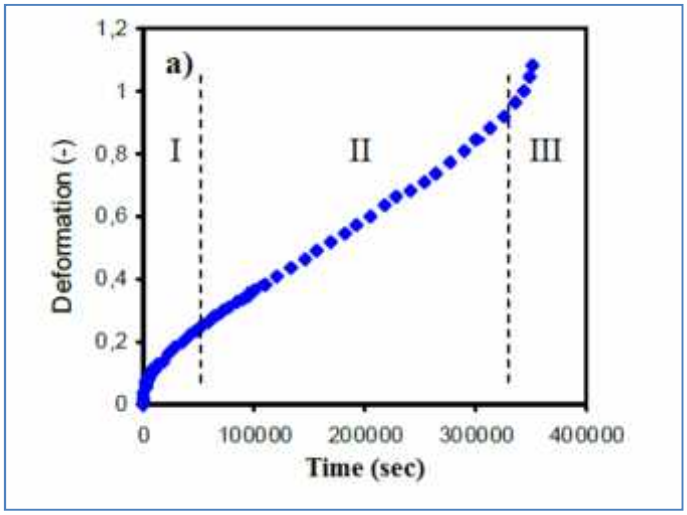

Fig.1.13: Creep deformation of HDPE [76].

The curve is characterized by three inelastic deformation domains: i) a primary domain where the deformation increases rapidly with time, ii) a second domain characterized by a stabilization of deformation and iii) tertiary domain where there is a rapid and constant re-increase of the deformation over time. This tertiary domain coincides with the necking formation. Indeed, when the test section decreases sharply, the macroscopic stress increases

rapidly due to the constant applied load, the deformation of the material accelerates consequently.

Shown on figure.1.14, the correlation between nominal and true creep behavior. In this study, HDPE is deformed by creep at 60°C under different constant stresses (nominal behavior) or constant stress (behavior true) [77]. These two behavior types are characterized by strain-time curves with a different curve trends. Indeed, when the section reduction is considered (real behavior), there is no tertiary creep domain. Thus, the true strain-time evolution is composed of two domains after the elastic deformation: i) one where the true strain increases rapidly with time and ii) another characterized by a stabilization of the true strain with time since the stress state was homogenized in the surveyed material volume. Higher stress resulted in an early beginning of the secondary creep domain. This agrees with Zhou's results on creep behavior of HDPE films [74], also, the films showed not only an orientation dependence of creep behavior but also higher stress results in larger creep strains.

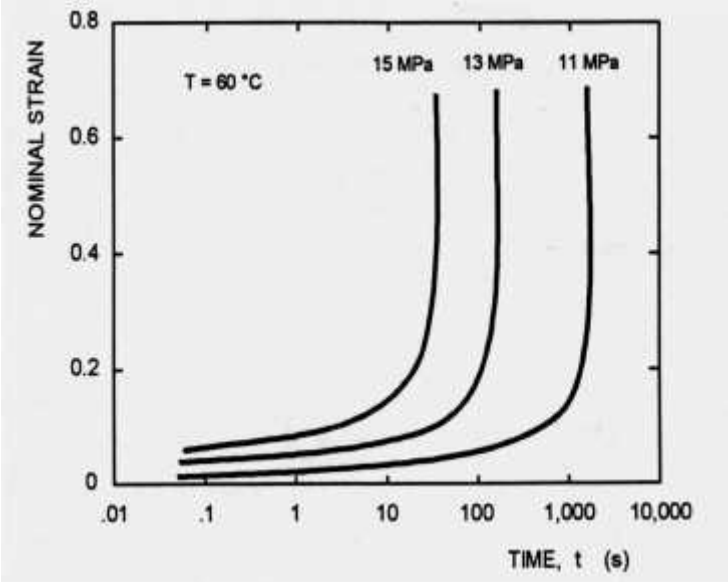

(a)

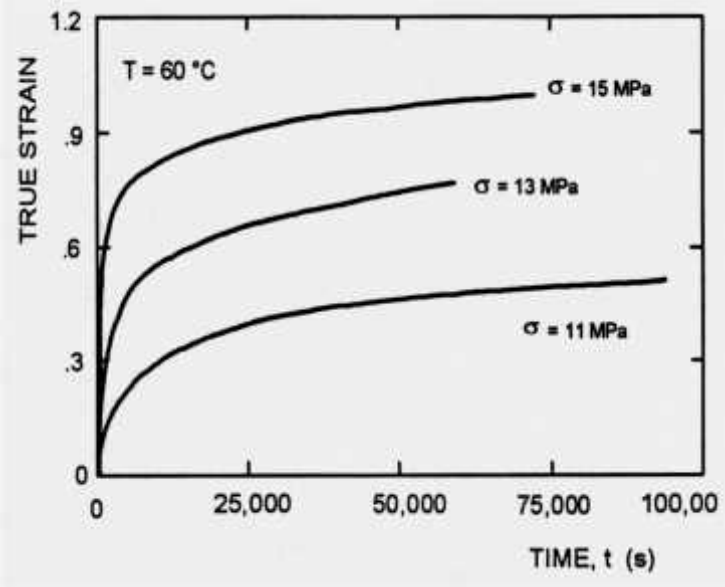

(b)

Fig.1.14: a) nominal, b) true creep test for HDPE at 60° [77].

3.1.Ageing effect on the creep-recovery behavior of PE

Most amorphous polymers are found to be of thermorheologically simple at temperatures above the glass transition temperature; therefore, the time-temperature superposition principle has also been used in the creep study of amorphous polymers [78-80]. According to this principle, the long time creep data can be “obtained” by performing experiments at higher temperatures in shorter time scales for the same material. For semicrystalline polymers, however, due to the complex coupling between the crystalline phase and the amorphous phase (thermorheological complexity), the time-temperature superposition principle is generally not applicable [81, 82]. In thermoplastic polymers, the rate-controlling creep mechanism involves a cooperative motion of molecular chain segments with respect to each other. Indeed, ageing increases the crosslinking density between the molecular chains in the amorphous phase which increases in return the average molecular weight. As a result, a decrease of the extent and the rate of the creep strain are usually observed [64]. The effect of the branching density on the creep behavior is known to decrease the total creep strain for long-test time deformation while they increase the creep strain and the creep rate for the short-term creep [62, 63, and 64]. Raburn et al (1994) on their studies on creep behavior of PE found that the SCB increases, the strain rate decreases in the different domains and the tertiary creep domain is delayed , thus the creep resistance increases as well [64]. Moreover, the creep rate is lowered by the methyl branch contents [6 from our creep paper].

The creep behavior in polyethylene films is mainly controlled by the deformation of the amorphous phase, which is itself strongly affected by the variation of the crystallinity and the tautness of the tie molecules [74].From morphological standpoint, the crystallinity affects directly the creep behavior of PE. Indeed, at iso-strain, the tertiary creep domain is retarded with increasing crystallinity [83]. Also, in chemical aging of HDPE, knowing that increasing in crystallinity which is equal to lowering of the molecular weight, thus increasing in aging time, decreases the strain rate [76].

However, many works dealing with the effect of structure and morphology on the creep behavior of polyethylene films can be found in literature but seldom on ageing effects. In this work the effects of ageing on the mechanical properties and on the creep behavior of a LDPE film tested in the two main directions of the plane are studied. The goal of this work is to apply a long-term mechanical deformation mode, much more sensitive than tensile to the elementary microstructural changes.

References

[1] J. Rault, *Les polymères solides*, Ed. CEPADUES, Toulouse, France, (2002).
[2] Ministry of Agriculture, Algeria, 2014.
[3] Al-Ayedh, A., Al-Doghairi, M., 2004. *Trapping efficiency of various colored traps for inserts in cucumber crop under greenhouse conditions in Riyadh, Saudi Arabia. In: International Symposium on Greenhouses, Environmental Controls and In-house Mechanization for Crop Production in the Tropics and Sub-tropics*, Pahang, Malaysia, June 15–17.
[4] G. Lozano, D. Gonzalez, E. Santos, *Growing lettuce in greenhouses clad with polychromatic films*. Plasticulture 110, 15-22, 1996.
[5] I. M. Ward, (1971), *Mechanical Properties of Solid Polymers*, Wiley-Interscience, Toronto.
[6] Encyclopædia Britannica, Inc.1997.
[7] F. Addiego, Ph.D Dissertation, *Caractérisation de la variation voluminique du polyethylene au cours de la déformation plastique en traction et en fluage.* INP de Lorraine, Nancy (France), March 2006.
[8] A. Lustiger, & R. L. Markham, *Importance of tie molecules in preventing polyethylene fracture under long-term loading conditions, Polymer*, 24 (12), (1983).
[9] X. Lefebvre, P.h.D dissertation, the school of mines Paris (France), 2002.
[10] Haudin J.M., G'sell C. *Introduction to the mechanic of polymers*, chapter structure and morphology of semicrystalline polymers, pp 97-115, ed. C. G'sell et J.M. Haudin, INP de Lorraine, Nancy (France), 1995.
[11] J.H. Magill, (2001). Review Spherulites: A personal review. *Journal of Materials Science*, 36, pp. 3143-3164.
[12] J.Audureau, *Industrial Synthesis of polyethylene*, Initiation to chemical and to physicochemical macromolecular, Ed. GFP, 4, 1-58, 1982.
[13] M. Hert, physical and mechanical properties of polyethylene , *Initiation to chemical and to physicochemical macromolecular* , Ed. GFP, 4, 59-100, 1982.
[14] J.P.Trotignon, J.Verdu, A. Dobracginsky, M. Piperaud, *Précis de matières plastiques*, Ed. Nathan, Paris, France, 1996.
[15] G. Dlubek, J. Stejny, T. Lupke, D. Bamford, K. Petters, C. Hubner, M.A. Alam, M.J. Hill, *Free-volume variation in polyethylenes of different crystallinities: Positron lifetime, density, and X-ray studies.* Journal of Polymer Science: Part B: Polymer Physics, 40, 65-81, 2002.
[16] D.R. Norton, A. Keller, *On the morphology of blends of linear and branched polyethylene.* Journal of Materials Science, 19, 447-456, 1984.
[17] D. Yan, W.J. Wang, S. Zhu, *Effect of long chain branching on rheological properties of metallocene polyethylene*, Polymer, 40, 1737-1744, 1999.
[18] J.Perez, *physics and mechanics of amorphous polymer -Techniques and documentation - Lavoisier*, Paris (France), 1992.
[19] B. Escaig, *Kinetics and thermodynamics of plastic flow in polymeric glasses*, Plastic deformation of amorphous and semi crystalline material, edited by Escaig B. and G'Sell C., Les Editions de Physique, Les Ulis (France), 187-225, (1982).
[20] S. Castagnet, J.L. Gacougnolle, P. Dang, *Correlation between macroscopical viscoelastic behaviour and micromechanisms in strained α polyvinylidene fluoride (PVDF).* Materials Science and Engineering, A276, 152 159, 2000.
[21] S.W. Allison, I.M. Ward, *The cold drawing of polyethylene terephthalate*, British Journal of Applied Physics, 18, 1151-1164, 1967.

[22] R. Corneliussen, A. Peterlin, *The influence of temperature on the plastic deformation of polyethylene*, Die Makromolekulare Chemie, 105, 193-203, 1967.
[23] V. Gaucher-Miri, R. Séguéla, *Tensile yield of polyethylene and related copolymers: mechanical and structural evidences of two thermally activated processes*, Macromolecules, 30, 1158-1167, 1997.
[24] R. Séguéla, V. Gaucher-Miri, S. Elkoun, *Plastic deformation of polyethylene and ethylene copolymers: Part I Homogeneous crystal slip and molecular mobility*, Journal of Materials Science, 33, 1273-1279, 1998.
[25] F.J. Balta-Calleja, A. Peterlin, *Plastic deformation of polypropylene. VI. mechanism and properties*, Journal of Macromolecular Science-Physics, B4 (3), 519-540, 1970.
[26] J. Petermann, J.M. Schultz, *Lamellar separation during the deformation of high-density polyethylene*, Journal of Materials Science, 13, 50-54, 1978.
[27] K. Friedrich, Advances in Polymer Science, *Crazing in polymers*, 52/53, Edited by Kausch H.H., Springer-Verlag, Berlin-Heidelberg, Germany, 225-274, 1983.
[28] E.J. Kramer, Advances in Polymer Science, *Crazing in polymers*, 52/53, Edited by Kausch H.H., Springer-Verlag, Berlin- Heidelberg, Germany, 1-56, 1983.
[29] A. Peterlin, *Molecular model of drawing polyethylene and polypropylene*, Journal of Materials Science, 6, 490-508, 1971.
[30] L. Lin, A.S. Argon, *Structure and plastic deformation of polyethylene*, Journal of Materials Science, 29, 294-323, 1994.
[31] A. Dahoun, *Ph.D dissertation*, INP de Lorraine, Nancy (France), 1992.
[32] C. G'Sell, A. Dahoun, *Evolution of microstructure in semi-crystalline polymers under large plastic deformation*, Materials Science and Engineering, A175, 183-199, 1994.
[33] J. Schultz, *Polymer Materials Science*, Prentice-Hill, Englewood Cliffs, New Jersey, 1974. Chapter.11.
[34] K.H. Nitta, M. Takayanagi, *Role of tie molecules in the yielding deformation of isotactic polypropylene*, Journal of Polymer Science, Part B: Polymer Physics, 37, 357-368, 1999.
[35] K.H. Nitta, M. Takayanagi, *Tensile yield of isotactic polypropylene in terms of a lamellar-cluster model*, Journal of Polymer Science, Part B: Polymer Physics, 38, 1037-1044, 2000.
[36] C. Fond, C. G'Sell, *Localisation des déformations et mécanismes d'endommagements dans les polymères multiphases*, Mécanique et Industries, 3, 431-438, 2002.
[37] Haudin J.M., Edited by B. Escaig and C. G'Sell, *Les Editions de Physique*, Les Ulis, (France), 291-311, 1982.
[38] M. Aboulfaraj, C. G'Sell, B. Ulrich, A. Dahoun, *In situ observation of the plastic deformation of polypropylene spherulites under uniaxial tension and simple shear in the scanning electron microscope*, Polymer, 36, 731-742, 1995.
[39] P.I. Vincent, *The necking and cold-drawing of rigid plastics*, Polymer, 1, 7-19, 1960.
[40] I.H. Hall, *The effect of strain rate on the stress–strain curve of oriented polymers. I. Presentation of experimental results*, Journal of Applied Polymer Science, 12, 731- 738, 1967.
[41] A. Peterlin, F.J. Balta-Calleja, *Diffraction studies of plastically deformed polyethylene*, Kolloid-Zeitschrift und Zeitschrift für Polymere, 242, 1093-1102, 1970.
[42] J.M. Andrews, I.M. Ward, *The cold-drawing of high density polyethylene*, Journal of Materials Science, 5, 411-417, 1970.
[43] G. Meinel, A. Peterlin, *Plastic deformation of polyethylene II. Change of mechanical properties during drawing*, Journal of Polymer Science: Part A-2, 9, 67-83, 1971.
[44] J. Amoedo, D. Lee, *Modeling the uniaxial rate and temperature dependent behavior of amorphous and semicrystalline polymers*, Polymer Engineering and Science, 32, 1055-1065, 1992.

[45] S.Hillmansen, S. Hobeika, R.N. Haward, P.S. Leevers, *Polymer Engineering and Science*, 40, 481-488, 2000.
[46] S. Hobeika, Y. Men, G. Strobl, *Temperature and strain rate independence of critical strains in polyethylene and poly (ethylene-co-vinyl acetate)*, Macromolecules, 33, 1827-1833, 2000.
[47] Q. Fu, Y. Men, G. Strobl, *Understanding of the tensile deformation in HDPE/LDPE blends based on their crystal structure and phase morphology*, Polymer, 44, 1927-1933, 2003.
[48] A. Rozanski , A. Galeski, *Plastic yielding of semicrystalline polymers affected by amorphous phase*, International Journal of Plasticity,41, 14–29, 2013.
[49] M. Sebaa, C. Servens, J. Pouyet, *Natural and Artificial Weathering of Low-Density Polyethylene (LDPE) : Calorimetric Analysis*, J. Appl. Polym. Sci., 47, 1897, 1993.
[50] S. F. Chabira, M.Sebaa, C. G'sell, *Influence of climatic ageing on the mechanical properties and the microstructure of low-density polyethylene films*, J. Appl. Polym. Sci.,110, 2516, 2008.
[51] A. Tidjani, *Comparison of formation of oxidation products during photo-oxidation of linear low density polyethylene under different natural and accelerated weathering conditions*, Polym. Degrad. Stab., 68, 465, 2000.
[52] S. F. Chabira, M.Sebaa, C. G'sell, *Oxidation and crosslinking processes during thermal aging of low-density polyethylene films*,J. Appl. Polym. Sci., 124, 5200–5208, 2011.
[53] O.Al Othman, S. Faiz, and M. A. Tuasikal, *Study of natural and accelerated weathering on mechanical properties of antioxidants modified low density polyethylene films for greenhouse*, International Journal of Polymer Science, 543930, 2014.
[54] F.P. La Mantia, M.C. Mistretta, M. Ceraulo, P. Koci, *Effect of the orientation on the photooxidation behaviour of polymer films*, European Polymer Journal, 83, 129-137, 2016.
[55] F.Sitek, J.E. Guillet, Journal of polymer science. Symp. N° 57, 343-355, 1976.
[56] F.Severini, R.Gallo, S.Ipsale, *Weathering Effects on the Microstructure Morphology of Low Density Polyethylene*, the arabian journal for science and enginnering, 13,4, 533-543, 1988.
[57] F.H. Winslow, W. Materyek, and A.M. Trozzolo, *weathering of polymers*, soc.plast.Eng.18:766-772, 1972.
[58] S. F. Chabira, M. Sebaa, R. Huchon, B. De Jeso, *The changing anisotropy character of weathered low-density polyethylene films recognized by quasi-static and ultrasonic mechanical testing*, J. Polym. Degrad. Stab. 2006, 91, 1887.
[59] S.Halim Hamid, M.B. Amin, A.G.Maadhan, *handbook of polymer degradation*, Mercel Dekker,Inc.
[60] Nielsen, L. E., *The Stress Dependence of Creep of Polyethylenes*, J. Appl. Polym. Sci. 1969, 13, 1800.
[61] Cowking, A., *Tensile creep and deformation mechanisms in oriented low-density polyethylene*, J. Mater. Sci. 1975, 10, 1751.
[62] Klein, P. G.; Woods, D. W.; Ward, I. M., *The Effect of Electron Irradiation on the Structure and Mechanical Properties of Highly Drawn Polyethylene Fibers*, J. Polym. Sci: Part B: Polym. Phys. 1987, 25, 1359.
[63] Ohta, Y.; Sugiyama, H.; Yasuda, H., *Short Branch Effects on the Creep Properties of the Ultra-High Strength Polyethylene Fibers*, J. Polym. Sci: Part B: Polym. Phys. 1994, 32, 261.
[64] Rasburn, J.; Klein, P. G.; Ward, I. M., *The Influence of Short-Chain Branching on the Creep Behavior of Oriented Polyethylene, and Its Effect on the Efficiency of Crosslinking by Electron Irradiation*, J. Polym. Sci: Part B: Polym. Phys. 1994, 32, 1329.

[65] Zhou, H.; Wilkes, G. L., *Creep behaviour of high density polyethylene films having well-defined morphologies of stacked lamellae with and without an observable row-nucleated fibril structure*, J. Polymer 1998, 39, 3597.
[66] Unigovski, Y. B.; Bobovitch, A. L.; Gutman, E. M.; Mogilansky, D., *Effect of Processing and Density on Morphology and Creep Behavior of Linear Low-Density Polyethylene*, Polym. Eng. Sci. 2011, 51, 1642.
[67] I. M. Ward, *Mechanical Properties of Solid Polymers*, John Wiley & Sons, 1983.
[68] H. Leadmann, *Trans. Soc. Rheol.*, 361, **6**, 1962
[69] B. Berstein, E. A. Kearsley and L. P. Zapas, *A study of stress relaxation with finite strain. Trans Soc Rheol, Trans. Soc. Rheol.*, 391, **7**, 1963
[70] K. C. Valanis and R. F. Landel, *Trans. Soc. Rheol.*, 243, **11**, 1967
[71] R. A. Schapery, *On the characterization of nonlinear viscoelastic materials, Polym. Eng. Sci.*, 295, **9**, 1969
[72] I. M. Ward and E. T. Onat, *Non-linear mechanical behaviour of oriented polypropylene , J. Mech. Phys. Solids*, 217, **11**, 1963.
[73] W. N. Findley, J. S. Lai and K. Onaran, *Creep and Relaxation of Nonlinear viscoelastic Materials*, North-Holland Publisher, 1976.
[74] Zhou, Hongyi and Wilkes, G. L., *Orientation-dependent mechanical properties and deformation morphologies for uniaxially melt-extruded high-density polyethylene films having an initial stacked lamellar texture* , J. Mater. Sci., 1998, 33, 287.
[75] R.O.Ebewele, *Polymer science and technology*, 2000 by CRC Press LLC.
[76] C. Devilliers, Ph.D dissertation, *Dégradation chimique du PE et influence sur le comportement, l'endommagement et la rupture en fluage :Application à la durabilité d'une canalisation sous pression*, Paris (France), 2012.
[77] G'Sell C., Dahoun A., Hiver J.M., Poinsot C., IUTAM symposium on micromechanics of plasticity and damage in multiphase materials, *Creep and yield behavior of semicrystalline polyethylene in uniaxial tension*, Sevres, France, 29 August – 1 September, (1995).
[78] J. Lai and A. Bakker, *An integral constitutive equation for nonlinear plasto-viscoelastic behavior of high-density polyethylene.*, Polymer, 36, 93 (1995).
[79] P. J. R. Leblans and W. M. Bastiaansen, *Viscoelastic properties of UHMW-PE fibers in simple elongation*, J. Polym. Sci., Phys. Ed., 27, 1009 (1989).
[80] Y. C. Bhuvanesh and V. B. Gupta, *Interaction between viscoelastic and structural relaxation in drawn polypropylene yarn*, Polymer, 36, 3669 (1995).
[81] L. C. E. Struik, *Physical aging in amorphous* polymers *and other materials.*, Polymer, 28, 1251 (1987).
[82] L. C. E. Struik, *Mechanical behaviour and physical ageing of semi-crystalline polymers* , Polymer, 90, 799 (1989).
[83] Gedde U.W., Jansson J.F., *Effect of orientation on mechanical properties of metallocene polyethylenes*, Polymer Engineering and Science, 19, (1979), 77-81.

CHAPTER 2.0

MORPHOLOGICAL ANALYSIS OF LOW DENSITY POLYETHYLENE FILMS INFLUENCED BY AGEING

Chapter 2.0 MORPHOLOGICAL ANALYSIS OF LOW DENSITY POLYETHYLENE FILMS INFLUENCED BY AGEING

1. Introduction

Polyolefins have been widely used owing to their high performance such as high modulus, high tensile stiffness, high chemical resistance and low cost for processing. Those materials have numerous applications such as cable and wire insulation, food packaging, medical components and many more [1]. One of the most weight consuming applications of this type of material is their use for greenhouses covering. In such an application, polyethylene film is subjected to a variety of environmental stresses, among them one can quote, temperature variation from day to night, sun irradiation, variable wind strength and creep [2, 3]. These environmental parameters can adversely affect the polymer thermal and structural properties. These are due to the microstructural changes undergone by the macromolecular structure mainly governed by chain scissions and cross-linking. The main event in a chemical point of view is the oxidation of the polymeric chains accompanied by the consummation of the existing vinylidene groups (CH_2=C<) and the formation of vinyl groups (CH_2=CH-) [4-6]. The consequences of these chemical changes on the material morphology are an increase of the crystallinity which affects adversely the mechanical properties by making it much more brittle. The structural morphology of polyethylene is an alternance of crystalline and amorphous layers (two-phase system). The oxidation damages are mainly confined in the amorphous phase which is responsible to the cohesiveness of the whole. Also, the damages (chain scissions) caused to the amorphous tie molecules contribute to increase the crystalline concentration. Elsewhere, Chabira et al. [4, 7] have analyzed the morphological changes undergone by LDPE films outdoor exposed in Sub-Saharan region (Laghouat). They have

shown that the short chain segments coming from chain scissions can either contribute to increase the thickness of the existing crystalline lamellae or to nucleate new crystallites.

Film ageing is more a surface phenomenon, where most of the chemical and morphological events take place. In a practical point of view, this means that degradation will follow a concentration profile with a decreasing effect in the direction of the film core.

The aim of this work is to highlight the effect of weathering on the morphology and the surface roughness of films in Sub-Saharan facilities. The variation of the crystallinity degree has been checked by means of DSC and WXRD. This last technique allows also identifying the type of crystalline lattice. Atomic Force Microscopy (AFM) is an effective and reliable method for visualization of the surface topography of PE films. As a matter of fact, the degradation of polyethylene film surface by different types of irradiation, plasma treatment etc…, have been conducted and led to an irremediable modification of the surface morphology by increasing the roughness [8, 9]. However, few or almost no work, who studied the surface modification of naturally weathered low density polyethylene films have been investigated by AFM. Nevertheless, it is a very powerful technique to get a 3D representation of the surface topography and the roughness parameters [9-12].

The analysis and the comparison of the results obtained by these different methods have allowed connecting the impact of the morphological changes of the material to that of the surface topography.

2. Experimental

2.1. Material and exposure

The LDPE utilized in this investigation is a commercial grade supplied by the Saudi Basic Industries Corporation (SABIC) as “LDPE 2100 T N00W”, (ρ_s= 0.92g/cm^3, MFI= 0.33g/ 10min). This polymer is a neat grade exempt of stabilizing agents. Films were produced by

blowing extrusion from the raw material in an Algerian industry (Sofiplast of Sétif). The drawing speed of the production line was fixed to 15 $cm.s^{-1}$. The melt was extruded at about 175°C and blown in a continuous process characterized by a bubble diameter of 4.4 m and a wall thickness of 160 µm. It is known that the properties in the machine direction (MD) depend on the draw down ratio (DDR) and those in the transverse direction (TD) to the blow up ratio (BUR) [13].

The exposition was carried out at Laghouat, Algeria (33° 48'N 2° 52'E) from December to August. The films were mounted on metallic frames, south oriented and inclined by 33° relatively to the horizontal according to the standard NF51-165. Samples were picked up periodically, during all the ageing period, from film zones sufficiently far away from the contact points with the holding frame. This precaution was taken to avoid uncontrolled overheating of the material. The maximum of eight months of exposure corresponds to the time at which the film became too brittle to resist to the wind strength; this corresponds to the limit of the experimental exposure.

2.2. Differential Scanning Calorimetry DSC

A Q2000 DSC apparatus was used to perform the thermal analysis of the non-weathered and weathered samples (two, four, six and eight months of exposure). A few milligrams (10 mg) were taken from the films and pressed in an aluminum pan and the whole is placed in the furnace. Then, they were subjected to a thermal cycle i) heating from 10°C up to 150°C with a heating rate of $10°C.min^{-1}$ ii) the sample is maintained at equilibrium for few second before being subjected iii) to a progressive cooling with a cooling rate of $10°C.min^{-1}$ up to 10°C. The measurements were performed under inert atmosphere (N_2). Indium is used for calibration. The melting temperature was determined at the maximum of the melting peak and the crystallization temperature at the maximum of the re-crystallization peak get from cooling.

The mass-based degree of crystallinity was calculated with reference to the thermodynamic heat of fusion of 100% crystallized polyethylene (ΔH_c= 290 J.g^{-1}). The specific heat (C_p) was determined from the fusion and the re-crystallization peaks respectively [14]. Furthermore, DSC melting endotherms can be used to calculate the lamellar thickness distribution. In this approach, a DSC profile, heat flow versus temperature, is transformed into a lamellar thickness distribution curve by using the Gibbs-Thomson equation expressed as [15]:

$$T_m = T_m^0 \left(1 - \frac{2\sigma_e}{\Delta H_f L}\right) \quad (1)$$

Where T_m^0= 143.5°C is the equilibrium melting temperature of the crystalline lamella of infinite thickness, σ_e= 90 mJ.m^{-2} is the basal surface energy of the crystalline lamella, ΔH_f= 290 J.cm^{-3} is the enthalpy of fusion for the crystalline phase [16].

2.3. Wide angle X-ray diffraction WXRD

The overall percent of crystallinity and crystallite sizes of the unaged and weathered PE samples were determined by WXRD. The X-ray measurements were carried out on a D8 Advance Power diffractometer (Bruker AXS GMBH, Karlsruhe, Germany) and performed at atmospheric pressure and at room temperature with nickel-filtered Cu target Kalpha radiation (λ= 0, 154056 nm) at 40 KV and 40 mA over a range of 2θ = 10-60°. The analyses of the spectra were carried out by means of the Eva 9.0 rev.0© software. The data were collected at a scanning rate of 6°.min^{-1} with a step size of 0.02°.

The mathematical treatment of the XRD data (peaks deconvolution) have been processed by means of the OriginPro 9 software. The overall crystallinity was calculated by the total crystalline peaks areas (A_{cr}) and the total scattering peaks including contribution of the amorphous phases ratio ($A_{cr} + A_{am}$) using the following equation:[17]

$$X_C(\%) = \frac{A_{cr}}{A_{cr} + A_{am}} \times 100 \quad (2)$$

2.4. Atomic force microscopy AFM

AFM analysis was performed on a Universal Scanning Probe Microscope [Nano Navi (E-Sweep)]. The samples are etched in specific chemical solutions. The etching protocol is done in two steps followed by a washing cycle. Each step takes one hour. The first sauce contain 0,7 % wt/v of $KMnO_4$ dissolved in a mixture of concentrated H_2SO_4 and H_3PO_4 in proportion of 2:1, The second sauce contain 1% wt/v of $KMnO_4$ dissolved in a mixture of concentrated H_2SO_4, H_3PO_4 and H_2O in proportion of 10:4:1.

The washing cycle begins with a frozen sauce of H_2SO_4 and H_2O in the proportions 2:7, during 20 minutes, followed by a H_2O_2 (30 %) rinsing during 20 minutes at room temperature. Then the samples are washed in distilled water during 5 minutes at room temperature. Finally, they are dropped during 20 minutes in acetone at room temperature and dried by compressed air.

This etching procedure allows removing only the detached impurities without modifying the material surface structure [18].

The surface morphology observations were conducted in the tapping mode with a constant force of 20 $N.m^{-1}$ and a resonance frequency of 0.15 KHz. From the analysis of the images, the root-mean-squared roughness (R_{rms}), the peak pitch and the average roughness (R_a) for the topographic profiles measured on 0.4×0.4 μm^2 images are evaluated.

Furthermore, to quantify the evolution of the peaks position in the X-range direction with ageing, characteristic of a change of the surface films topography, relevant to microstructural and morphological modifications has been processed as follows. A measure of the peaks distance (named in this work “peaks-spacing” or “$\bar{d}$”) for the image in the X-range direction

and for four different equidistant positions in the Y-range direction has allowed calculating their average values "$\overline{d}$" and that for each ageing time (Fig.2.1), where;

$$\overline{d} = \frac{\sum_{i=0}^{n} L}{n} \quad (3)$$

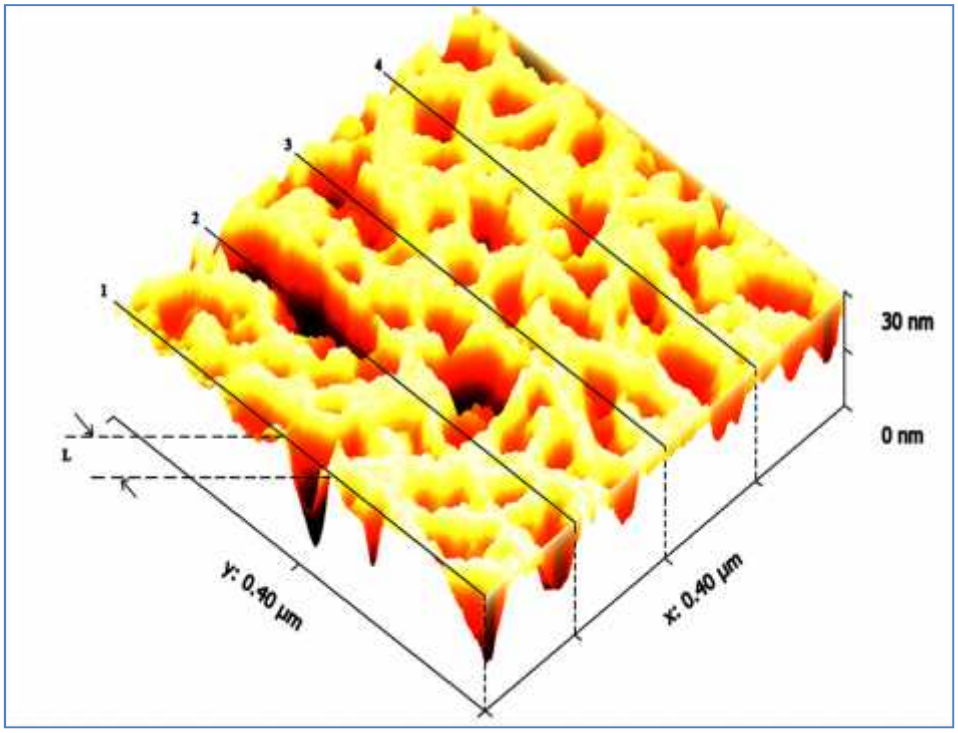

Fig.2.1: Average values of peaks-spacing.

3. Results and discussion

3.1. Ageing effects on the thermal behavior

Figure 2.2 displayed the heating and cooling DSC curves of unaged and weathered LDPE films. It appears that the total heat of fusion and that of re-crystallization slightly increases with ageing. It is still very important to notice that the crystalline concentration obtained initially was restored after ageing during the cooling process. Indeed, it was expected that after melting, the crystallinity history would have been completely lost and the re-crystallization of the aged sample might have delivered a small peak very similar to that of the unexposed sample. The most surprising in the cooling process is that even the transition

temperature (T_r) around 55°C is restored. This means that despite the melting of all the crystallites the material, whatever its ageing stage, it maintains its initial morphology.

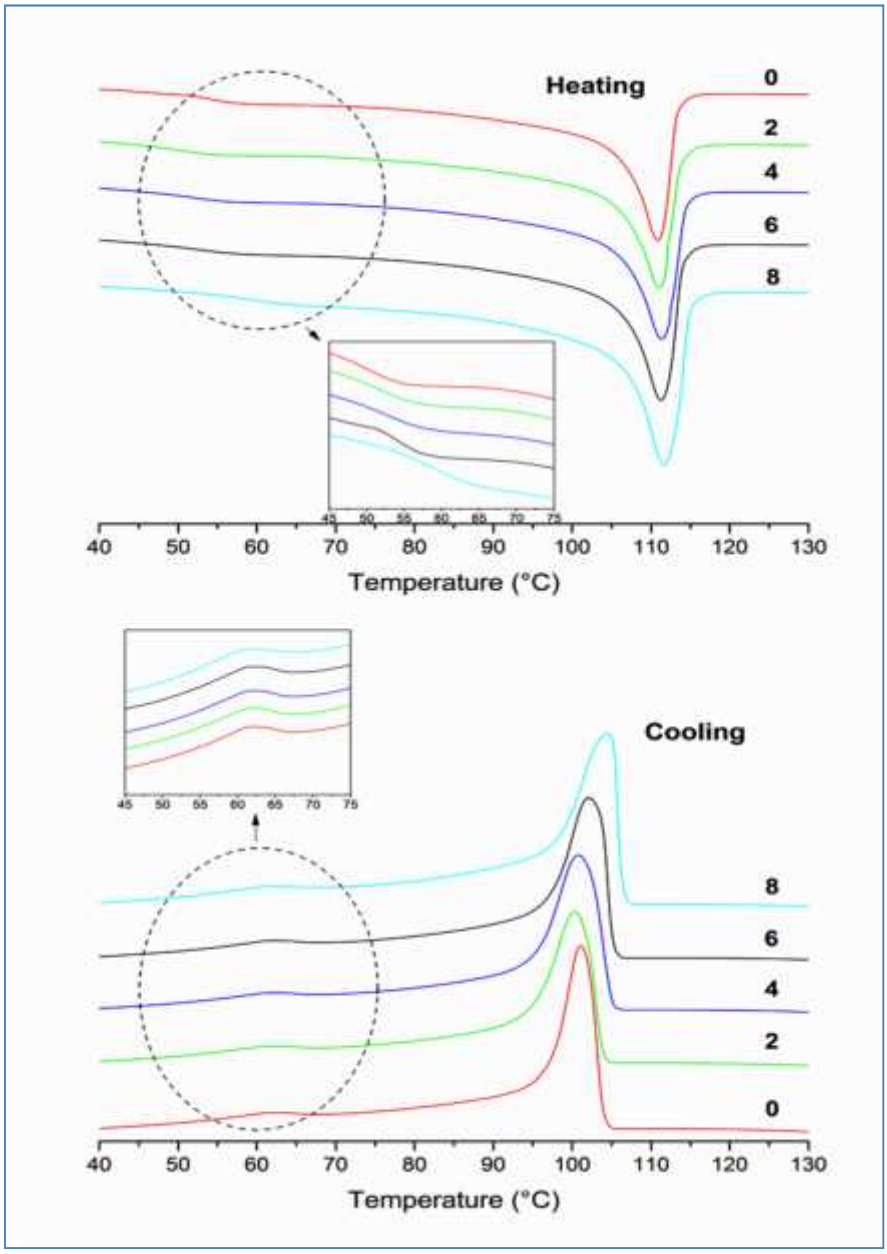

Fig.2.2: DSC heating and cooling curves of unaged and weathered LDPE films.

A comparative approach and an accurate analysis of the changing thermal properties of the material show the impact of ageing on the material morphology. First of all, the melting temperature occurs around 111 °C and increases very slightly with exposure. A transition temperature (T_r) appearing only as a very weak shoulder around 54°C becomes more visible

with ageing and shift to higher values up to 65°C (Table.2.1). According to Pabiot et al.[19], this could correspond to the onset of the melting peak because of the presence of small crystallites nucleated after the diffusion of the small chain segments provided by chain scissions. The melting peak surface is increasing with ageing time and a calculus of the crystallinity shows that it goes from 39.5 % to 51.9 %; meaning a global increase of almost 34%. The same comparison with the cooling process shows that the difference between the initial re- crystallization and that of the most aged one is about 20.6%. This difference could be explained by the fact that, when melting the sample, a partial recombination of the damaged molecular chains could occur increasing as such the average molecular weight. This makes more difficult to the material to recover its original crystallinity degree gained by chain scissions during either the processing and/or ageing process. Indeed, longer macromolecules make difficult chain mobility which favors the secondary crystallization also known as chemo-crystallization process [7].

Table.2.1: Transition temperature of first order, T_m, and of second order, T_r, degree of crystallinity X_c , crystallization temperature, T_c, for unaged and aged LDPE films.

Ageing	**Heating**				**Cooling**			
(months)	T_m	T_r	X_c	C_p	T_c	T_r	X_c	C_p
	$(°C)$	$(°C)$	(%)	$(J.g^{-1}.K^{-1})$	$(°C)$	$(°C)$	(%)	$(J.g^{-1}.K^{-1})$
0	110.9	54.2	39.5	0.29	101.1	62.2	35.9	0.26
2	111.1	54.6	40.9	0.29	100.3	62.1	35.7	0.26
4	111.4	55.5	43.3	0.31	101.2	62.1	37.6	0.27
6	111.3	57.6	44.7	0.32	101.8	62.1	38.8	0.28
8	111.7	65.3	51.9	0.38	104.4	61.7	43.3	0.31

Figure 2.3 reported the lamellar thickness distribution determined thanks to the Gibbs Thomson equation (Equation 1) and it is applied to the DSC melting peaks data. On a statistical point of view each point of the curve corresponds to a lamellar thickness population. Of course the higher population is the one corresponding to the maximum of the curve (i.e. the melting temperature, T_m). An accurate observation of the figure showed that, with the ageing, there is an increase in the intensity of maxima of the curves accompanied by broadening. The right side of the peak shifts towards higher lamellar thickness values. In fact, the maximum of the peak goes from 7.93 nm for the unaged sample up to 8.13 nm for the more aged and the largest lamellar thickness, determined at the end of the peaks baseline goes from 9.01 nm up to 9.49 nm. From these results it can be deduced that short chain segments coming from the chains scission process due to ageing promote as much the thickening of the existing lamellae by their diffusion toward the exiting crystallites as the nucleation of new small ones. Both effects responsible to the global increase of the crystalline concentration are favored either by the incident solar energy absorbed by the film or by warming due to temperature.

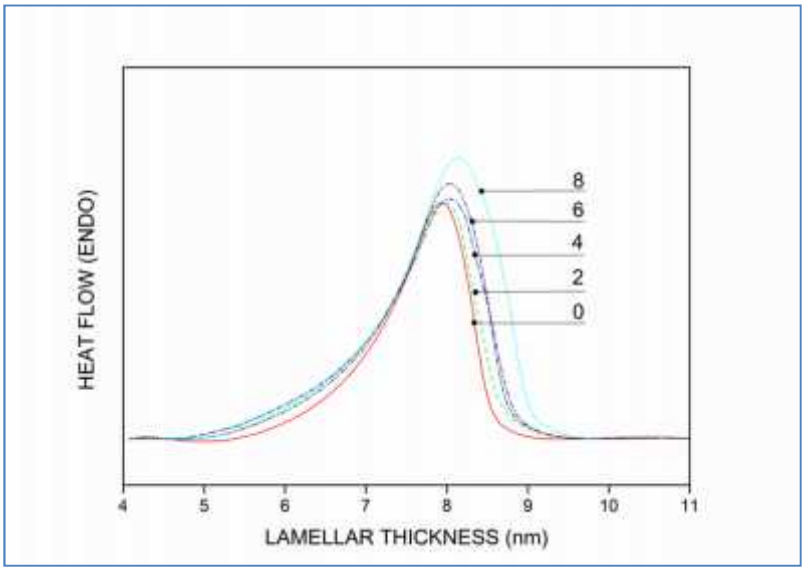

Fig.2.3: Lamellar thickness distribution curves for unaged and weathered LDPE films.

3.2 Crystal structure and unit cell parameters

The WXRD patterns of LDPE films for different ageing stages were represented in Fig.2.4. All the samples showed two distinguishable reflection peaks (110) and (200) at 21.29° and 22.52° respectively, corresponding to the crystallographic plane of the elementary orthorhombic lattice of polyethylene. The diffraction curves are combination of an amorphous halo and crystalline peaks, specific to semi-crystalline polymer. The deconvolution of the peaks and the calculation of their respective area allows to fit the contribution of the crystalline peaks and the amorphous bump (amorphous 'halo') which give access to the crystallinity degree. As a matter of fact it has been observed a sensitive increase of the peak surfaces and their respective maximum.

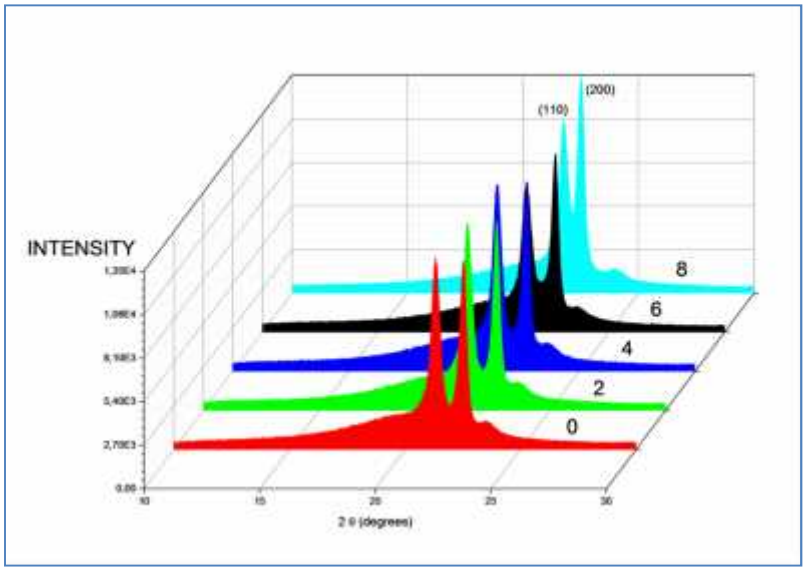

Fig.2.4: The WXRD patterns of LDPE films for different ageing stages.

On the other hand, the crystalline concentration has been calculated using the data of the XRD technique which is based on the optical properties of the material. Comparatively, crystallinity determination by DSC is based on the melting of the whole crystalline structures, displaying a broad enthalpic peak of fusion [7]. Also, the crystallinity concentration as function of ageing time measured by the two methods is expected to be different because of

the distinctive physical principle respective to the two techniques. Indeed, the crystallinity values recorded by the XRD method seem to be a little bit lower to those of DSC (Fig.2.5). For XRD, the crystalline concentration (38.64% at 0 month) tends to remain constant till the sixth month, and then it knows a significant increase at the last stage (45.38% at 8 months). For DSC, crystallinity increases progressively until the last month of exposure.

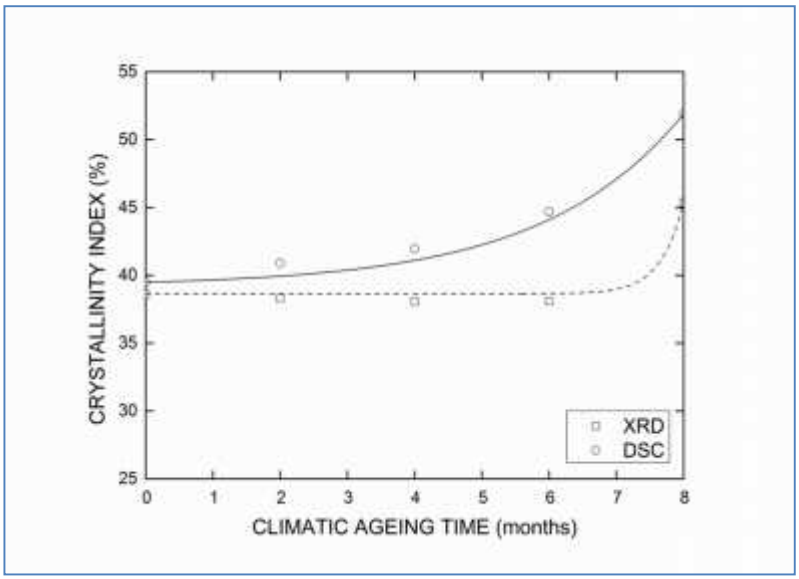

Fig.2.5: Evolution of the crystallinity (X_c) of the LDPE films during climatic ageing.

The unit cell parameters and full width at half maximum (*FWHM*) are reported in Table.2.2. The crystalline peaks of the (110) and (200) planes of the unaged film have d-spacing of 4.17 and 3.95 Å, respectively. These results corroborate with the *FWHM* results. Indeed, the values of *FWHM* generally associated with the internal strains, crystallite size and the perfectness of the polyethylene crystallites change with ageing. If we analyze and compare separately the *FWHM* and d-spacing of each crystallographic plane it appears that they vary differently. The widths of (110) plane diffraction peak become larger, its d-spacing decreases and its peak position shifts to higher values with exposure time. Whereas, the width of the (200) plane diffraction, its d-spacing and its peak position do not change significantly.

From those observations one can deduce that the fact that the 110 crystallographic planes

get closer with ageing and the shift of the peak maximum to higher values of (2θ) accompanied by the broadening of the peak argue in favor of an increase of crystallinity, crystallites size and their perfectness. Therefore, ageing seems to reduce the internal strain because of the progressive chain rearrangement combined to the relaxation of the internal stress acquired during the film processing [20, 21].

Table.2.2: Unit cell parameters of LDPE films for different ageing stages.

Ageing (months)	**(110)**			**(200)**		
	d-spacing			d-spacing		
	2θ	(°$\AA$)	FWHM	2θ	(°$\AA$)	FWHM
0	21.29	4.17	0.47	22.52	3.95	0.37
2	21.35	4.16	0.481	22.64	3.93	0.37
4	21.42	4.15	0.46	22.68	3.92	0.35
6	21.44	4.14	0.52	22.66	3.92	0.37
8	21.76	4.08	0.53	22.50	3.95	0.36

3.3 Ageing effect on the surface morphology

Figure.2.6 reported the AFM 2D pictures and the roughness profile which highlight on the surface topography of the unaged and weathered LDPE films. A cursory observation of the roughness profiles displayed an increase in the peak number and the valley height. As a matter of fact, a rapid sight of the 3D representation of the aged samples supports the previous observation and reveals significant changes of the surface films aspect (Fig. 2.7).

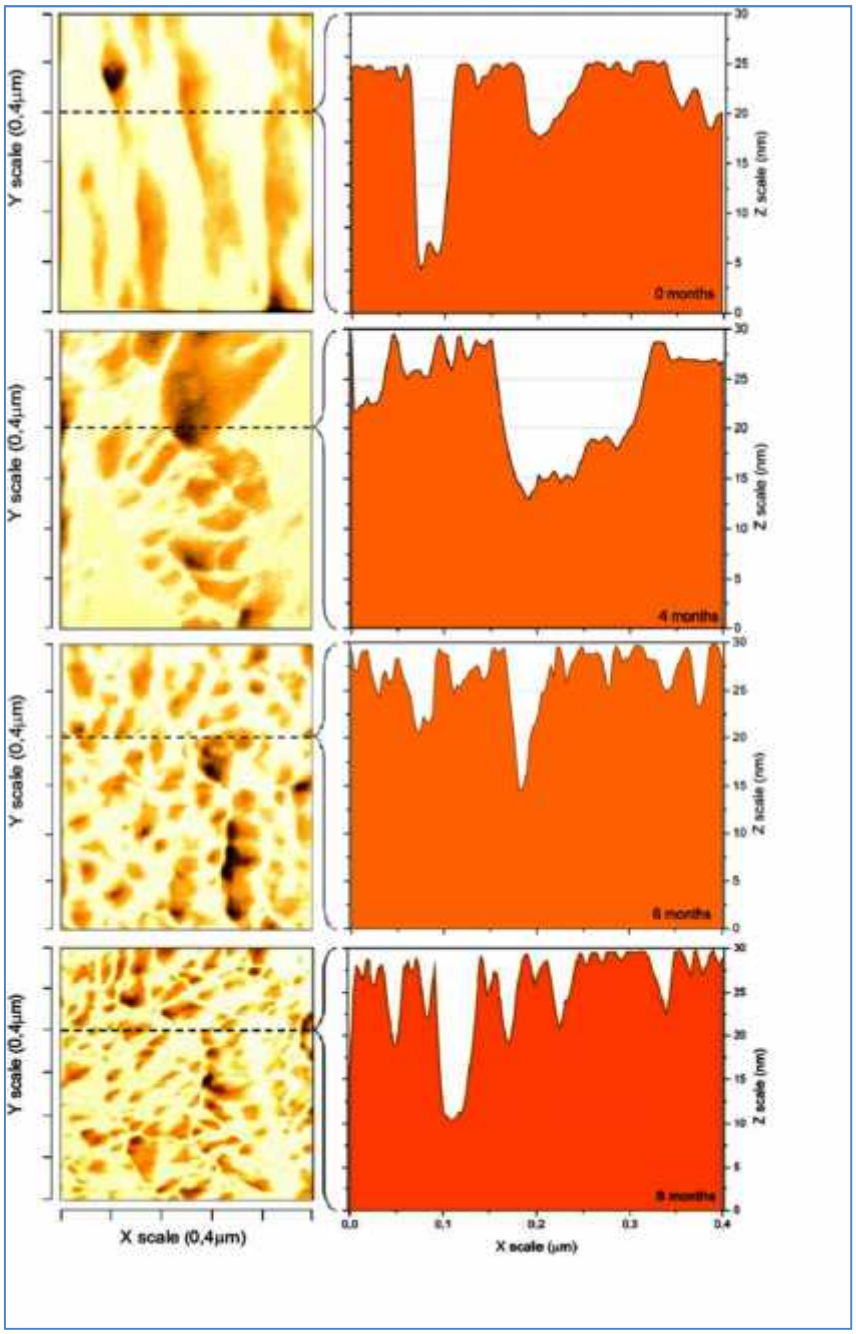

Fig.2.6: AFM 2D roughness profile of weathered LDPE film surfaces for different exposure time.

Table.2.3 reported the roughness parameters determined by the analysis of the topography scans of the sample's surface. The surface profile parameters include average roughness (R_a), the root-mean-squared roughness (R_{rms}), maximum peak to valley height (R_t), for different exposure times. The obtained results illustrate that the variations of the average roughness

values (R_a) and maximum peak to valley height (R_t) values have the same trend as the variations of RMS roughness (R_{rms}) values they all tend to globally increase.

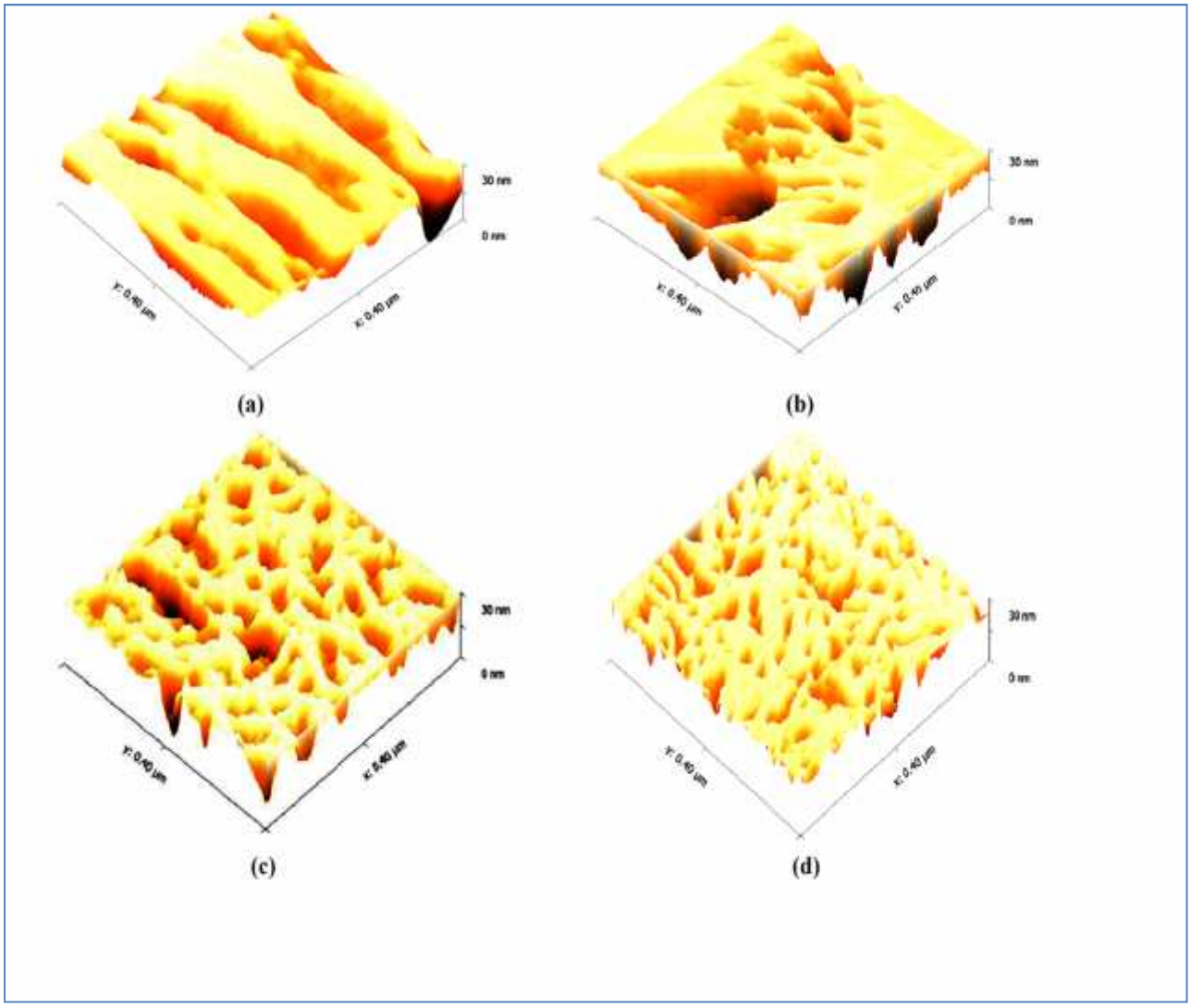

Fig.2.7: AFM 3D topographic representations of weathered LDPE film surfaces for different exposure times: 0, 4, 6 and 8 months.

To make more evident the effect of ageing on the sharpness and the increasing density of the peaks number on the film surface, it has been suggested a method to quantify them and to support the observation.

Table.2.3: Roughness parameters of LDPE films for different ageing time.

Exposure time (months)	R_{rms} **(nm)**	R_t **(nm)**	R_a **(nm)**
0	3.57	14.69	2.78
4	4.42	18.57	3.54
6	4.73	15.15	3.69
8	5.26	23.91	3.13

Also, in figure.2.8 are displayed the variations of the peaks-spacing ($\bar{d}$) and the R_{rms} with ageing time. It can be observed that it decreases progressively and almost linearly with exposure time for the first, while the second increases but likewise linearly. This seems reasonable since these two parameters are logically inversely related. Peaks-spacing follows a regression line which can be expressed by a mathematical equation (-6.49 t + 90.04), this is applicable for the whole range of the exposure time (0-8 months). The same thing is observable for R_{rms} (0.21t + 3.56). Roughness and peak spacing vary inversely and both obey to a mathematic law, thus demonstrating that they are surprisingly linearly related to ageing time.

These results tend to demonstrate that ageing, which is a complex photo-oxidative process accompanied by morphological changes, affects dramatically the surface aspect of the films [22, 4]. Lamantia et al. have demonstrated that film ageing obeys to a gradient of chemical and physical defects along the thickness [22]. As a matter of fact, the crystalline formation being more important at the film surface than in the core this reduces the amorphous zones in favor of the crystalline ones. Therefore this dramatically increases the surface roughness.

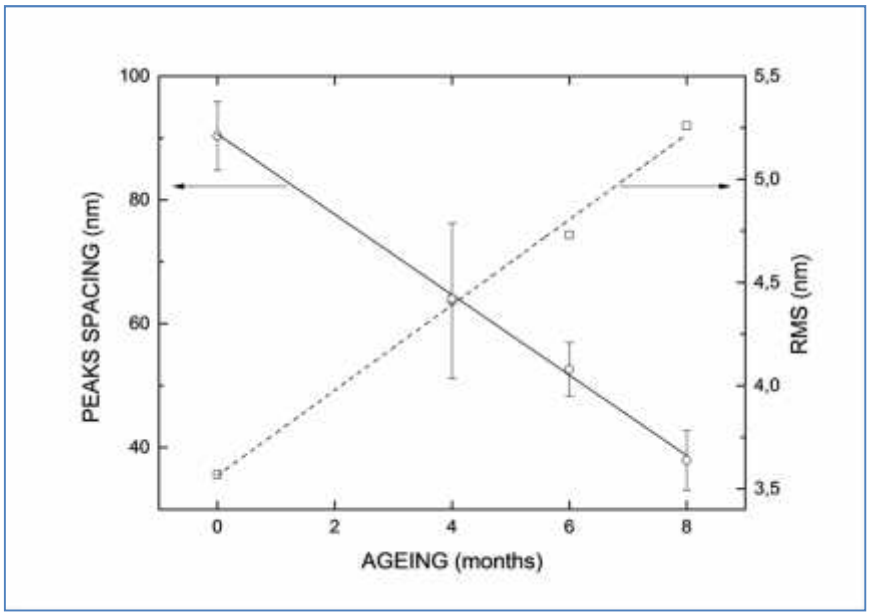

Fig.2.8: Evolution of peaks-spacing $\bar{d}$ and RMS with ageing.

These relations are approved by FESEM cross-section scan. Figures 2.9.a and b present the FESEM micrographs of pristine and altered films. It can be seen clearly the broadening of existing micro-voids and birth of new ones.

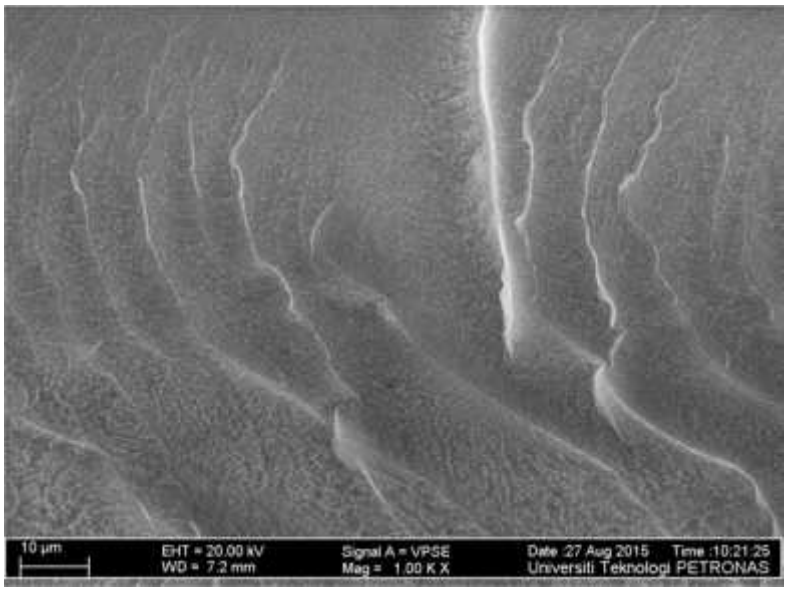

(a)

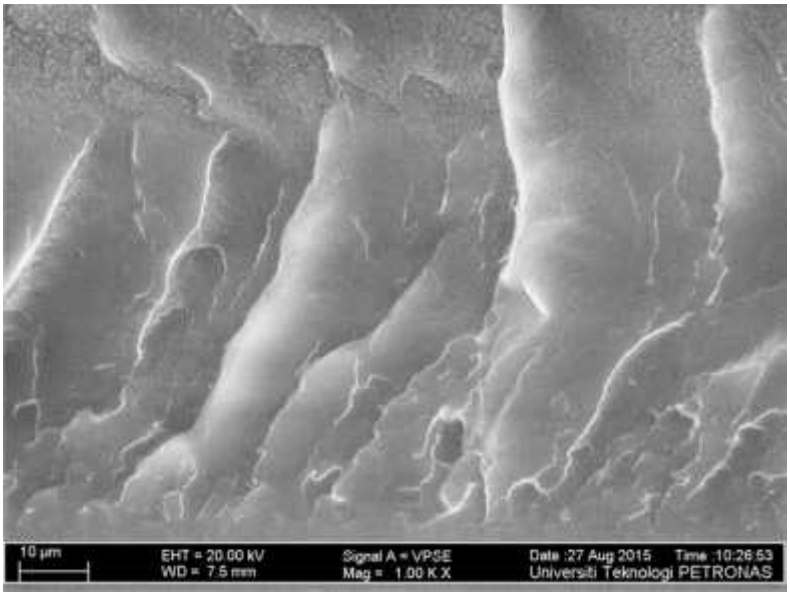

(b)

Fig. 2.9: FESEM micrographs showing surface of unaged (a) and weathered (b) LDPE films. EHT:20kV, magnification x1.00 K.

4. Conclusion

The present work has been concluded with the observation that natural weathering lead to a rapid change of the morphological and surface properties of the studied film.

The complex photochemical mechanism taking place during ageing increases progressively the crystalline concentration by increasing either the lamellar thickness or by nucleating new crystallite via a chemo-crystallization process.

These results corroborate with those of AFM which demonstrate that the surface aspect of the film changes significantly with natural exposure. Indeed, the roughness and the height valley increase in reason of the increase of the surface crystalline zones. This result supports the hypothesis that the material degradation follows a gradient of physicochemical defects from the surface to the core through the film thickness. Surprisingly, it has been found that the peaks-spacing and R_{rms} which logically progress inversely, followed an evolution that obeys to linear mathematical relationships.

References

[1] Friedmen, M. and Walsh, G., High Performance Films: Review of New Materials., *J. Mater. Sci.* **2002**, 42, 1756-1788.

[2] Mendes, L. C., Rufino, E. S. 0., De Paula, F. O. C. and Torres, Jr. A. C., Mechanical, thermal and microstructure evaluation of HDPE after weathering in Rio de Janeiro City., *Polym. Degrad. Stab.* **2003**, 79, 371-383.

[3] Puig, C. C., Albano, C., Laredo, E., Quero, E. and Karam, A., Thermal characterization of the HDPE/LDPE blend (10/90) irradiated using g-rays., *Nucl. Instruments. Methods. Phys. Res. Sect. B: Beam. Interact. with. Mater. Atoms.* ***2010***, 268, 1466-1473.

[4] Chabira, S. F., Sebaa, M. and G'sell, C., Influence of climatic ageing on the mechanical properties and the microstructure of Low-Density Polyethylene films., *J. Appl. Polym. Sci.* **2008**, 110, 2516-2524.

[5] Chabira, S. F., Sebaa, M. and G'sell, C., Oxidation and Crosslinking Processes During Thermal Ageing of Low-Desnity Polyethylene Films., *J. Appl. Polym. Sci.* **2012**, 124, 5200-5208.

[6] Singh, R., Samra, K. S., Kumar, R. and Singh, L., Proton (3 MeV) and copper (120 MeV) ion irradiation effects in low-density polyethylene (LDPE)., *Radiat. Phys. Chem.* **2008**, 77, 53-57.

[7] Chabira, S. F., Sebaa, M., Huchon, R. and De Jeso, B., The changing anisotropy character of weathered low-density polyethylene films recognized by quasi-static and ultrasonic mechanical testing., *Polym. Degrad. Stab.* **2006**, 91, 1887-1895.

[8] Hirotsu, T., Ketelaars, A. A. J. and Nakayama, K., Plasma surface treatment of PCL/PC blend sheets., *Polym. Eng. Sci.* **2000**, 40, 2324-2331.

[9] Sanchis, M. R., Blanes, V., Blanes, M., Garcia, D. and Balart, R., Surface modification of low density polyethylene (LDPE) film by low pressure O2 plasma treatment., *Eur. Polym. J.* **2006**, 42, 1558-1568.

[10] Ortiz-Magán, A. B., Mercedes Pastor-Blas, M., Ferrándiz-Gómez, T. P., Morant-Zacarés, C. and Martín-Martínez., Surface modifications produced by N2 and O2 RF plasma treatment on a synthetic vulcanized styrene-butadiene rubber., J. M. *Polym.* **2001**, 6, 81-105.

[11] Park, S. C., Koh, S. K. and Pae, K. D., Effects of surface modification by Ar+ irradiation on wettability of surfaces of poly(ethylene terephthalate) films., P*olym. Eng. Sci.* **1998**,

38, 1185-1192.

[12] Wickson, B. M. and Brash, J. L., Surface hydroxylation of polyethylene by plasma polymerization of allyl alcohol and subsequent silylation., C*olloids. Surfaces. A: Physicochem. Eng. Asp.* **1999**, 156, 201-213.

[13] Yilmazer, U., Effects of the processing conditions and blending with linear low-density polyethylene on the properties of low-density polyethylene films., J. *Appl. Polym. Sci.* **1991**, 42, 2379-2384.

[14] Medel, F. J., García-Álvarez, F., Gómez-Barrena, E. and Puértolas, Ja., Microstructure changes of extruded ultra high molecular weight polyethylene after gamma irradiation and shelf-aging., *Polym. Degrad. Stab.* **2005**, 88, 435-443.

[15] Huang, X., Jiang, P., Kim, C., Duan, J. and Wang, G., Atomic Force Microscopy Analysis of Morphology of Low Density Polyethylene influenced by Al Nano-and Microparticles., *J. Appl. Polym. Sci.* **2008**, 107, 1763-1772.

[16] Zhou, H. and Wilkes, G. L., Comparison of lamellar thickness and its distribution determined from DSC, SAXS, TEM and AFM for high-density polyethylene films having a stacked lamellar morphology., *Polymer.* **1997**, 38, 5735-5747.

[17] Mo, Z. and Zhang, H., The Degree of Crystallinity in Polymers by Wide-Angle X-Ray Diffraction (Waxd) ., *J. Macromol. Sci. Part C: Polym. Rev.* **1995**, 35, 555-580.

[18] Hamoudaa, H.B.H., Simoes-betbedera, M., Grillona, F., Blouetb, P., Billonc, N. and Piquesa, R., Creep damage mechanisms in polyethylene gas pipes., *Polymer.* **2001**, 42, 5425-5437.

[19] Pabiot, J. and Verdu, J., The change in mechanical-behavior of linear-polymers during photochemical aging., *J. Appl. Polym. Sci.* **1981**, 21, 32-38.

[20] Lyulin, A. V., Hudzinskyy, D., Janiaud, E. and Chateauminois, A. *J. Non. Cryst. Solids.* **2011**, 357, 567-574.

[21] Flores, A., Ania, F. and Baltá-Calleja, F., From the glassy state to ordered polymer structures: A microhardness study., J. *Polymer*. **2009**, 50, 729-746.

[22] La Mantia, F.P. and Gardette, J.L., Improvement of the mechanical properties of photo-oxidized films after recycling., *Polym. Degrad. Stab.* **2002**, 75, 1-7.

CHAPTER 3.0

ORIENTATION DEPENDENCE OF MECHANICAL PROPERTIES AND DEFORMATION MORPHOLOGIES FOR BLOWN EXTRUDED LOW DENSITY POLYETHYLENE FILM

Chapter 3.0 ORIENTATION DEPENDENCE OF MECHANICAL PROPERTIES AND DEFORMATION MORPHOLOGIES FOR BLOWN EXTRUDED LOW DENSITY POLYETHYLENE FILM

3.1. Introduction

Polymers represent a very important and still rapidly growing class of engineering materials. Among them, semicrystalline polymers such as polyethylene films used for greenhouses covering are of particular interest. Solid state processing techniques, such as stretching films, depend upon the plastic deformation characteristics of the given polymer. During solid state processing, macromolecular chains are often preferentially oriented along a specific direction, e.g. the machine direction, so that the final products possess the desired properties at this particular orientation, this generally being the loading direction in most applications. From an engineering point of view, in order to optimize the material properties during their service, it is important to understand the physical orientation process and how it can affects the material response when subjected to mechanical solicitation, therefore to be able to choose the optimal orientation. On the other hand, the lifetime is also an interesting topic for fundamental research. Thus, it is not surprising that there has been a tremendous amount of research that has been focused on this area [1-11].

Semicrystalline polymers that crystallize under quiescent conditions often have a spherulitic morphology. For these unoriented semicrystalline polymers, there are three basic levels of microstructures that are important in the deformation process [13]: i) the 2 to 20 level, which represents the interactions between neighboring chain segments in both the crystalline phase and the amorphous phase; ii) the 100 to 300 level, which represents the thickness of the crystalline lamellae and of the amorphous layers between the crystalline lamellae; iii) the 0.5 to 100 mm level, which represents the dimension of larger scale superstructures such as spherulites, which are complex arrangements of crystalline lamellae and amorphous regions. Therefore, semicrystalline polymers possessing a spherulitic morphology must be regarded as microstructural and mechanical complex systems, as depicted in Fig. 3.1 (according to ref.13), in which all the three levels of structure influence the deformation process. Certainly, there are cases where all the above three levels are not always present such as, for example, semi-crystalline polymers that have already undergone extensive drawing.

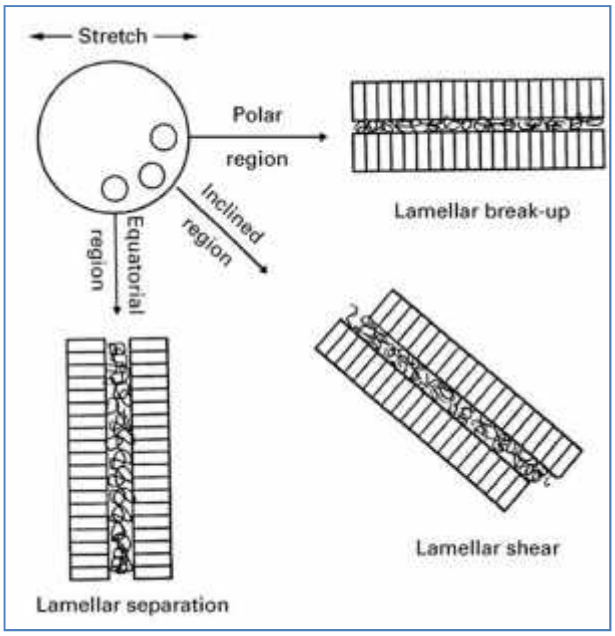

Fig.3.1: A schematic drawing that shows the complexity in the deformation of spherulitic morphology.

The study now presented is divided on two parts, the first one goal to check the orientation and ageing effect on the displacement plans of low density polyethylene films by means of an extensometer realized in the laboratory and using a camera which follows the displacement of drawn lines for defined extension rates. The methodology and the results achieved in three directions are presented. This is also accompanied by a brief description of the stretching rate effect on the lateral contraction in different direction. Furthermore, the ageing effects on the longitudinal extension and its lateral contraction have been studied. The second part deals with the microscopic morphologies, developed during the deformation, which have been related to the macroscopic properties, as measured by direct tensile tests. The mechanical properties have been explained by the development of the deformation induced morphologies. The specific morphological features of these films also allowed us to carry out plastic deformation at different orientations with respect to the original machine direction; it is possible therefore, to present a model structure-property study about the effect of orientation on the deformation morphology and the mechanical properties. In addition, the following of tensile tests on the weathered samples allowed us not only to check the mechanical properties during their service, but also to choose optimal tensile resistance direction.

3.2 Experimental

***Plans deformation and lateral contraction*:**

The lateral contraction results for all the samples were obtained by using a mechanical device at room temperature. The apparatus is constituted by two clamps one is fixed and another movable. The moving part is monitored by concentric bars and the displacement of the mobile clamp is controlled by a screw. Both clamps are covered with rubber to help clamping and to prevent samples slippage during deformation. Rectangular samples of $110mm \times 10mm$ were used for tests, with a calibrated portion of length L_0 = 80 mm, W_0 = 10 mm and thickness T_0 = 0.16 mm. They were cut directly from the LDPE films at one of tree angles, 0°, 45°, and 90° deformations accordingly, corresponding to MD, TD/2, and TD respectively. Different marks are placed on the right and the left of the middle of the sample to follow the material deformation by optical measurements. "r_i" is defined as the distance between the middle and marks situated on the right of the middle sample. The distance "l_i" is the distance between the middle and the marks situated on the left of the middle sample. At a selected distance, a fixed camera is placed above the montage to keep the same test conditions for all the tests. The picture resolution is set at its maximum (7.2 mega pixel); this allows a maximum magnification for further treatment and for the calculations of the elongation and the deformation. The pictures obtained are treated then using Matlab. Hence, the optical measurements results are converted from pixel to millimeter. The use of this software allows a physical measurement with fairly good accuracy. Samples are subjected to strain rates ranging from 0 to 50% of the initial length. The sketch of Fig.3.2 shows the motion of the marks measured on the photograph of a sample subjected to a mechanical stress under an overall strain rate of 8%. Fig.3.3 shows the photograph of sample placed in the device before and after stress.

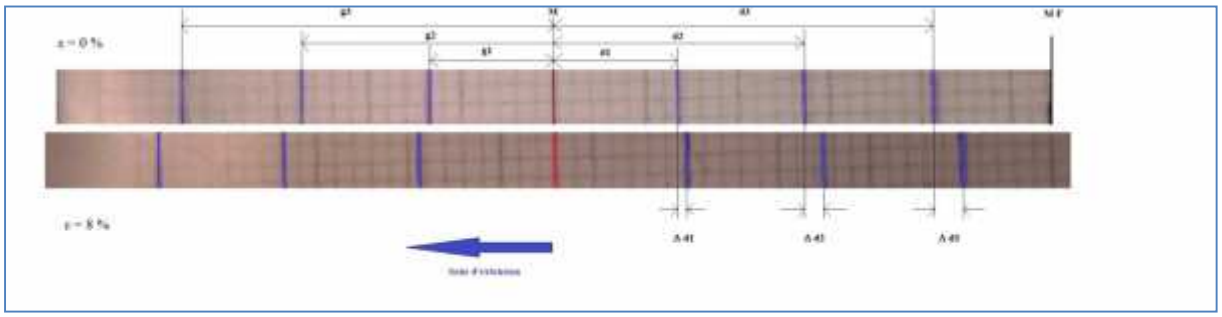

Fig.3.2: Sample subjected to a mechanical stress under an overall strain rate of 8% (initial distance between the drawn lines = 10 mm).

We defined in this study the true strain as [14, 15]:

$$\varepsilon_i = Ln\frac{L_i}{L_{i0}} \quad (3.1)$$

So in our case, for both sides of the specimen the deformation between markers is defined as $\varepsilon_{ri} = Ln\frac{L_{rij}}{L_{ri}}$ for the right side; $\varepsilon_{li} = Ln\frac{L_{lij}}{L_{li}}$ for the left side. Where $i = 1, 2\ and\ 3$ represent the increasing distance from the center. $j = 0, 1, 2 \ldots etc$; is an index indicating de degree of the applied strain (4, 8,…., 50%).

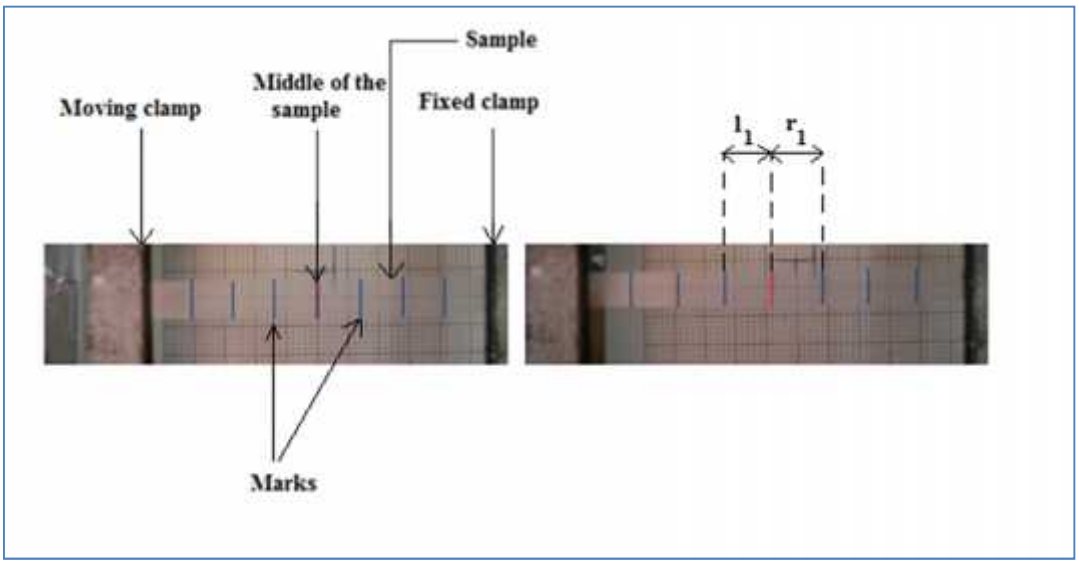

(a) (b)

Fig.4.3: Clamped sample in the device, (a): before deformation, (b): after deformation.

However, marks displacement and their relative true strains are measured. Furthermore, lateral contraction of samples subjected to controlled deformation rates has also been carried out. Such measurements are very useful to calculate then the Poisson's ratio which is the lateral contraction per unit breadth divided by the longitudinal extension per unit length [16]. Therefore, the thickness of the specimen decreases according to equation [4].

$$h = h_0(1 - \upsilon\varepsilon) \quad (3.2)$$

Where: h_0: initial thickness of the film;
h: thickness of the film after stretching;
υ: Poisson's ratio;
ε: true strain.

Knowing that the sample width varies proportionally with the thickness; for that purpose we tried to see the response of the relative width according to the true relative strain, since there is an inverse relationship between length and width deformations when stretching the material, we can write then:

$$l/l_0 = 1-\upsilon\varepsilon \qquad (3.3)$$

Where: l_0: initial width of the film;
l: film's width after stretching.

To optimize the accuracy of the measurements for each curve an average of 5 test pieces has been tested and this for all directions. Also the curves presented in this work have been plotted with these average values. The standard deviation for each point around the average value never exceeded 5%.

***Mechanical properties and plastic deformations*:** The stress-strain curves for all the samples were obtained by using a Roell zwik machine (Fig.4.5) at room temperature (T=21°C, ± 1°C) at a nearly constant relative humidity (RH=50%, ± 5%). The test pieces were cut out from the original and the aged films. The dimensions of the rectangular test pieces were 70 mm × 10 mm, with a calibrated portion of length L_0 = 40 mm, W_0 = 10 mm and thickness T_0 = 0.16 mm. The results of the tensile test are presented in terms of true stress, $\sigma = F(1+\varepsilon)/A_0$, and true strain $\varepsilon(t) = \ln(L(t)/L_0)$. To optimize the duration of the test the strain rate was fixed at a low value to the yield point ($d\varepsilon/dt = 3 \times 10^{-4}\ s^{-1}$) (determination of the Young modulus) and then stepped to a higher value ($d\varepsilon/dt = 3 \times 10^{-2}\ s^{-1}$) for the rest of the test until fracture occurred. To check the anisotropy of the film the test pieces were cut and tested in the two main directions corresponding to the machine direction (MD) and the transverse direction (TD).

Fig.3.5: LDPE samples under tensile test.

Tensile tests on LDPE films aim to i) to determine to determine the characteristics of the material relating to the viscoelastic domain: Young's modulus (E), yield stress ($\pm_y$) and strain ($£_y$), These input data will be used to better understand the behavior of PE at short time, particularly; during the loading phase of creep tests. The stress range over which will be performed creep tests, is also determined from the tensile tests, which will be addressed later in chapter 5.0 ii) to determine the break stress ($\pm_b$) and strain ($£_b$) and its variation with ageing. Additionally, the strain rate effect on deformations in the elastic domain from stress-strain curve has been addressed.

3.3 Results

3.3.1 Unexposed LDPE

Measurement of the film planes displacement for different strain rates: Reported in Table 3.1 the distance variation (Δr_i and Δl_i) for different strain rates. The values represent the increasing distance between the marks relative to their initial distance. As the Fig.3.2 shows, the displacement of the ink marks is parallel which means that the film's planes deform in parallel to each other.

Table 3.1: Marks distances for different strain rates from the elastic domain for the unaged LDPE films (2100 T N00W) investigated.

Strain rate "*j*" (%)	4			8			12			16		
Orientation	MD	TD	45°	MD	TD	45°	MD	TD	45°	MD	TD	45°
Δr_1^j	0.46	0.49	0.62	0.67	1.08	0.92	0.99	1.54	1.72	1.33	1.76	2.03
Δl_1^j	0.52	0.49	0.54	0.65	1.08	0.82	1.02	1.54	1.43	1.30	1.76	1.83
Δr_2^j	0.37	0.54	0.51	0.68	0.72	1.13	1.03	0.93	1.64	1.44	2.06	2.09
Δl_2^j	0.45	0.49	0.57	0.74	0.64	1.02	0.95	0.86	1.33	1.4	1.69	1.51
Δr_3^j	0.57	0.08	0.45	0.85	0.41	0.97	1.30	0.99	1.27	1.55	0.99	1.67
Δl_3^j	0.48	0.16	0.10	0.61	0.49	0.43	0.81	0.82	0.72	0.99	0.84	1.17

Relative true strain: Shown on Figs.3.6 at three orientations (0°, 45° and 90°) the variation of the relative true strains($\ln(d_i^j \; d_{i0})$) of the film planes situated on the right [$\ln(r_i^j \; r_{i0})$] and the left [$\ln(l_i^j \; l_{i0})$] for an overall strain rate "*j*" of 50% from its original length. As expected, these curves showed a distinct orientation dependence of the relative true strain. The growth of the curves for the three different distances (*r* and *l*) is almost linear.

For the 0° stretch, the samples displayed almost the same true strain in both sides ε= 40% so it decrease by 5% in l_2 and l_3. For the 45° stretch, the film behaves similarly to the 0° with higher values, the difference is about of 10% in the different part of the specimen. The relative true elongations of the film for 90° stretch are similar in behavior to 0° and 45°deformation direction with intermediary rates except in "r_2" and "l_2" which rise to higher values at the end of test ~80% and 50% respectively. However, the deformations in the right side are more pronounced whatever the stretching direction is.

The film planes deformation for all orientations can be illustrated by the following equation:

$$\varepsilon(t) = \sum_{\substack{i=1 \\ j=0}}^{\substack{i=3 \\ j=n}} ([\Delta d_i^j / d_{i0}] \times 100/3) = [(L - L_0)/L_0] \times 100 \qquad (3.4)$$

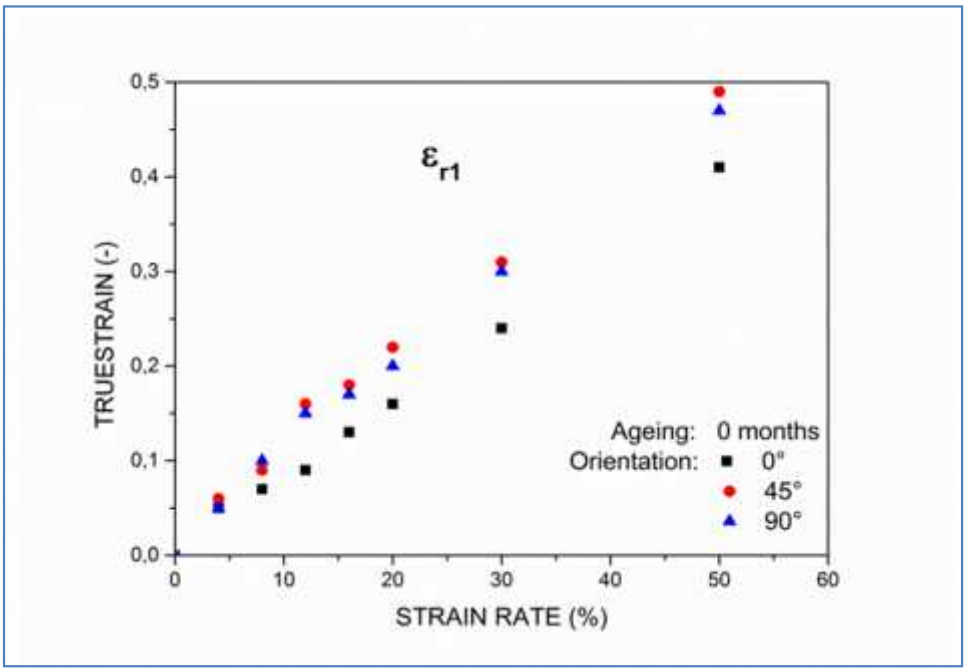

(a)

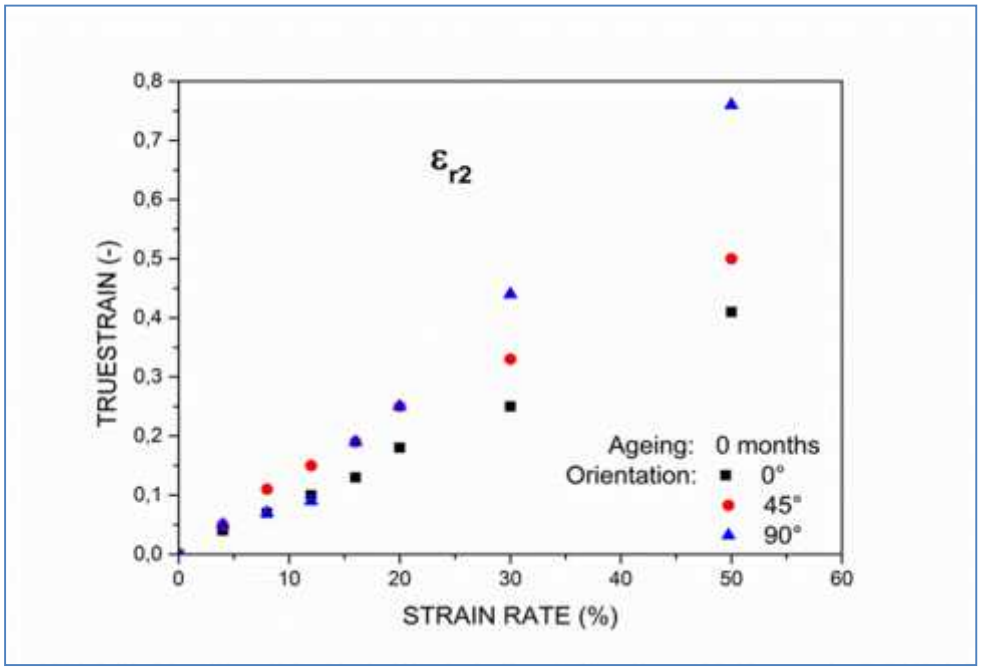

(b)

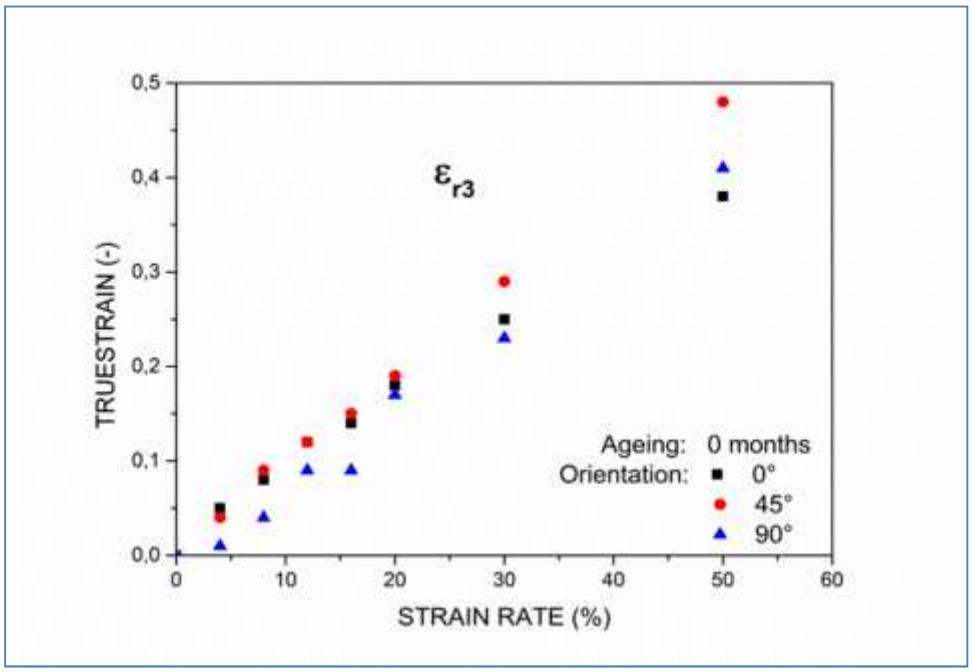
ε_{r3}
TRUESTRAIN (-)
STRAIN RATE (%)
Ageing: 0 months
Orientation: 0°
45°
90°

(c)

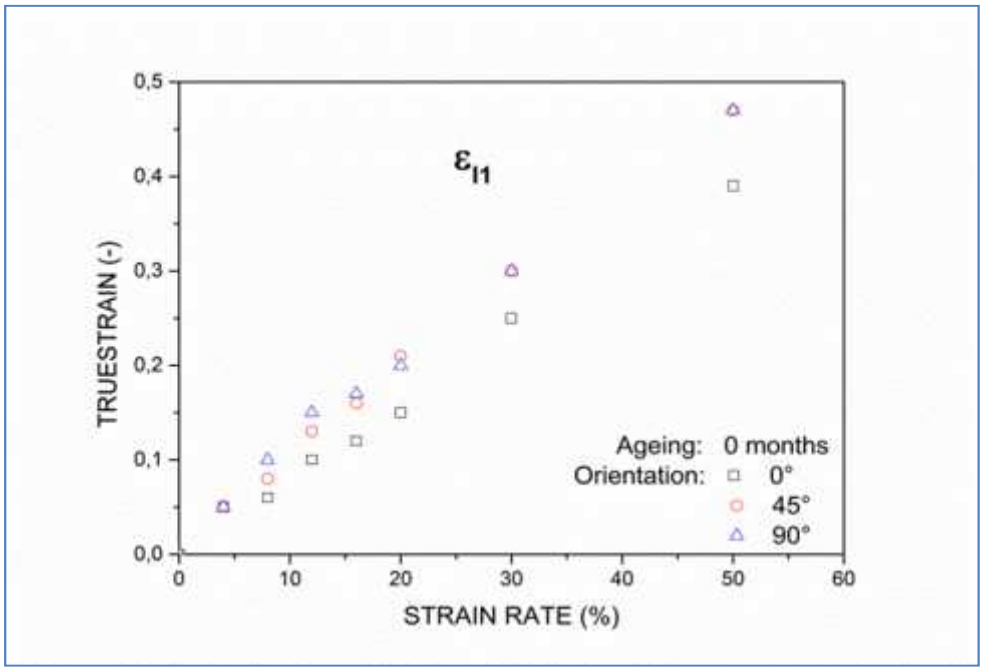
ε_{l1}
TRUESTRAIN (-)
STRAIN RATE (%)
Ageing: 0 months
Orientation: 0°
45°
90°

(d)

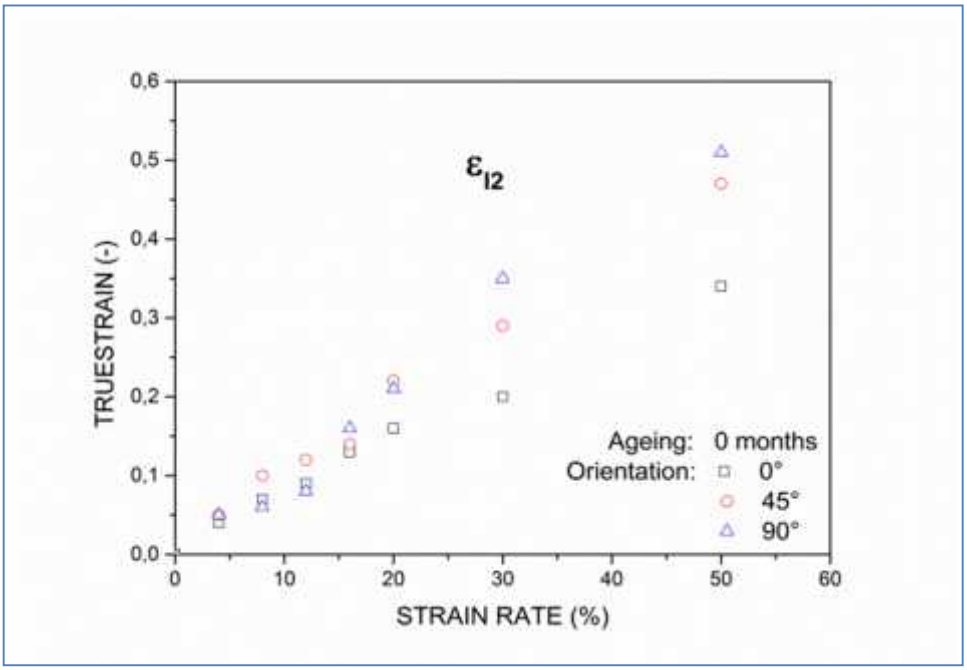

(e)

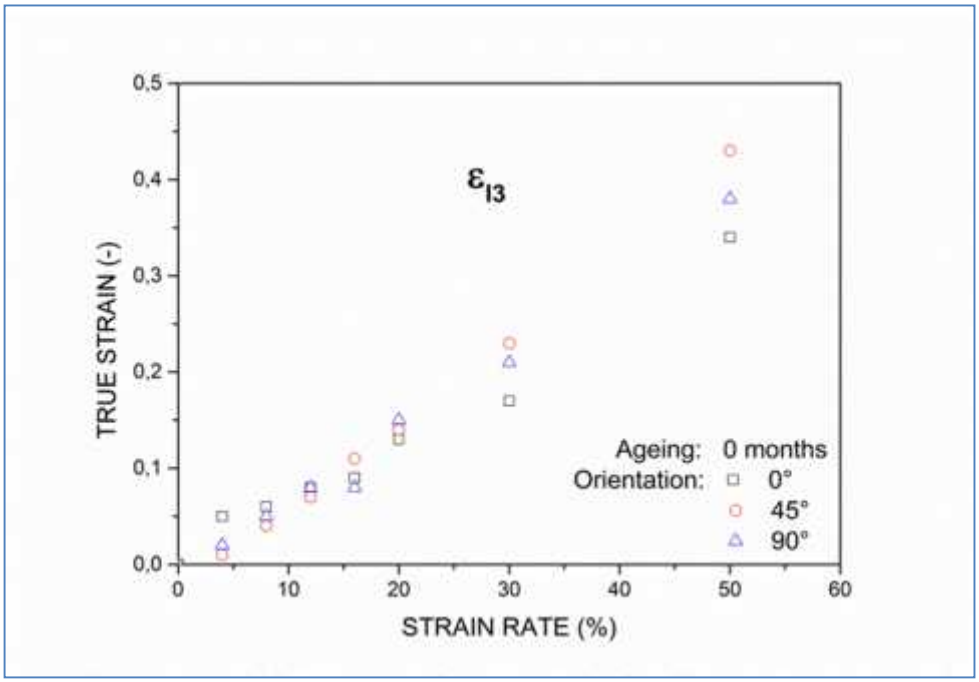

(f)

Fig.3.6: Relative true strain versus strain rate; (a-c): Right side, (d-f): Left side for the LDPE films at three directions of 0°, 45° and 90°.

Lateral contraction during stretching: The lateral contraction response of the film in the three directions are presented in Figures 3.7 where lateral contraction is plotted against true strain in the interval of strain rate: $j \in [0 - 16]$. For both sides the decreasing variation of the width is almost linear (i.e; left and right and for all the marks) with a negative slopes (-υ). These data, by their side, highlight the orientation dependence to the film deformation, with the 0° deformation being the least in terms of elongation and contraction, followed by the 90° and finally the 45° orientation displaying the higher elongation and contraction. This is maybe due to the molecular chains rearrangement of the polymer in equilibrium state. Data presented in these figures have been well reproduced by using another set of samples at each of the orientation angles.

The lateral contraction measurement in the middle of the sample, indicated M in the graph, allows the lateral contraction rate comparison between the two sides. For the 0°stretch, the lateral contraction rate for different parts of sample is almost the same, farther from mobile clamp lower in contraction. For the 45° stretch, the lateral contraction is more important between M and r_1. Regarding the 90° stretch, samples displayed a significant contraction in the middle.

Furthermore, the Poisson's ratio value (-υ) determined from these graphs for different strain rates is (-0.33) whatever the stretching direction. This value is consistent with literature [17], when the material is subjected to deformation; the atoms are moved away from their equilibrium position; we can say then that the material obeys the plans mechanism, i.e. that all points of mobile elements describe a movable curves situated in parallel plans.

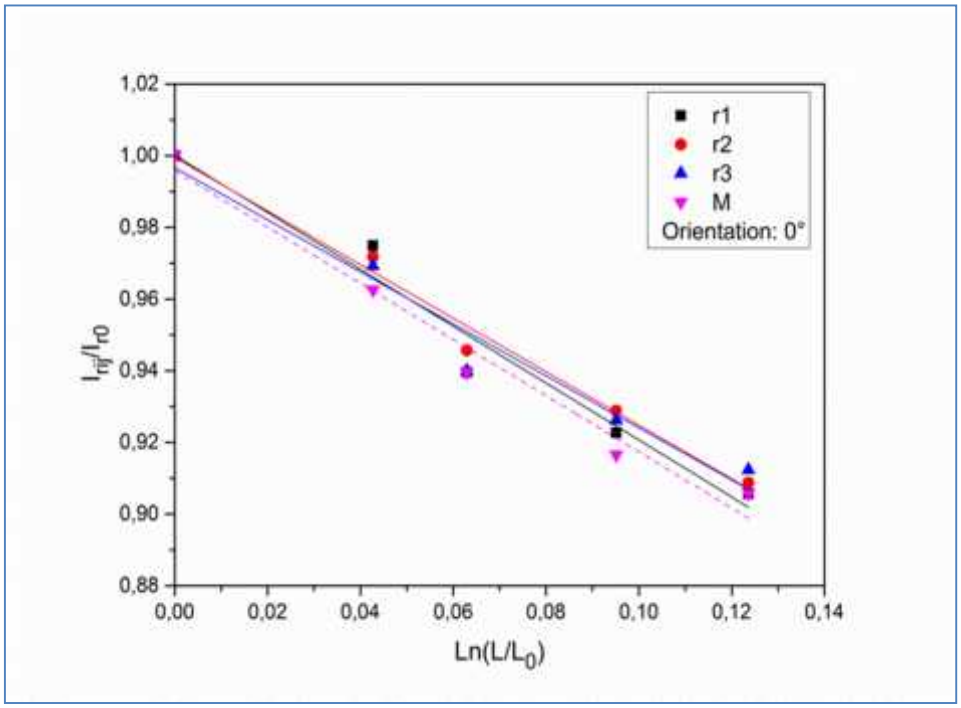
r1
r2
r3
M
Orientation: 0°
I_{rij}/I_{r0}
Ln(L/L0)
1,02
1,00
0,98
0,96
0,94
0,92
0,90
0,88
0,00
0,02
0,04
0,06
0,08
0,10
0,12
0,14

(a)

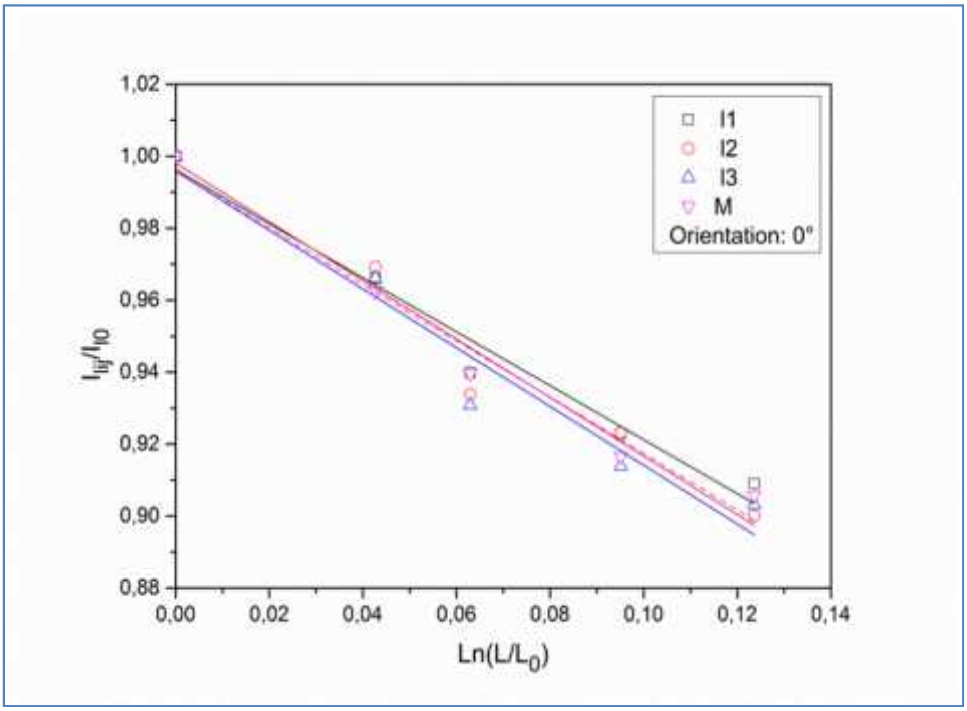
I1
I2
I3
M
Orientation: 0°
I_{lij}/I_{l0}
Ln(L/L0)
1,02
1,00
0,98
0,96
0,94
0,92
0,90
0,88
0,00
0,02
0,04
0,06
0,08
0,10
0,12
0,14

(b)

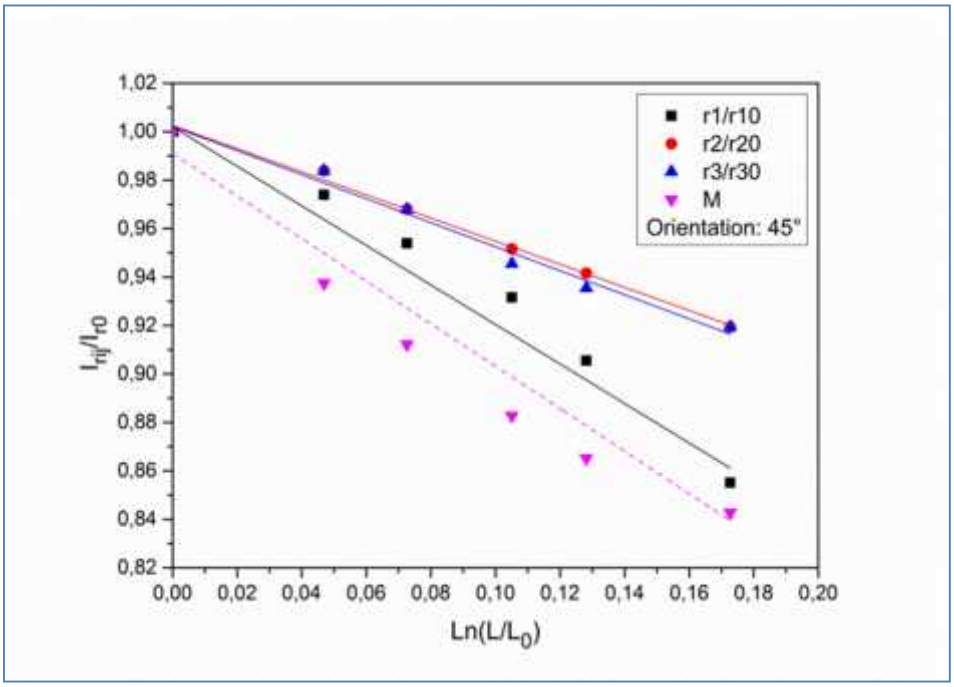
r1/r10
r2/r20
r3/r30
M
Orientation: 45°
I_{rij}/I_{ri0}
Ln(L/L0)

(c)

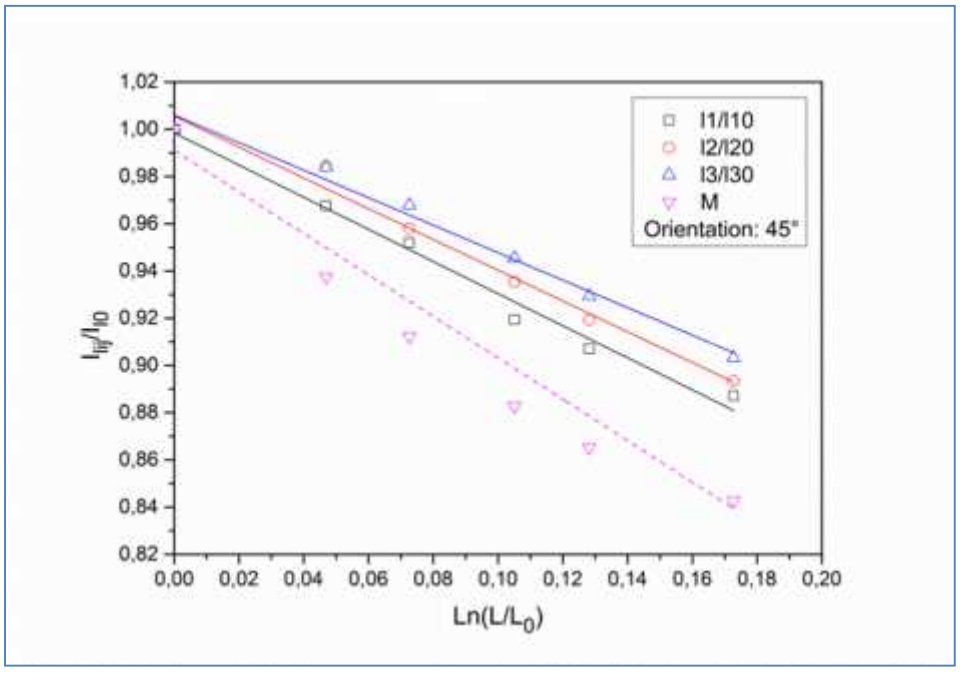
I1/I10
I2/I20
I3/I30
M
Orientation: 45°
I_{rij}/I_{ri0}
Ln(L/L0)

(d)

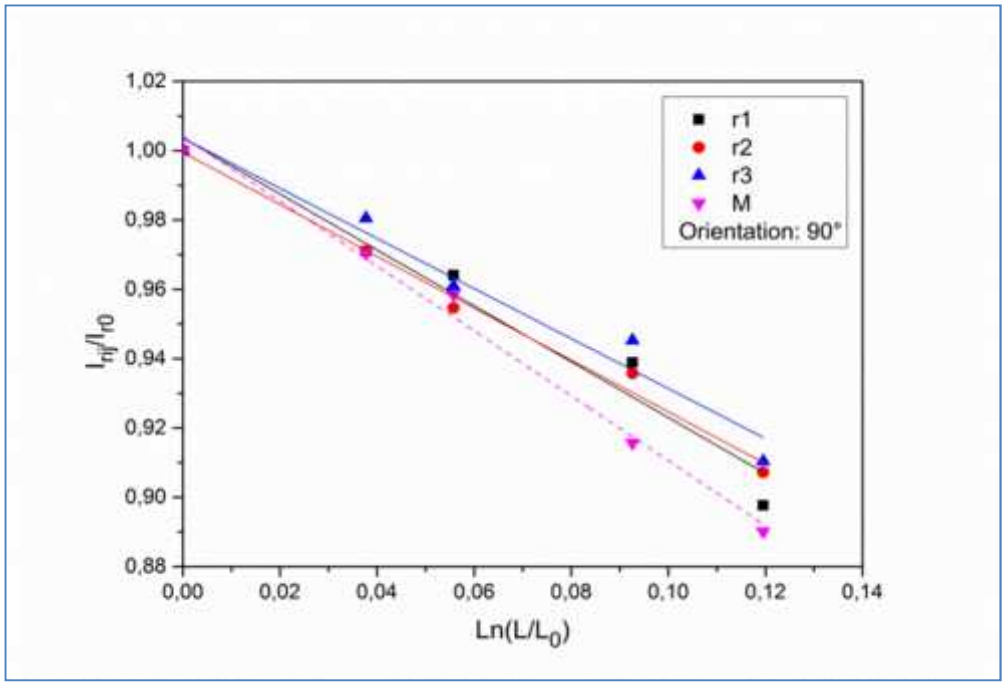

(e)

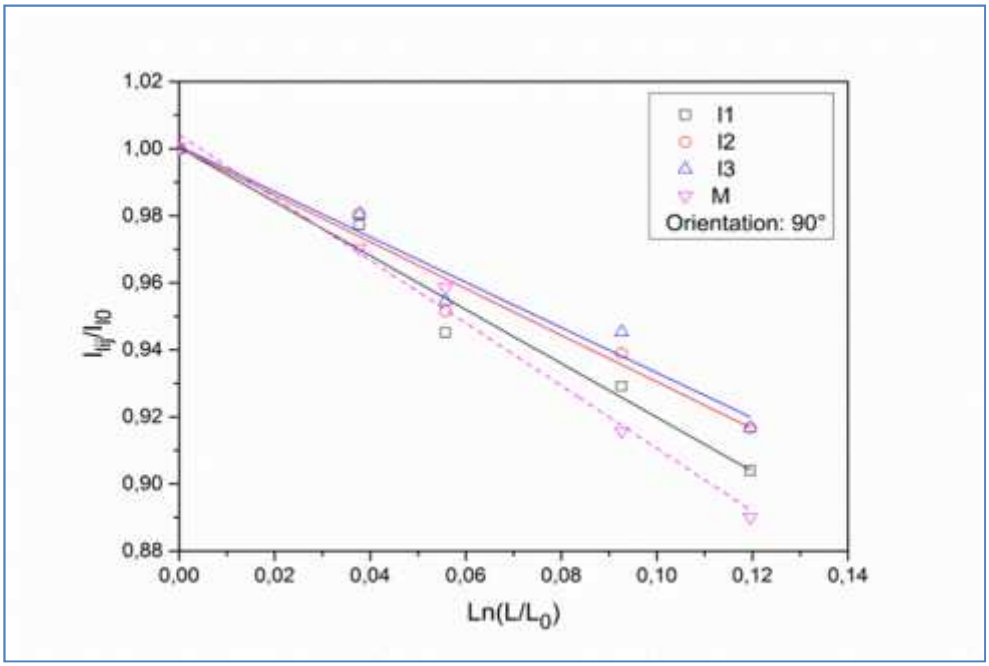

(f)

Fig.3.7: Lateral contraction versus the true strain; (a), (c) and (e): Right side, (b), (d) and (f): Left side for the LDPE films at three directions of 0°, 45° and 90°.

3.3.2. Naturally weathered LDPE films

Relative true strain versus the relative elongation: Shown in Figs.3.8 are the variation of the relative true strain of the planes situated on the right (a-c) and the left (d-f) at the 0° deformation before and after six ageing months. Again, the figures show a larger rate of elongation in right side.

With ageing, the samples display the same forms of Data as unaged films. These data clearly demonstrate the loss in the mechanical properties of the film, particularly at advanced exposure time. This revealed by the decrease of true strains. At the same strain rate, the true strains for six-aged sample is less than that for unaged samples, at the end of the tests (50%), the partial true strains on the right side go from ε_{r1}=0.41, ε_{r2}=0.41, ε_{r3}=0,38 to ε_{r1}=0.38, ε_{r2}=0.34, ε_{r3}=0,37 for the six-aged samples so those for the left side go from ε_{l1}=0.39, ε_{l2}=0.34, ε_{l3}=0,34 to ε_{l1}=0.36, ε_{l3}=0.35, ε_{l3}=0,36.

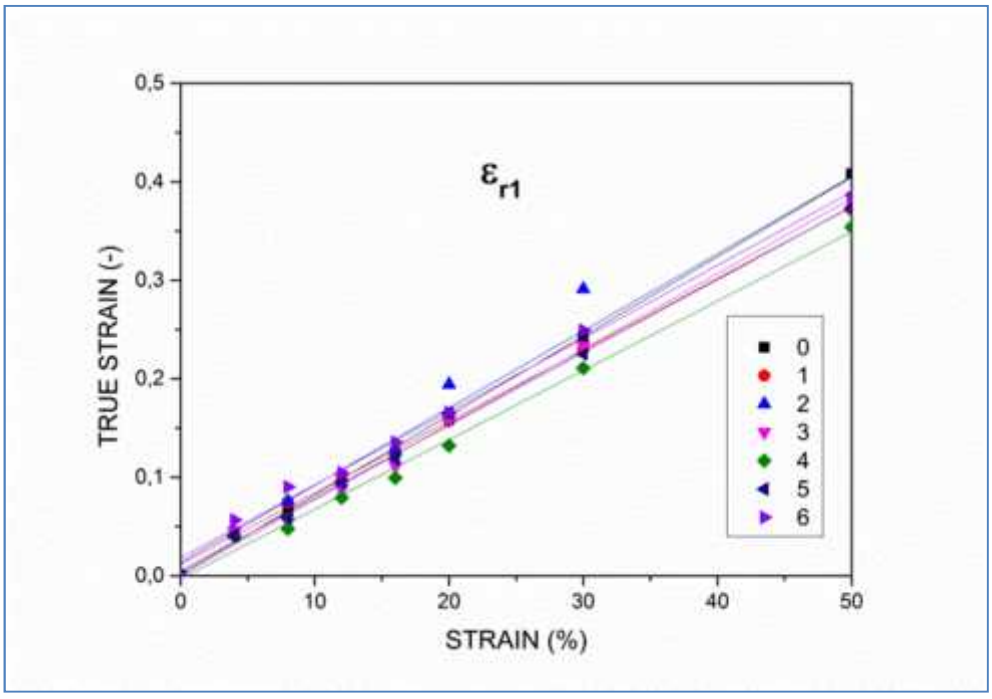

(a)

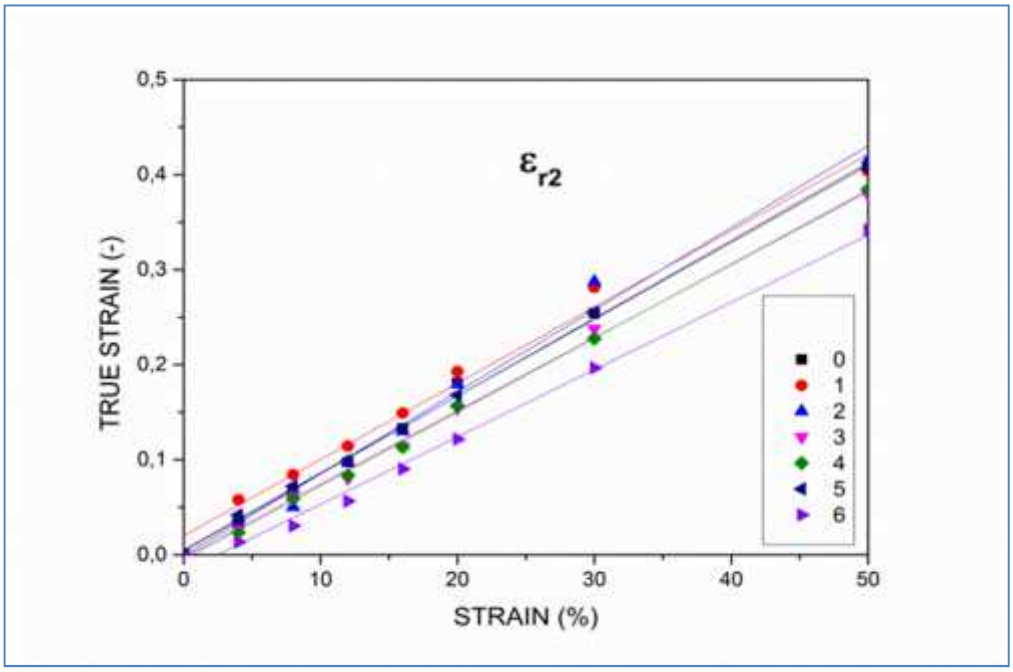
ε_{r2}
TRUE STRAIN (-)
STRAIN (%)
0,0
0,1
0,2
0,3
0,4
0,5
0
10
20
30
40
50
0
1
2
3
4
5
6

(b)

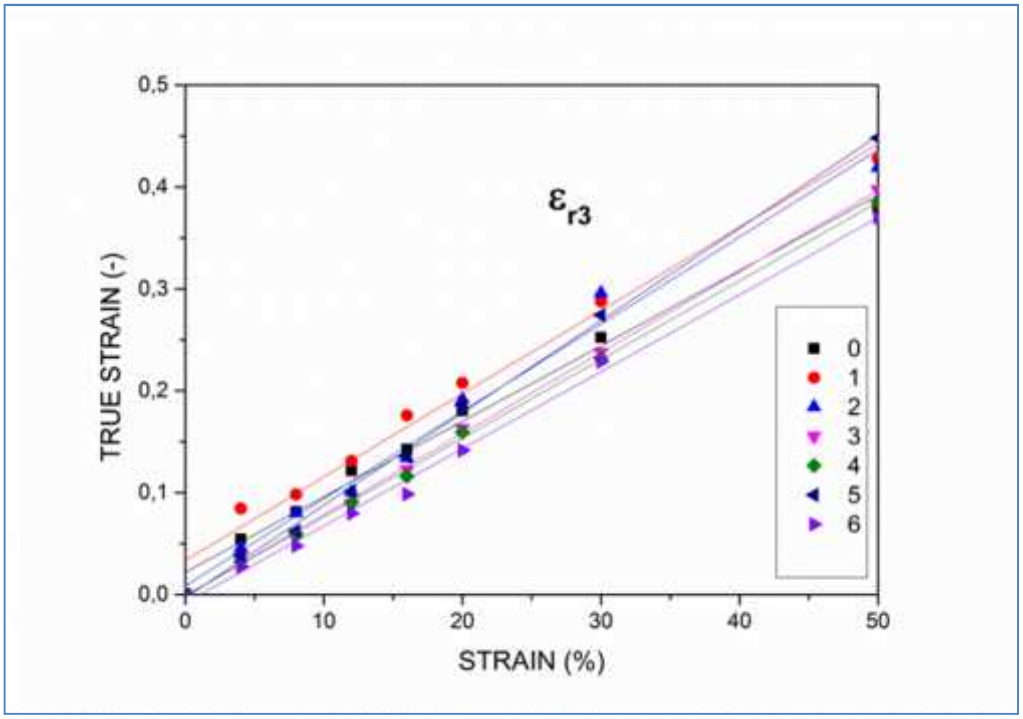
ε_{r3}
TRUE STRAIN (-)
STRAIN (%)
0,0
0,1
0,2
0,3
0,4
0,5
0
10
20
30
40
50
0
1
2
3
4
5
6

(c)

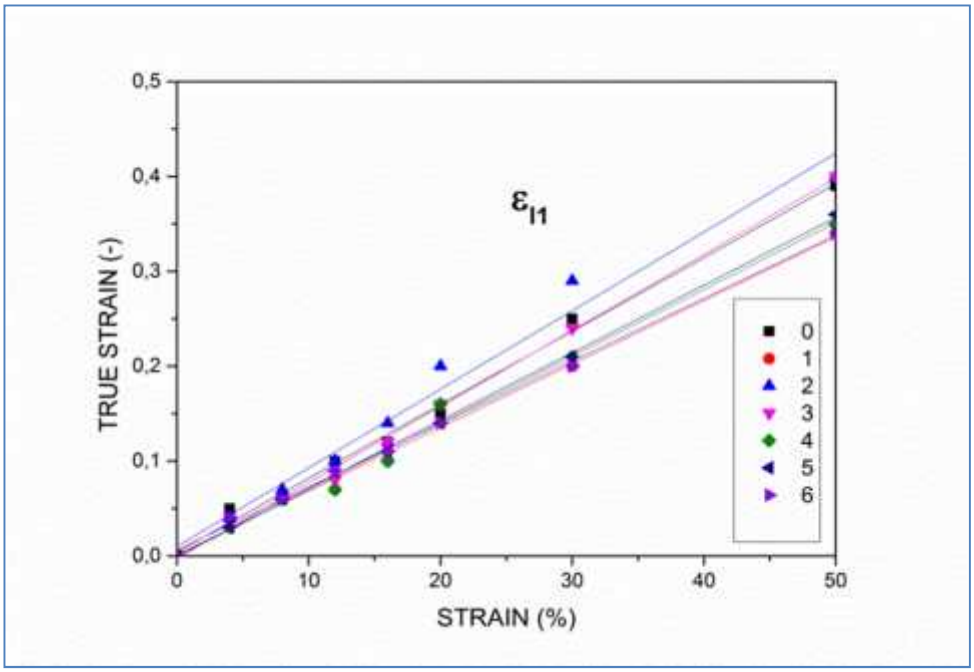
ε_{l1}
TRUE STRAIN (-)
STRAIN (%)
0,0
0,1
0,2
0,3
0,4
0,5
0
10
20
30
40
50
0
1
2
3
4
5
6

(d)

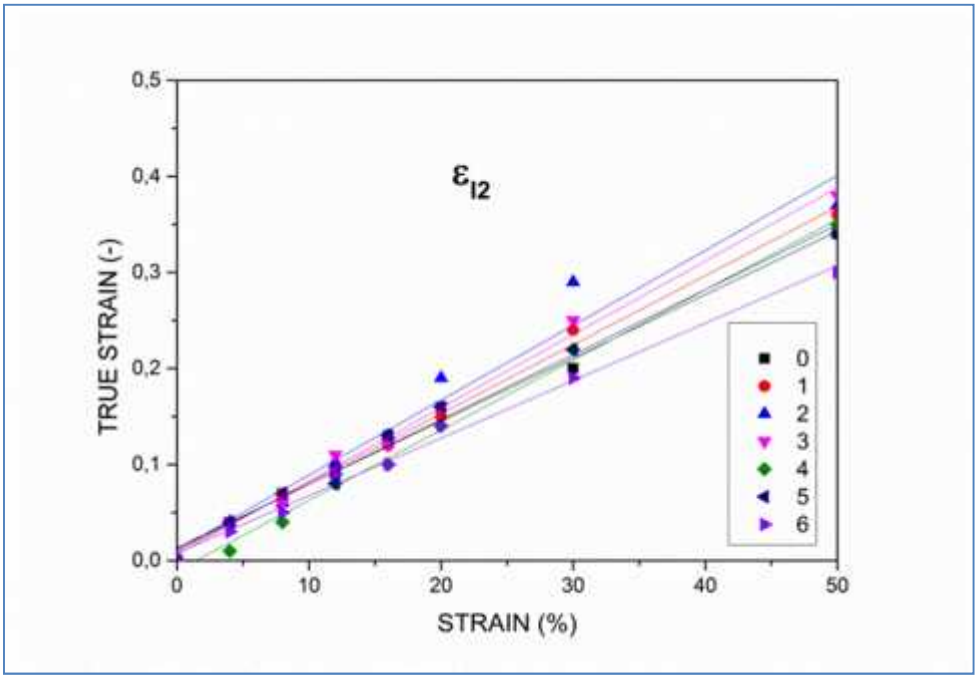
ε_{l2}
TRUE STRAIN (-)
STRAIN (%)
0,0
0,1
0,2
0,3
0,4
0,5
0
10
20
30
40
50
0
1
2
3
4
5
6

(e)

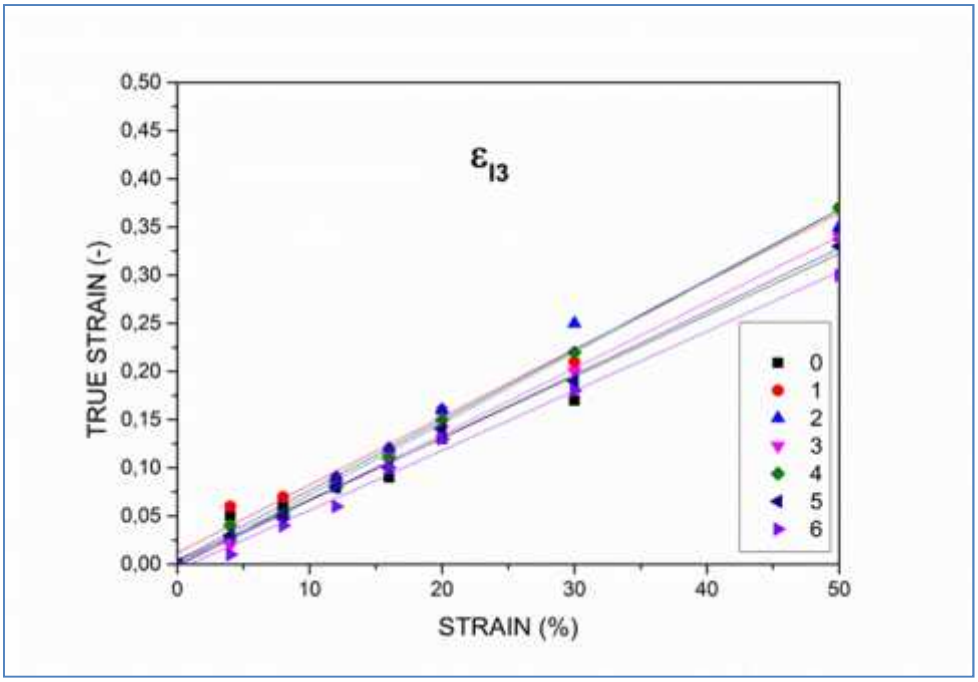

(f)

Fig.3.8: Relative true strain versus strain rate; (a-c): Right side, (d-f): Left side for the unexposed and aged months LDPE films at the 0° direction.

Lateral contraction during stretching: Shown on Figures 3.9 the lateral contraction response of the film before (a and c) and after (b and d) ageing in the interval of strain rate: $j \in [0-16]$. Data presented in these figures have been well reproduced by using another set of samples at each ageing state. For both sides the decreasing variation of the width is almost linear for all marks with negative slopes (-υ) following the Eq.3.3. With ageing each of longitudinal elongation and lateral contraction decrease in both sides displaying lower rates especially in I_3. This is may be due to film processing. As expected, the Poisson's ratio value (υ) determined from these graphs for different strain rates is (0.33) whatever the ageing state because this is characteristic is specific to the material.

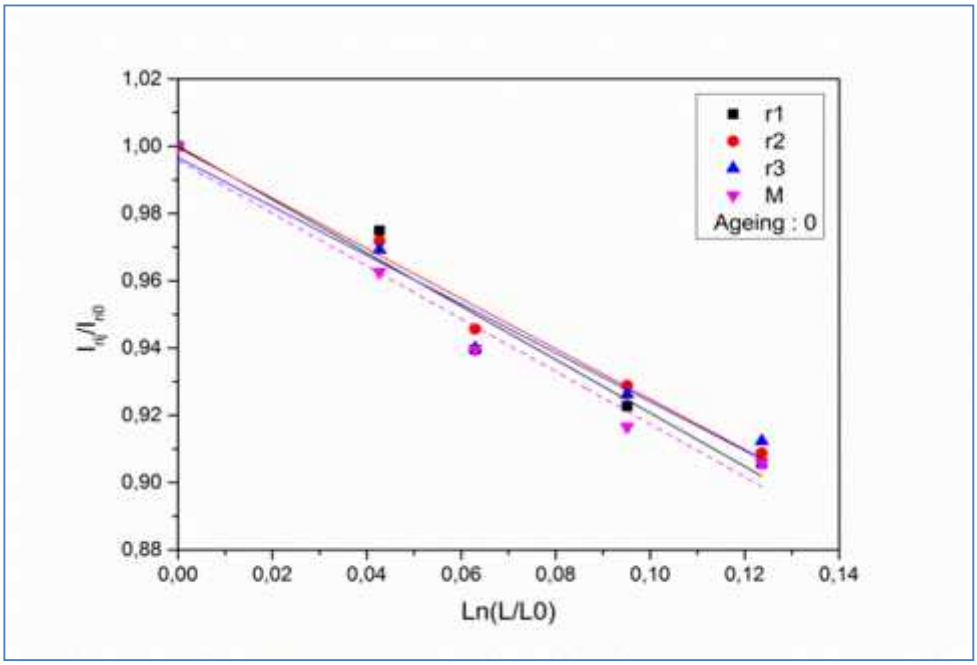
1,02
1,00
0,98
0,96
0,94
0,92
0,90
0,88
0,00
0,02
0,04
0,06
0,08
0,10
0,12
0,14
Ln(L/L0)
r1
r2
r3
M
Ageing : 0

(a)

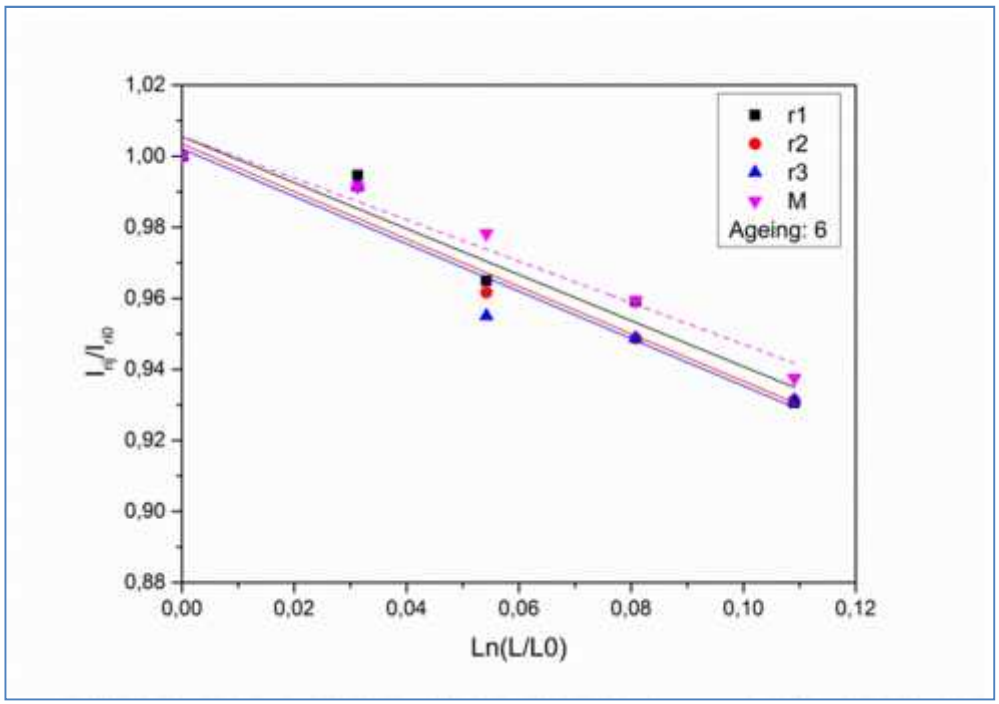
1,02
1,00
0,98
0,96
0,94
0,92
0,90
0,88
0,00
0,02
0,04
0,06
0,08
0,10
0,12
Ln(L/L0)
r1
r2
r3
M
Ageing: 6

(b)

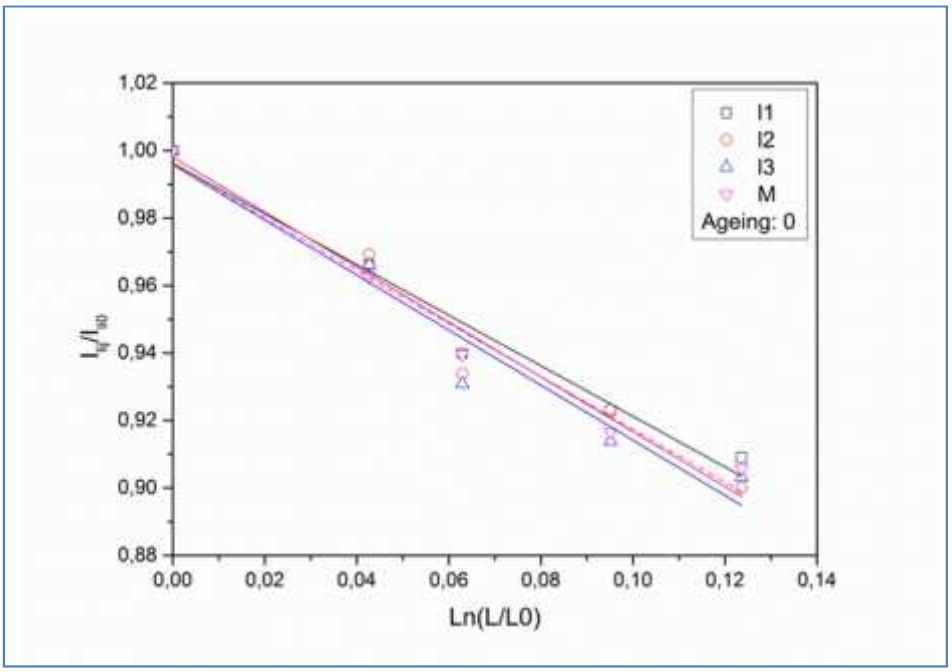

(c)

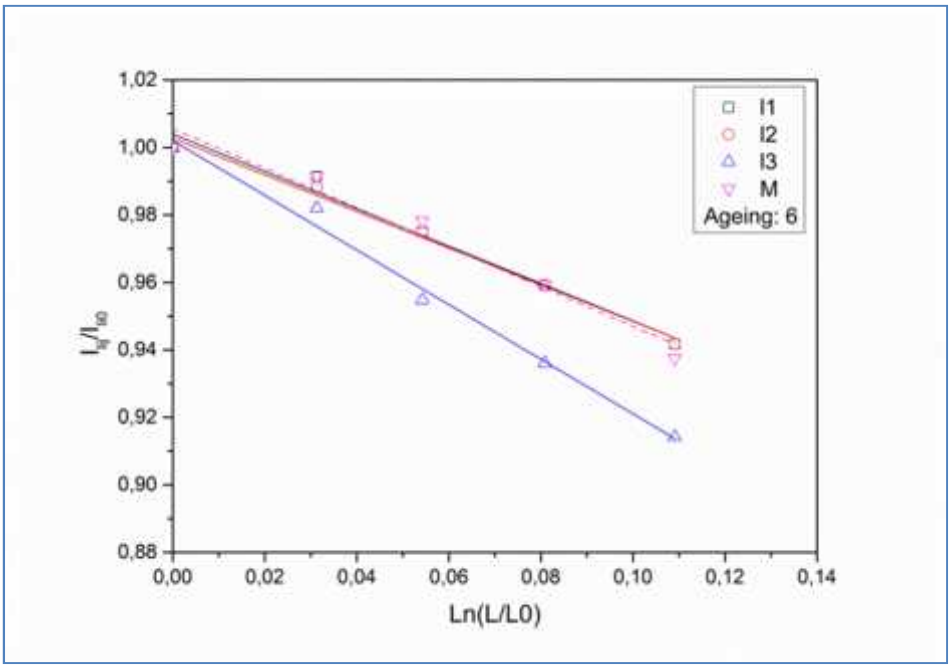

(d)

Fig.3.9: Lateral contraction versus the true strain before (a and c) and after (b and d) ageing of LDPE films at the 0° direction.

Stress-strain curves of LDPE films: Shown in Figs.3.10 the stress-strain curves at the MD and TD deformations for LDPE 2100T films. The same forms of data for the unaged and weathered samples are shown in Fig.3.11.a and 3.11.b. During ageing, the LDPE knows stiffening accompanied by a loss of clarity of its surface (sign of a physical alteration of the material). These data highlight the dramatic differences in the mechanical properties of this film; particularly those with ageing. The properties of Young's modulus (E), yield stress ($\pm_y$) and strain ($£_y$), cold-drawing stress ($\pm_d$), break stress ($\pm_b$) and strain ($£_b$), determined from these curves are listed in Table 3.2 and will be discussed later. It needs to be pointed that, although the data presented in Table 3.2, the Young's modulus (E) calculated from strain-stress curves with different crosshead speed of 3×10^{-4} s^{-1} and 3×10^{-2} s^{-1}, the observed mechanical behavior at each orientation is very representative and can be reproduced in the range of ±5%.

The progression of Young's modulus is similar for both direction but it is not monotonous since it is very slow during the two first months to suddenly increase the fourth month of about 7% for MD and 8% for TD. Then the progression is almost linear and it is about 7% for MD and 4% for TD, meaning that the overall progress of the modulus is about 15% for MD and 13% for TD.

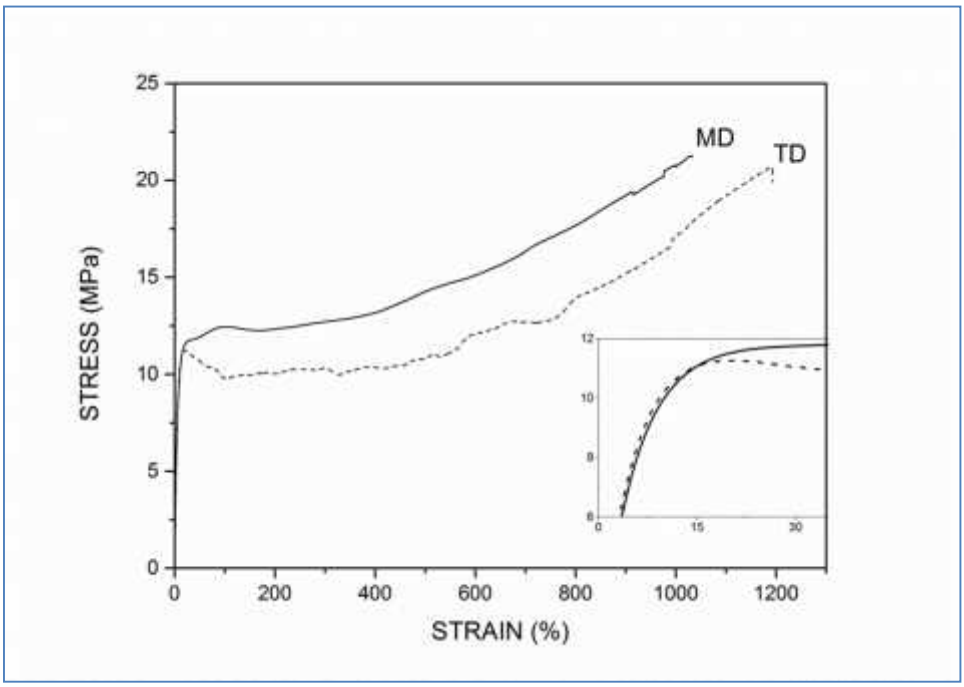

Fig.3.10: Stress-strain curves for the LDPE 2100T films at two main directions.

For the MD deformation, after yielding, which in this case is denoted by where a deviation from initial linearity occurs, followed by neck formation. The samples underwent then cold drawing to different amount of strains to display finally a significant degree of strain hardening, indicated by the large positive slopes following cold drawing. For the TD deformation, all samples displayed a very different yielding style - a sharp "conventional" yield peak, as compared with the case of MD deformation, and necked at earlier stages of the deformation (20% strain). The samples underwent then a larger range of cold drawing followed then by a lower range of strain hardening before failure.

With ageing, the curve shape remains unchanged. However, an increase in linearity slopes but lowering in strain hardening.

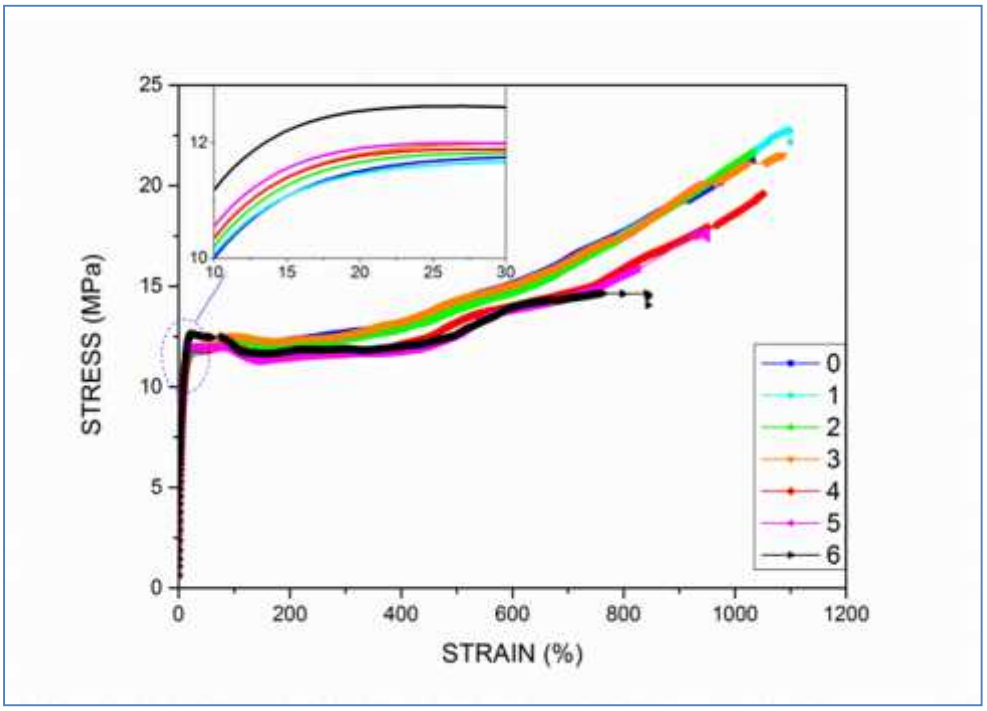

(a)

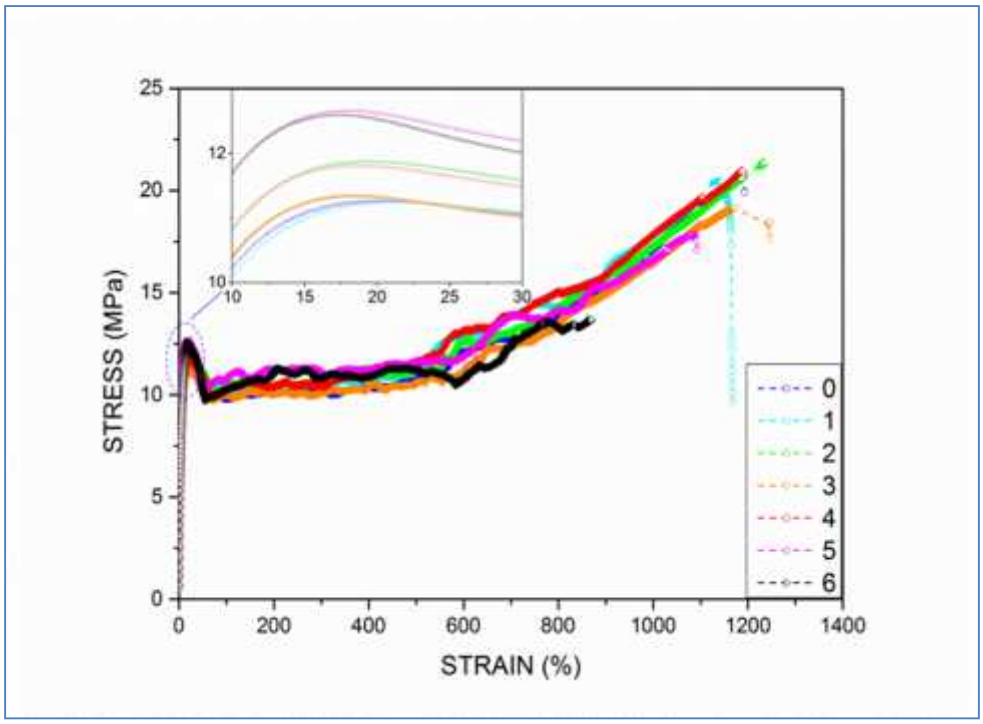

(b)

Fig.3.11: Stress-strain curves for the LDPE 2100T films at different exposure time in two main directions (a) machine direction (MD), (b) transverse direction (TD).

Fig.3.12 shows the stress-strain curves obtained in the elastic domain, for two grades of PE at two different crosshead speed which are 2 and 200 mm.min^{-1}, corresponding to 3×10^{-2} and 3×10-4 s^{-1} respectively. It provides information on:

- The influence of ageing and crystallinity degree for a given strain rate;
- The influence of the strain rate for a given ageing degree.

Young's Modulus Data obtained from stress-strain curves are summarized in Table 3.2.

The variation of break strain (ε_b) is similar for both directions; its initial values of the initial length are 1006% and 1103% for MD and TD, successively. Up to 4 months of exposure, the elongation at break is almost constant. After 5 months of exposure, this greatness knows a sudden drop. At the final stage of ageing, the material undergoes an overall loss of 24% and 26% of its initial elongation, for MD and TD respectively.

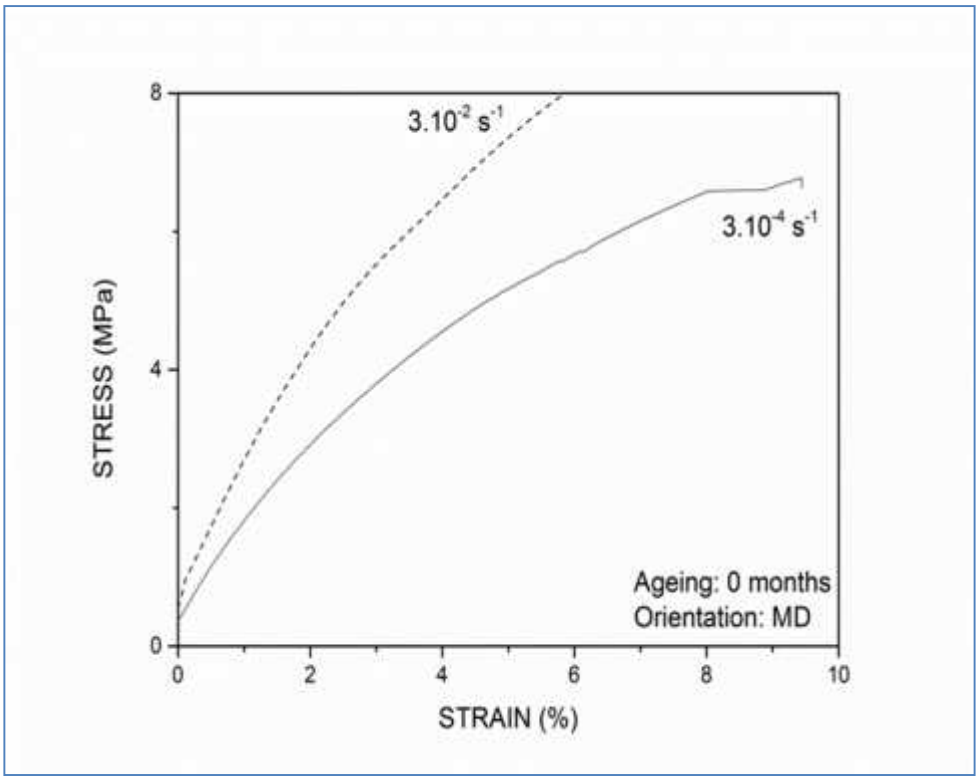
3.10-2 s-1
3.10-4 s-1
STRESS (MPa)
STRAIN (%)
Ageing: 0 months
Orientation: MD
0
4
8
0
2
4
6
8
10

(a)

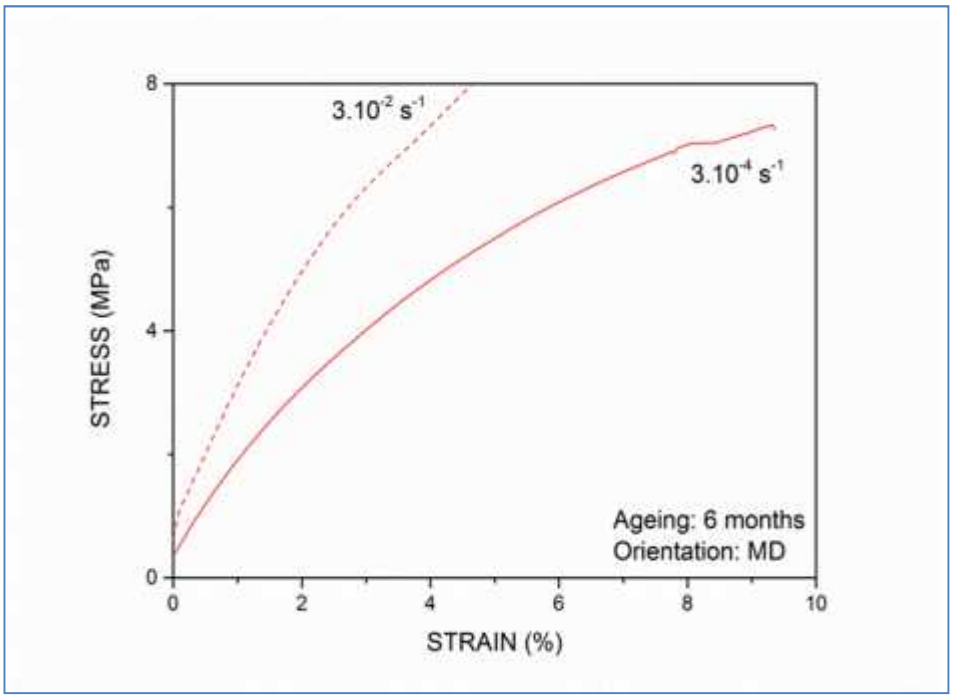
3.10-2 s-1
3.10-4 s-1
STRESS (MPa)
STRAIN (%)
Ageing: 6 months
Orientation: MD
0
4
8
0
2
4
6
8
10

(b)

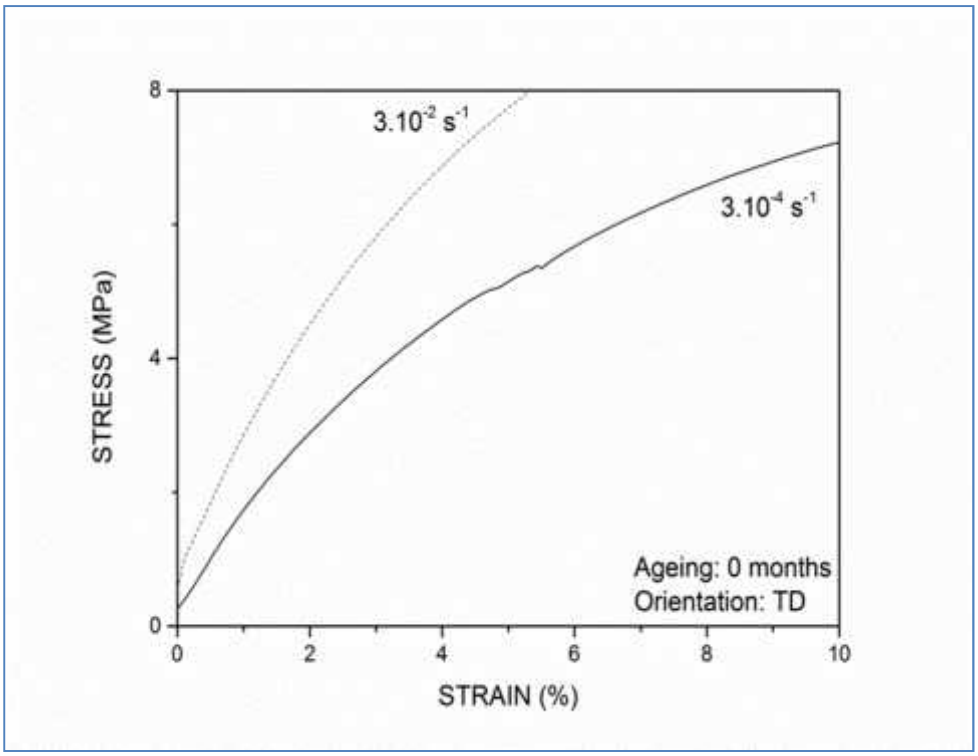

(c)

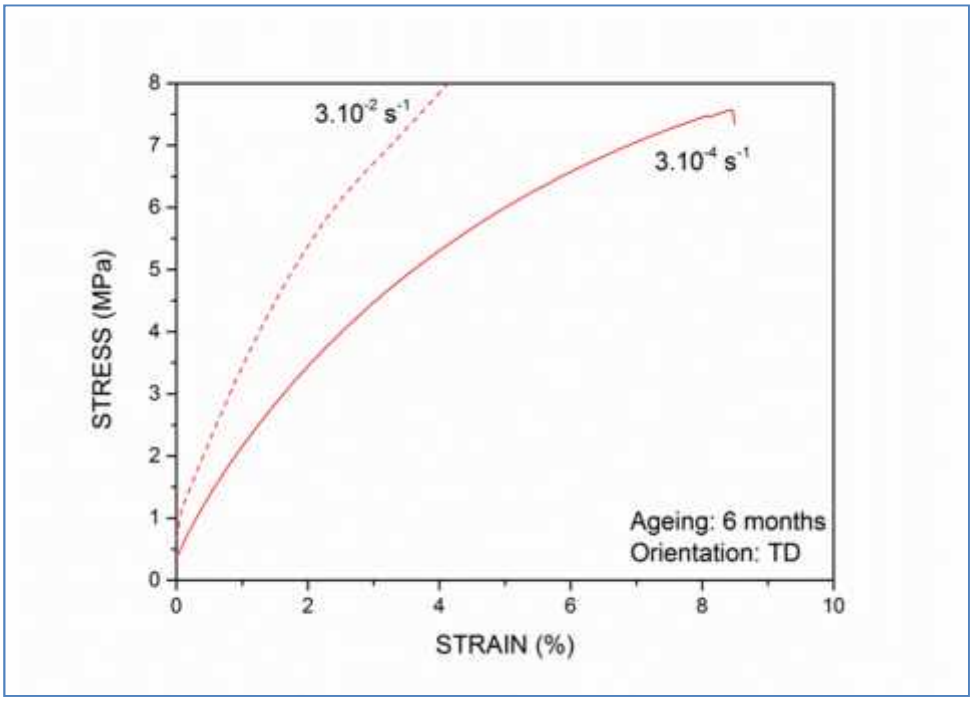

(d)

Fig.3.12: Stress-strain curves of the unaged (a and c) and weathered (b and d) LDPE films for two head speed of 3×10^{-2} s^{-1} and 3×10^{-4} s^{-1} , and two directions of MD and TD.

The break stress results (σ_b) present a similar behavior to that of the strain. The initial stress which is a little bit more than 20 MPa for MD and 19 MPa for TD, remains almost unchanged during the first months and known a significant drop at the last stage of ageing. The last stress values recorded of 14.79 MPa for MD and 13.27 MPa for TD, represent an overall loss of 27% and 44% of its initial values, respectively. The cold drawing stress (σ_d) remain almost unchanged, however it is higher for MD.

Table 3.2: Values of Young's modulus, *E*, yield stress,=±$_y$,and strain, £$_y$, cold-drawing stress, ±$_d$, breaking stress,=±$_b$, and strain,=£$_b$, for the LDPE films (2100 T N00W) investigated.

Property (units)	Orientation	Ageing						
		0	**1**	**2**	**3**	**4**	**5**	**6**
E[200mm.min^{1}](MPa)	MD	197,03	199,55	199,55	204,95	205,85	211,98	227,48
	TD	209,51	203,66	215,2	218,49	226,25	246,96	250,18
E[2mm.min^{-1}] (MPa)	MD	136,24	132,46	136,12	138,64	154,06	157,68	158,03
	TD	153,41	153,77	154,23	157,96	165,18	167,47	171,72
±$_y$ *(MPa)*	MD	11,76	11,79	11,8225	12,02	12,38	12,57	12,63
	TD	11,24	11,42	11,85	11,84	11,81	12,16	12,62
£$_y$ *(%)*	MD	27,76	27,36	27	26,27	24,35	23,18	22,53
	TD	20,46	20,065	18,54	18,41	18,54	17,7	16,99
±$_d$ *(MPa)*=	MD	12.25	12.05	11.96	12.29	11.40	11.38	11.65
	TD	10.02	10.38	10.29	10.08	10.40	11.24	10.84
±$_b$ *(MPa)*	MD	20,41	21,3	21,84	20,58	19,30	17,12	14,79
	TD	19,18	18,62	18,95	18,95	18,95	16,585	13,27
£$_b$ *(%)*	MD	1006,36	1038,88	1049,90	1035,01	1000,15	888,72	764,4
	TD	1103,13	1130,455	1141	1120,14	1053,07	944,845	810,98

Young's Modulus at Different Orientations: The variation in mechanical properties listed in Table 3.2 can be explained by the specific *initial* morphologies and also those *developed* during the deformation processes of these LDPE films and this before and after ageing. We will first address the Young's modulus, since it depends on the low deformation elastic behavior of the materials.

For the two types of films, the crystalline lamellae of the films are uniaxially oriented with the lamellar normal preferentially aligned parallel to the MD. Therefore, as a first approximation, these materials can be considered as a "laminated composite" of a hard

crystalline phase and a soft amorphous phase stacked along the MD. At the MD deformation, the material can be considered as the composite being deformed in an iso-stress case, i.e., the crystalline phase and the amorphous phase are deformed in series; therefore the modulus is dominated by that of the soft amorphous phase. On the other hand, at the TD deformation, the material can be considered as the composite being deformed in an iso-strain case, i.e., the crystalline phase and the amorphous phase are deformed in parallel; therefore the modulus is dominated by that of the hard crystalline phase. The modulus for the *sample* at the TD orientation (perpendicular to the chain direction) is *higher* than that for sample at the MD orientation (more parallel to the chain direction). The increase of the Young's modulus reflects an increase on its stiffening with ageing. Moreover, the mechanical response for a given type of PE depends on the strain rate, whatever its oxidation degree. This highlights the viscous component of the PE at short times which will be a parameter to take into account for the creep tests.

Plastic Deformation Morphologies at Different Orientations: Other properties, namely yield stress (σ_y) and strain (ε_y), cold-drawn stress (σ_d) and strain (ε_d), and break stress (σ_b) and strain (ε_b), are related to the plastic deformation behavior of the materials. As can be seen from the stress-strain curves in Fig. 3.11, the mechanical behavior of the films strongly depended on i) the ageing stage, ii) the orientation of the deformation, both will be discussed separately below. Other factors, such as molecular weight distribution will also certainly affect these properties.

1) MD deformation: Considering the "laminated composite" model proposed earlier for the investigated films, its deformation along the MD direction would occur by lamellar separation. Such a deformation mechanism can be justified by the appearance of strain whitening for samples stretched along the MD direction and the disappearance of such a phenomenon for relaxed samples upon removal of the stress. Similar statements have been made from the deformation studies on other polyethylene [18], hard-elastic polyethylene [19] and polypropylene [20], which have an aproximative morphology to LDPE samples deformed along the MD direction. Lamellar separation cause crystalline lamellae to "open-up" or splay, and this results in the strain-whitening shown by all the samples. As the deformation proceeded, the crystalline lamellae have to be deformed to generate higher strains, and this promotes the yielding of the sample. Since the c-axis in the crystal is more or less oriented along the stress direction (MD), chain slip is the dominant deformation mode for the

crystalline phase, especially [100] chain slip. The slip of the crystalline phase also causes the large degree of strain hardening, as shown in the stress-strain curves.

2) TD deformation: At this orientation, since the c-axis (chain axis) in the crystalline lamellae was more or less perpendicular to the direction of the applied stress (SD), the deformation on the level of the crystalline lamellae and amorphous layers, via lamellar separation, lamellar shear and lamellar rotation, was significantly limited. Therefore, the samples yielded sharply after a small amount (20%) of iso-strain elastic deformation of the crystalline phase and amorphous phase, and what followed was the localized break-up (decrystallization) of the crystalline lamellae, by transverse slip in the crystal. During the decrystallization process, polymer chains are pulled-out of the crystalline lamellae and realigned and recrystallized parallel to the SD, which is perpendicular to the original MD. The pull-out of the chains is basically a cold-drawing process and, therefore, it occurred as a horizontal plateau in the stress-strain curves at the TD deformation. The cold-draw strains at the TD deformation seemed to be higher than that at the MD deformation, due to a greater degree of chain-slip rather than chain pull-out.

With ageing and on a mechanical point of view, the stress-strain curve reduces resulting from a decrease of the stress break (σ_b) and strain (ε_b). This last one, its initial value indicates the highly ductile character of the virgin material. Other of us found this greatness about 600% [5]. However, its reduction behind the stress break (σ_b) is the consequence of a progressive loss of the ductility of the film which becomes progressively more and more brittle with the exposure time. On a structural point of view the stiffening can be explain by the effect of radiation on the molecular structure which reduce dramatically the average molecular weight via different chain scissions process [3, 5]. Also the reduction of the chain length has an adjacent effect on the morphology by increasing the crystallinity concentration via a chemo-crystallization process [5]. The ultimate mechanical properties highlight more on the effect of chain scissions which contribute to the transition for large deformation from a ductile behavior before ageing to a very brittle behavior after ageing.

In industry it is estimated that a loss of 50% of elongation at break is a criterion sufficient to determine the end of life of a plastic film.

3.4. Conclusion

By carrying out deformation studies on LDPE films having semi-crystalline morphology, the study of the polyethylene film deformation under controlled deformation rates is allowed. The

optical measurements carried out on samples with marks have revealed that relative elongation and true strain are strongly dependent on the angle of the deformations with respective the original orientation direction, they are greater in the 45° stretch followed by 90° then 0°. Also, it has been found that the deformation in the right side is more pronounced. However, it should be noticed that the planes delimited by the marks remain uniform during the whole deformation meaning that the lines of ink remains parallel during the total duration of the experiment. The lateral contraction measurement performed at different orientations and zones of the specimen shows in all the cases that the contraction remains linear despite the fact that the plans delimited by the marks shrink with slightly different rates. This explains why in a mechanical tensile test conducted up to break, necking appears randomly. With ageing the material showed loss in mechanical properties by decrease in true strain and lateral contraction. In general and in all the cases, the Poisson's ratio could be determined and it is estimated to be 0, 33. This value is close to that of the literature.

In another hand, comparing the mechanical properties obtained from tensile tests and the deformation morphology taken from literature at specific strain, a model structure-property investigation has been presented. Stretching parallel to the MD results in lamellar separation, followed by break-up of the crystalline lamellae via chain slip. Stretching perpendicular to the MD causes the crystalline lamellae to break-up or rupture by chain pull-out. With ageing, the properties at the break decrease indicating the loss of ductile character of the material.

References

[1] P. A. Dilara, D. Briassoulis., Standard Testing Methods for Mechanical Properties and Degradation of Low Density Polyethylene (LDPE) Films Used as Greenhouse Covering Materials: A Critical Evaluation., *J. Poly. Test.*, 17 (**8**), 1998.

[2] M. A.Tuasikal, O.Y. Alothman, M. Luqman, S. M. Al-Zahrani, M. Jawaid., Influence of Natural and Accelerated Weathering on the Mechanical Properties of Low-Density Polyethylene Films., *Int. J. Poly. Analy. And. Charac.*, 19 (**3**), 2014.

[3] S. F. Chabira, M. Sebaa, C. G'sell., Influence of climatic ageing on the mechanical properties and the microstructure of Low-Density Polyethylene films., *J. Appl. Polym. Sci.*, 2008, 110 (**4**), 2516.

[4] P. G. Klein, D. W. Woods, and I. M. Ward, *J. of. Poly. Sci: Part B Poly. Phys.*, 25, 1987.

[5] S. F. Chabira, M. Sebaa, R. Huchon, B. De Jeso., The changing anisotropy character of weathered low-density polyethylene films recognized by quasi-static and ultrasonic mechanical testing.,*J. Polym. Deg. And. Stab.*, 91 (**8**), 2006.

[6] I. M. Ward, J. Sweeney, Mechanical Properties of Solid Polymers, 2013.

[7] F. P. La Mantia., Natural weathering of low density polyethylene—III: Mechanical properties., *Eur. Poly. J.*, 20 (**10**), 1984.

[8] X.M. Zhang, S. Elkoun, A. Ajji, M.A. Huneault., Oriented structure and anisotropy properties of polymer blown films: HDPE, LLDPE and LDPE., *Polym.J.*, 45 (**1**), 2004.

[9] S. F. Chabira, R. Huchon, M. Sebaa., The changing anisotropy character of weathered low-density polyethylene films recognized by quasi-static and ultrasonic mechanical testing., *J. Appl. Polym. Sci.*, 90 (2), 2006.

[10] H. Zhou, G. L Wilkes., Orientation-dependent mechanical properties and deformation morphologies for uniaxially melt-extruded high-density polyethylene films having an initial stacked ., *J. Mat. Sci.*, 39 (**2**), 1998.

[11] O.Al Othman, S.Faiz, and M. A. Tuasikal, *Int. J.of.Poly.Sci.*, 2014

[12] J. M. Schultz., Microstructural aspects of failure in semicrystalline polymers ., Polym. *Eng. And .Sci.*, 20 (**10**), 1984.

[13] R. J. Samules, Structured Polymer Properties, Wiley-Interscience, New York (1974).

[14] S. Cantournet. Bases physiques contitatives des lois de comportement mécanque.

[15] C.JA Christensen,TA Ejerton. *Poly.J.*, 44 (19), 2003.

[16] F.Détrez. Nanomécanisme de deformation des polymers semi-cristallins, 2008.

[17] L.Romdhane, and A.Benaamara. Analyse des systèmes mécanique, 2006.

[18] H.Zhou. Structure-property relationships: model studies on melt extruded uniaxially oriented high density polyethylene films having well defined morphologies. 1997.

[19] B. Cayrol and J. Petermann., Elastic hard polyethylene fibers., *J. Polym. Sci., Phys. Ed.,* 12 (**10**), 1974.

[20] C. J. Chou, A. Hiltner and E. Bear., The role of surface stresses in the deformation of hard elastic polypropylene., *Polymer*, **27** (1986) 369.

CHAPTER 4.0

CREEP-RECOVERY BEHAVIOR AND LOADING EFFECT ON PRISTINE BLOWN EXTRUDED LOW DENSITY POLYETHYLENE FILM

Chapter 4.0 CREEP-RECOVERY BEHAVIOR AND LOADING EFFECT ON PRISTINE BLOWN EXTRUDED LOW DENSITY POLYETHYLENE FILM

1. Introduction

Creep is the time-dependent strain (elongation) for a material under constant stress. For polymers, the creep deformation is an important and powerful experimental method to study many physical properties such as the viscoelastic behavior, physical aging, etc.

On the other hand, the creep is also a common phenomenon for engineering applications where the products are under specific loads, and the lifetime of the product during service is a major concern. For this reason, it is essential to understand the origin of creep deformation and to be able to predict the long term creep behavior for a given polymer material under specific conditions. For this, and in order to replicate as accurately as possible the loading undergone by the greenhouse in service, These tests aim to reproduce, on the scale of laboratory test specimens, the mechanisms of deformation undergone by the films in service.

The creep-recovery behavior of different grades of polyethylene has been extensively studied [1-7]. Figure.4.1 shows a typical creep-recovery curve of polyethylene. It provides a crude qualitative representation of the phenomena generally observed with viscoelastic materials where the following deformations can be defined: instantaneous elastic strain "ε_1", delayed elastic strain "ε_2", viscous flow "ε_3", instantaneous elastic recovery"ε_a", delayed elastic recovery"ε_b", and plastic deformation (permanent set) "ε_c".Under creep, the total strain is the sum of three components ($\varepsilon_1, \varepsilon_2, \varepsilon_3$), as shown in the following equation [8, 9]:

$$\varepsilon(t) = \varepsilon_1 + \varepsilon_2 + \varepsilon_3 \qquad \text{Eq.4.1}$$

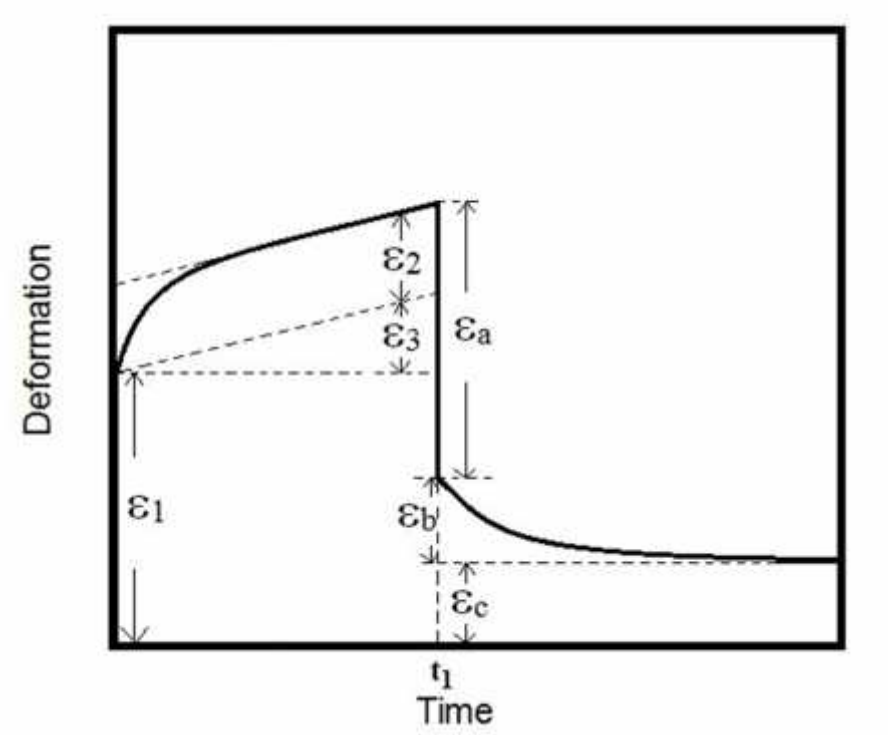

Fig.4.1: Typical creep-recovery curve of PE.

Neither the simple Maxwell nor Voigt model accurately predicts the behavior of real polymeric materials. Various combinations of these two models may more appropriately simulate real material behavior. We start with a discussion of the four-parameter model, which is a series combination of the Maxwell and Voigt models (Fig.4.2). We consider the creep response of this model.

Under creep, the total strain will be due to the instantaneous elastic deformation of the spring of modulus E_1, and irrecoverable viscous flow due to the dashpot of viscosity η_2, and the recoverable retarded elastic deformation due to the Voigt element with a spring of modulus E_3 and dashpot of viscosity η_3. Thus, the total strain is the sum of these three elements. That is,

$$\varepsilon(t) = \sigma_0\{1/E_1 + t/\eta_2 + \sum_{i=1}^{n} 1/E_3[1 - \exp(-t_i/\tau_3)]\} \qquad \text{Eq.4.2}$$

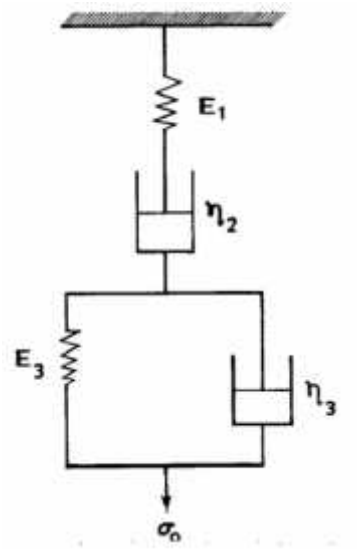

Fig.4.2: Schematic of the four-parameter model.

Where σ_0 is the imposed constant stress and τ_3 equals "η_3/E_3" and is referred to as the retardation time. In recovery, when the load is removed at time t_1; the deformation "σ_0/E_1" due to the spring of modulus "E_1" is recovered instantaneously. This will be followed by the retarded elastic creep recovery due to the Voigt element given by ε_3 or

$$\varepsilon_3 = \sigma_0/E_3[1 - \exp(-t_i/\tau_3)] \qquad \text{Eq.4.3}$$

Only the deformation due to the dashpot of viscosity η_2 is retained as a permanent set. The creep recovery curve of this model is shown in Fig.4.1.

The constants E_1 and η_2 are immediately determined from the intercept and the slope of the asymptote to the curve, thus:

$$\begin{cases} E_1 = \sigma_0/\varepsilon_0 \\ \quad and \\ \eta_2 = \sigma_0/\tan\alpha \end{cases} \qquad \text{Eq.4.4}$$

However, it remains to determine E_3 and η_3, this is done using the method based on mathematical analysis of INOKICHI.

Whether $\tau_i = \eta_i/E_i$, the time corresponds to the 1st solid KELVIN. Whereas the distance at the time "τ_i" between the asymptote to the curve and the curve is expressed by:

$$Q(t) = \sigma_0 \sum \exp(-t/\tau_i)/E_i \qquad \text{Eq.4.5}$$

If τ_3 is the longer delay time among τ_i, so :

$$Q(t) = \sigma_0 \exp(-t/\tau_3)/E_3 \qquad \text{Eq.4.6}$$

And

$$\ln Q(t) = \ln(\sigma_0/E_3) - t/\tau_3 \qquad \text{Eq.4.7}$$

The plot of $\ln Q\ t$ versus time lets generate the parameters E_3 and η_3 ;

E_3 deduced from $\ln(\sigma_0/E_3)$ (intercepts);

$\tau_3 = \eta_3/E_3 = -1/\tan\theta$ (inverse of the slope of the straight to opposite sign).

The four-parameter model provides a crude qualitative representation of the phenomena generally observed with viscoelastic materials: instantaneous elastic strain, retarded elastic strain, viscous flow, instantaneous elastic recovery, retarded elastic recovery, and plastic deformation (permanent set). Also, the model parameters can be associated with various molecular mechanisms responsible for the viscoelastic behavior of linear amorphous polymers under creep conditions. The analogies to the molecular mechanism can be made as follows.

1. The instantaneous elastic deformation is due to the Maxwell element spring "E_1". The primary valence bonds in polymer chains have equilibrium bond angles and lengths. Deformation from these equilibrium values is resisted, and this resistance is accompanied by an instantaneous elastic deformation.

2. Recoverable retarded elastic deformation is associated with the Voigt element. This arises from the resistance of polymer chains to coiling and uncoiling caused by the transformation of a given equilibrium conformation into a biased conformation with elongated and oriented structures. The process of coiling and uncoiling requires the cooperative motion of many chain segments, and this can only occur in a retarded manner.

3. Irrecoverable viscous flow is due to the Maxwell element dashpot η_3. This is associated with slippage of polymer chains or chain segments past one another.

To aid our visualization of viscoelastic response we introduce models that represent extremes of the material response spectrum. This is followed by the treatment of mechanical models that simulate viscoelastic response. These concepts are developed further by discussion of the superposition principles.

2. Experimental

Material: The LDPE utilized in this investigation is a commercial grade supplied by the Saudi basic industries corporation (SABIC) as "LDPE 2100 T N00W", (ρ_s= 0.92g/cm^3, MFI= 0.33g/ 10mn). This polymer is a neat grade exempt of stabilizing agents. Films were produced by blowing extrusion from the raw material in an Algerian industry (Sofiplast of Sétif). The

drawing speed of the production line was fixed to 15 cm/s. The melt was extruded at about 175°C and blown in a continuous process characterized by a bubble diameter of 4,4 m and a wall thickness of 160 µm. It is known that the properties in the machine direction (MD) depend on the draw down ratio (DDR) and those in the transverse direction (TD) to the blow up ratio (BUR) [10].

Tensile tests: The stress-strain curves for all the samples were obtained by using an Roell zwik machine at room temperature (T=21°C, ± 1°C) at a nearly constant relative humidity (RH=50%, ± 5%). The test pieces were cut out of the original and the aged films. The dimensions of the rectangular test pieces were 70 mm × 10 mm, with a calibrated portion of length L_0 = 40 mm, W_0 = 10mm and thickness T_0 = 0.16 mm. The results of the tensile test are presented in term of true stress, $\sigma = F(1 + \varepsilon)/A_0$, and true strain $\varepsilon(t) = \ln(L(t)/L_0)$. To optimize the duration of the test the strain rate was fixed at a low value to the yield point ($d\varepsilon/dt = 3 \times 10^{-4}\ s^{-1}$) (determination of the young modulus) and then stepped to a higher value ($d\varepsilon/dt = 3 \times 10^{-2}\ s^{-1}$) for the rest of the test until fracture occurred. To check the anisotropy of the film the test pieces were cut and tested in the two main directions corresponding to the machine direction (MD) and the transverse direction (TD).

Creep experiments : The creep test has been run on a creep tester (Fig.4.3.a) developed in the laboratory of mechanic (Laghouat university) with Rectangular specimens of dimension 110mm, with a calibrated portion of length L_0 = 80mm, width W_0 = 10 mm, and thickness T_0 = 0,16 mm. the test pieces were cut in two main directions of the film (MD and TD) and the tests were conducted at room temperature (T= 20°C ± 1°C, temperature very far above Tg = -110°C).

An equidistant markers perpendicular to the stretching direction (Fig.4.3.b), were drawn on the surface of the sample and symmetrically distributed with respect to the middle of the specimen, and separated by 1 cm respectively. The monitored section of the test pieces (or effective length) is delimited by ink marks distant of 6 cm respectively.

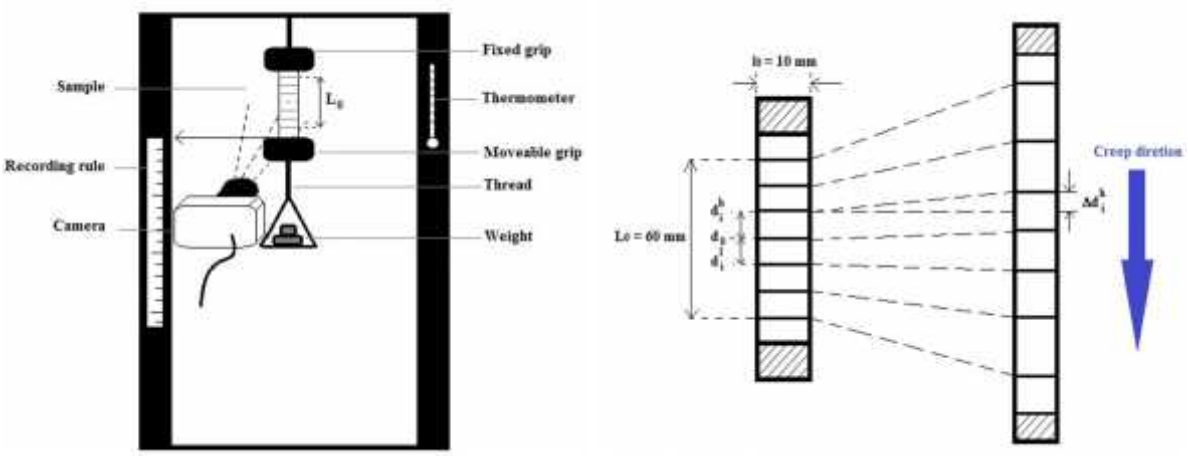

(a) (b)

Fig.4.3: (a) Creep tester, (b) Markers displacement during the creep.

Furthermore, other measuring instruments were used regularly to get more information:

- A CCD camera with resolution of 16.2 megapixels to ensure an optical monitoring of each test recording the evolution of markers on the sample surface.
- Matlab software for a digital correlation in the calculation of deformation.

The principle consists in measuring the distance between two markers previously positioned on the specimen. The displacement Δl measured by optical means corresponds to the spacing between the two end markers; it provides information on the local deformation of the specimen. The deformation of the effective length is checked through a number of partial deformations, this precaution has been taken to verify that the deformation is homogeneous in the total effective length. The details of calculation and equivalence of deformation measurements are discussed in Appendix 1.

Des photos sont prises tout au long le test de fluage à des intervalles des temps régulier, la fréquence d'acquisition est choisie relativement élevée pour être sûr de ne pas rater des points expérimentaux importants. Les données sont ensuite traitées par Matlab et lissées pour éviter de traiter des fichiers de données trop volumineux.

A photograph are taken throughout the creep test at regular time intervals, the frequency acquisition is chosen relatively high to be sure not to miss important points data. The whole is then processed by means of the Matlab software and smoothed to avoid dealing with too large data files.

Different nominal stresses are applied (6.6, 7.6, 8.6, 10.69, 11.69, 12.15 and 13.6 MPa). The loading phase (creep) has a duration of 8 hours, followed by the recovery phase begins

immediately following the unloading is that lasts 8 hours. This duration is limited by the most aged film samples which will be presented in chapter 5.0.

To optimize the accuracy of the measurements for each creep-recovery curve an average of 5 test pieces has been tested and this for all the different applied stresses. Also the curves represented in this work have been plotted with these average values. The standard deviation for each point around the average value ever exceeds 5%.

3. Results

The creep-recovery curves of LDPE films under different stresses at two main directions (MD, TD) are presented in Fig.4.4.a and Fig.4.4.b. A cursory observation of the curves shape, lets appear for both directions, during the loading phase, that after the instantaneous strain ε_1, the creep rate decreases progressively (primary creep) ε_2 till to reach a minimum value ($\dot{\varepsilon}_{min}$). Then, the secondary creep occurs ε_3, which is higher in the transverse direction than in the machine direction. After stress removal, during the recovery for both directions and for all ageing stages, much of the deformation is almost instantaneously recovered, then the delayed recovery tends quickly to a minimum value. It can be noticed that for this material, whatever is the stretching direction, it does not appear a tertiary creep regime; this behavior is typical for LDPE materials [11].

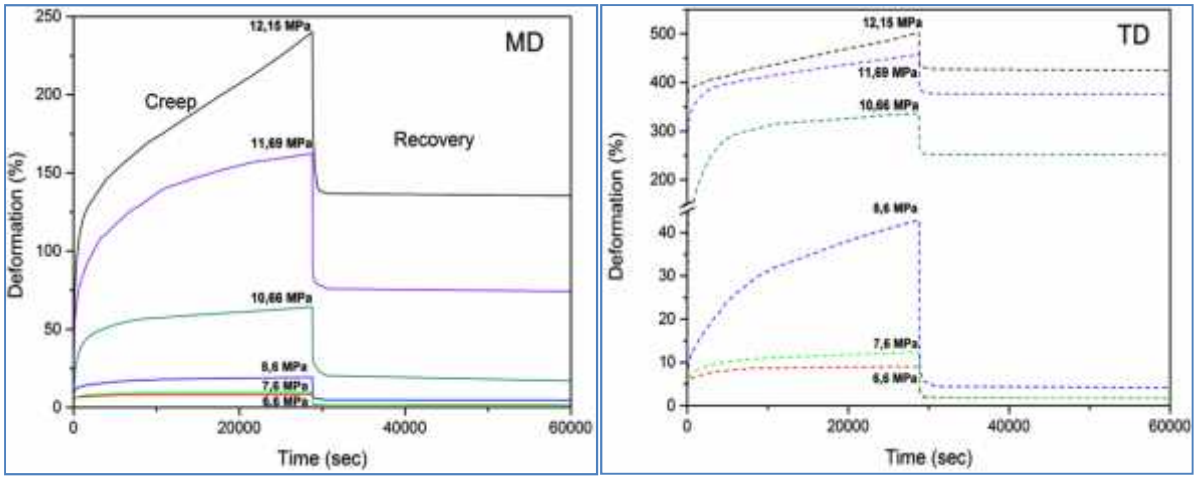

(a) (b)

Fig.4.4: Creep-recovery behavior of LDPE films 2100T at two directions (a) machine direction (MD), (b) transverse direction (TD).

We were interested to the loading phase where the creep deformation is plotted function to logarithmic time Fig.4.5.a and 4.5.b. At each orientation, a higher stress resulted in a larger creep strains (Table.4.1) and a larger creep rate (upward curvature at the end of the creep

curves). At the same stress level, samples at different orientations with respect to the MD also showed different amount of initial creep strains and plateau creep rates which is always higher in the TD. However, in the case of creep in TD, a necking have been developed during the test when applying a high stress, when this happens, the creep curve undergoes dramatically a rapid rise in the first test time.

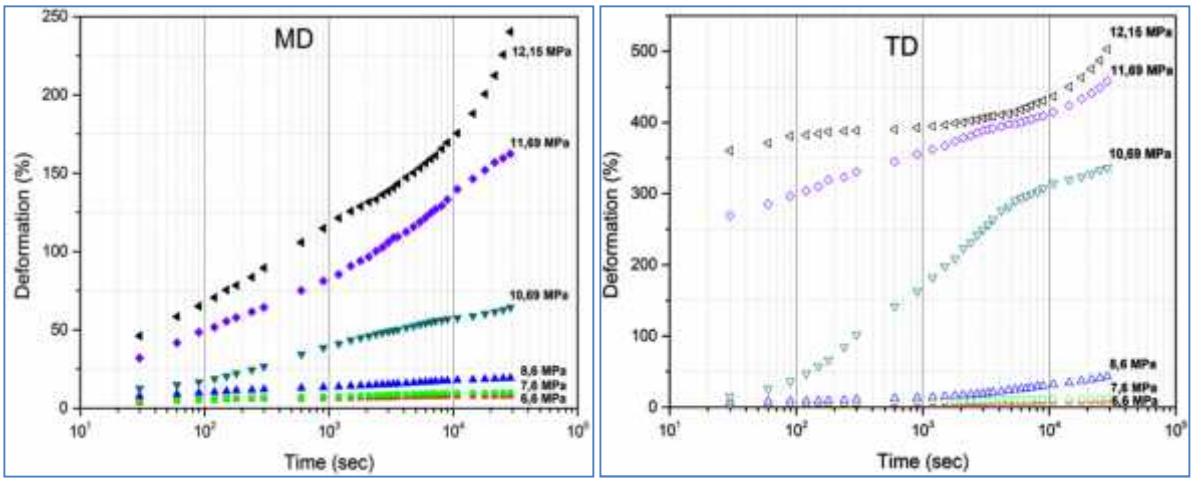

(a) (b)

Fig.4.5: semi-logarithmic curves of creep-recovery curves for LDPE films 21 00T at two main directions (a) machine direction (MD), (b) transverse direction (TD).

Table.4.1: Effects of applied stress on the different deformations identified in the creep-recovery curves of LDPE for the two main directions (a) MD, (b) TD.

Stresse (MPa)	Orientation	$\varepsilon_1(\%)$	$\varepsilon_2(\%)$	$\varepsilon_3(\%)$	$\varepsilon_a(\%)$	$\varepsilon_b(\%)$	$\varepsilon_c(\%)$
6.6	MD	5.13	2.95	0.2	5.05	2.01	1.22
	TD	4.95	3.64	0.16	5.05	2.82	1.12
7.6	MD	4.86	4.32	0.69	4.80	3.57	1.49
	TD	4.79	5.49	2.14	4.78	5.90	1.74
8.6	MD	10.48	6.87	1.99	9.59	5.09	4.63
	TD	9.52	16.04	17.56	26.22	10.42	6.35
10.69	MD	24.49	28.88	15.35	24.49	25.97	13.87
	TD	84.21	215.6	36.47	72.13	12.56	251.69
11.69	MD	51.89	85.03	26.17	51.9	37.89	72.64
	TD	290.25	96.84	71.82	68.16	15.03	374.89
12.15	MD	70.93	66.39	101.85	54.01	51.94	134.27
	TD	375.44	21.06	107.16	64.26	15.54	423.21

In order to show the plateau creep rate for the above creep curves, shown in Figs.4.6.a and 4.6.b the creep rate (which is the derivation of creep curve with respect to the time) plotted against the creep strain.

It can be clearly seen that at long loading times, a plateau creep rate is indeed achieved by the material for each individual creep experiment.

The creep curves under different stresses are higher in TD than the MD. However, the minimum strain rate $(\dot{\varepsilon}_{min})$ achieved in the secondary creep can be determined easily. This greatness will be considered as an intrinsic feature of a creep test.

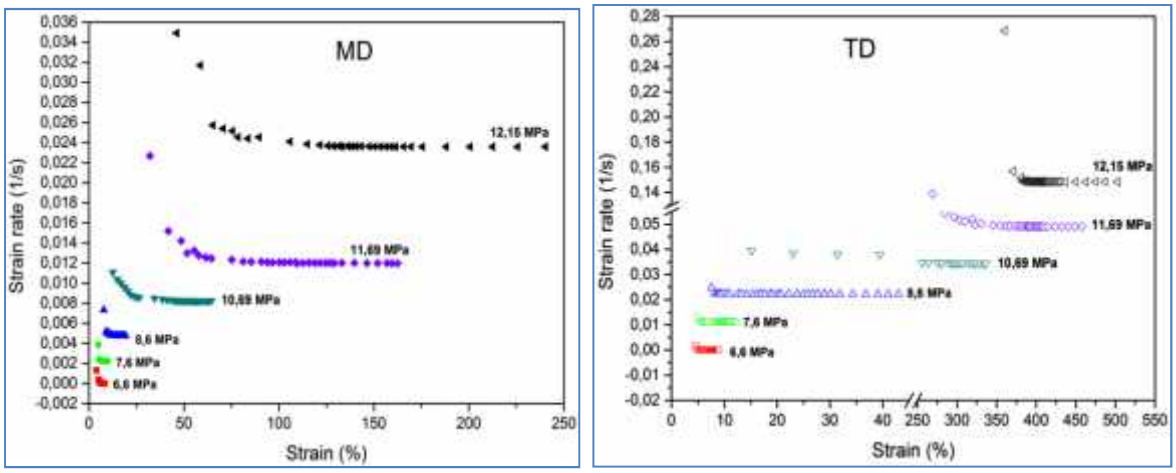

(a) (b)

Fig.4.6: Evolution of strain rate vs. strain for both directions (a) Machine direction (MD), (b) Transverse direction (TD).

3.1. Variation of minimum strain rate with stresses "activatin volume, V"

We report on logarithmic diagram (Fig.4.7), the variation of the minimum strain rate $(\dot{\varepsilon}_{min})$ verssus the applied stresses for both directions. For each direction, the results show that there are two straights. The minimum strain rate may therefore be related to the applied stress by a kind of power law (Eq.4.8):

$$\dot{\varepsilon}_{min} = A_1\sigma^{n_1} + A_2\sigma^{n_2} \qquad \text{(Eq.4.8)}$$

Where $\begin{cases} A_1, A_2, n_1 \; et \; n_2 \text{ are adjustable parameters} \\ n_1 \; et \; n_2 \; slopes \; of \; each \; straight \end{cases}$

The parameter n called the strain rate sensitivity coefficient.

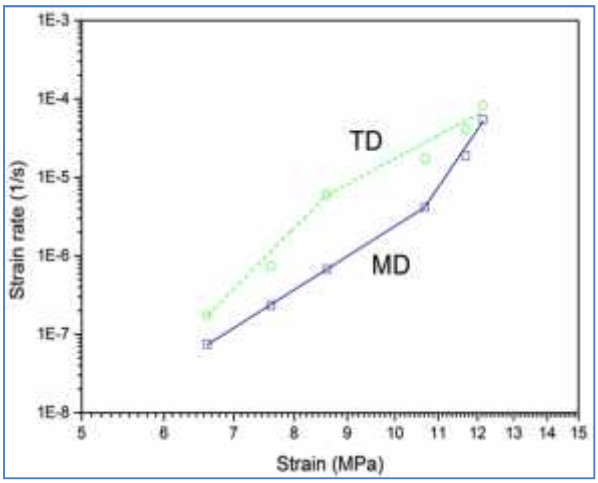

Fig.4.7: Evolution of the minimum strain rate versus applied stress, for the two main directions of LDPE films 21 00T.

This law called **Norton's law** [6]. The values of different parameters are reported on Table.4.2.

Table.4.2: Parameters obtained from Norton law for LDPE deformed in the two directions.

Parameters	A_1	A_2	n_1	n_2	V (nm^3)
MD	1.02289E-14	3.54845E-26	8.36911	19.51425	8.6
TD	1.84567E-18	1.27597E-12	13.38683	7.13634	10.69

The activation volume (V) is the one of the three parameters (i.e: activation energy (U) and the availability of creep sites ($\dot{\varepsilon}_0$)), definding the Eyring-rate model which are used to understand the plateau creep rate. The activation volume (V) was obtained by fitting the creep rate at different stress (Fig.4.7). This parameter is listed in Table.4.2.

The results show very clearly that the behavior cannot be represented by a single activated process, moreover the activation volume (V); which is the breaking slope point on the graphs, for the MD and TD creep were not the same. From the Figure.4.7 and Table.4.2, the breaking slope point (activation volume (V)) for MD is situated around 8.6 MPa and that for TD is situated around 10.69 MPa, and this implies that the molecular mechanisms involved at the two orientations are not the same. As already mentioned, in the case of yield behavior this has been noted by several previous workers who have proposed that a satisfactory representation is given by the superposition of two thermally activated processes, acting in parallel so that the stresses are additive [12, 13]. Moreover, it is appropriate to assume that one process (process 1), with a comparatively large activation volume, predominates at low strain rates

and that a second process (process 2) with a smaller activation volume comes into operation at high strain rates so that the two processes are then acting together.

In his manuscrit, C. Regrain highlighted the existence of two creep regimes on PA6, the one for low stresses and the other for high stresses, the breaking slope point was situated around 70 MPa. Also, Devilliers found the same thing for unaged HDPE but the studies wasn't completed to confirm this tendency [14].

From the creep curves, the isocrones curves could be plotted. They represent the stresses function to the strains at given times from the creep or the recovery, and could be used to determine the linearity limit of the viscoelastic material with respect to applied stresses.

3.2. Linear and non linear viscoelasticity

Fig.4.8 shows the isochronous curves of the creep tests realized on LDPE films in the two directions. The curves are parallel in evolution of ε versus σ in the two directions. From curves we can determine the linear limit of the viscoelastic behavior of the material, the linear-non linear transition is situated around 7.6 MPa and this is true for both directions.

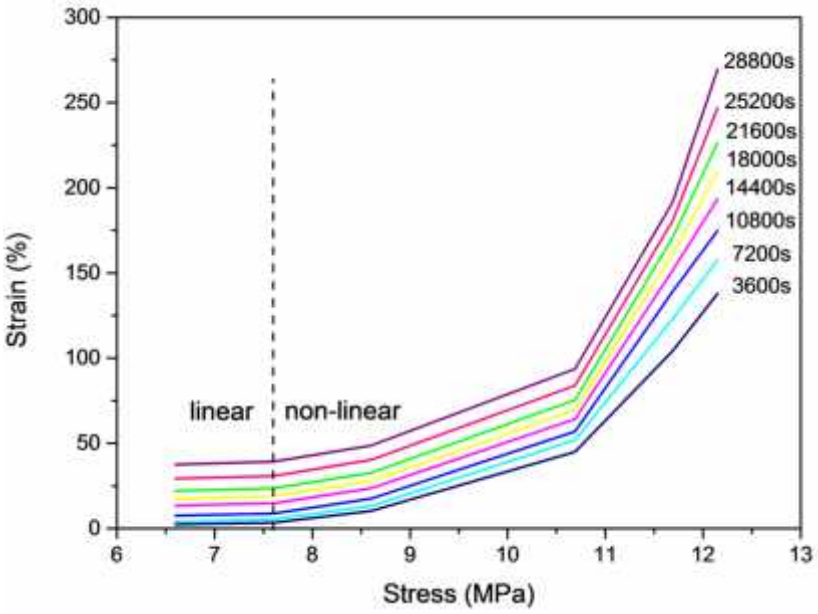

(a)

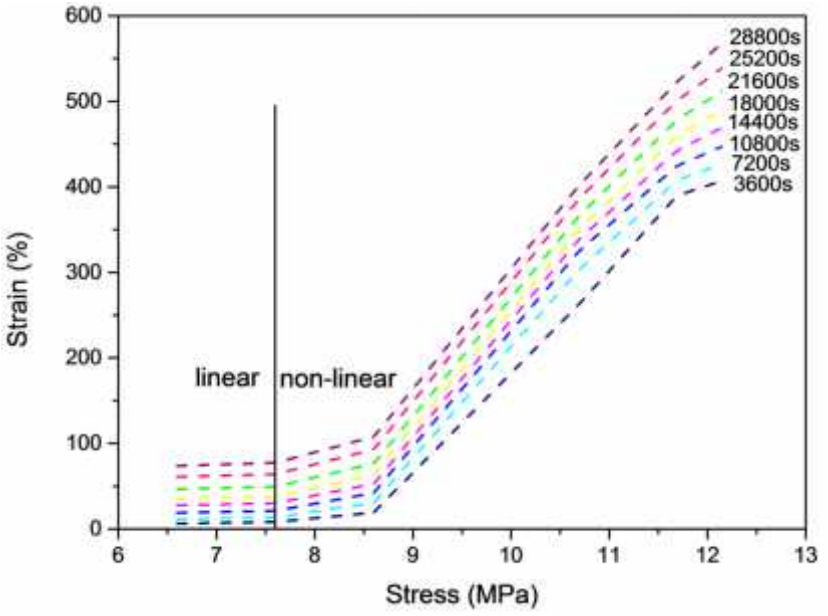

(b)

Fig.4.8: Linear-nonlinear transition of stress-strain relationship with respect to different time levels. (Isochronous creep curve of LDPE deformed in the two directions, data are taken from creep test at different stresses), (a) MD, (b) TD.

After loading, at an arbitrary time t chosen from the linear domain, ε_1 and ε_2 linear with σ_1 and σ_2, the strains at the two stresses can be expressed as

$$\frac{\varepsilon_1(t)}{\sigma_1(t)} = \frac{\varepsilon_2(t)}{\sigma_2(t)} \qquad \text{(Eq.4.9)}$$

For all tests, the strains are proportional to the imposed stresses. In general, for stress σ, the creep compliance D(t) can be given as the ratio of strain to stress at a certain time.

$$\frac{\varepsilon(t)}{\sigma} = D(t) \qquad \text{(Eq.4.10)}$$

This property is often characterized as *linear viscoelasticity* which corresponds to BOLTZMANN's principal, we can considerate the body as linearly viscoelastic. In this domain (linear domain), the compliance is independent to the stress, which means that the compliance is the same whether the stress level chosen from this interval.

However, up to 7.6 MPa, the material will assume *nonlinear viscoelastic* behaviors which will not obey the linear relation between stress and strain described above (Eq.4.9).

Since nonlinear behavior is very important to determine material behavior at moderate or higher stress levels, some models have been suggested for different kind of polymers [15].

In the next section, we will study BURGERS's model where it is representative of a viscoelastic material. It corresponds to series association of MAXWELL's liquid and some number of KELVIN-VOIGT.

3.3. Creep response of viscoelastic materials "The four-parameter model"

As it has been provided in introduction section of this chapter, the viscoelastic material is characterized by equation (Eq.4.2).

The obtained values of E_1 and η_2 are presented in Table.4.3 and Table.4.4.

Table.4.3: The four-parameter model for MD.

	6.6 MPa	**7.6 MPa**	**8.6 MPa**	**10.69 MPa**	**11.69 MPa**	**12.15 MPa**
E_1	148.98	152.30	111.83	84.37	35.85	26.22
η_2	8,54E+11	9,9217E+10	1,276E+11	2,8206E+10	9,28E+09	3,39E+09
E_3	79,60	59,81	44,33	16,32	7,07	4,79
η_3	1768,98	318,98	277,09	81,59	29,45	9,59

Table.4.4: The four-parameter model for TD.

	6.6 MPa	**7.6 MPa**	**8.6 MPa**	**10.69 MPa**	**11.69 MPa**	**12.15 MPa**
E_1	145.37	160	114.06	70.98	4.33	3.32
η_2	4,40E+11	9,76E+10	1,36E+10	8,55E+09	4,69E+09	3,27E+09
E_3	72,03	59,81	19,23	3,16	2,51	2.36
η_3	1241,88	398,72	40,07	25,25	13,92	9,82

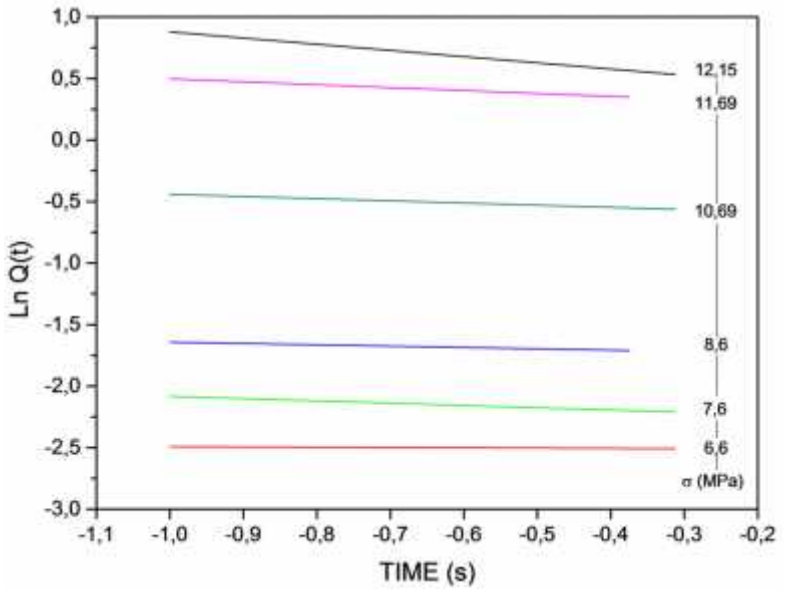

(a)

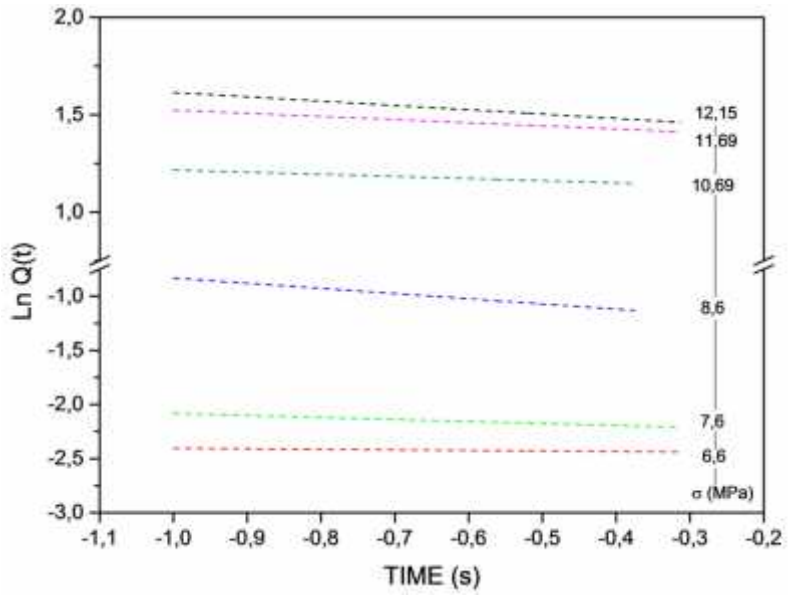

(b)

Fig.4.9: Ln Q(t) versus time for LDPE films deformed in (a) MD and (b) TD.

The figure.4.9 shows ln $Q(t)$ versus time relative to the LDPE films for different applied stresses. For both directions, the plot trend is a straight with increasing slope with increasing applied stresses. However, the slopes of TD are slightly greater than MD. The presence of one straight can be explained in fact that the viscoelastic material possesses one KELVIN-VOIGT solid where its parameters (E_3 , η_3) are presented in Table.4.2 and Table.4.3.

According to Table.3.3 and Table.3.4, both of E_1 and η_2 decrease with increasing applied stresses. However, E_3 and η_3 increase.

The behavior of LDPE against the creep is similar. It is representative to the creep response of thermoplastic polymer in general, this response contains:

- An instantaneous elastic deformation when loading, comparable to the response of a HOOKIEN solid.
- An intermediary viscoelastic behavior, comparable to the response of a KELVIN-VOIGHT solid.
- A viscous behavior for advanced loading time, comparable to the response of a NEWTONIEN liquid.

In chapter 5.0 we will see how the four parameters determined change with ageing, which will be interesting to simulate the creep behavior of weathered LDPE films under different applied stresses in both directions. Thing which never has been focused on in previous creep works.

The creep resistance is better for the films deformed in MD. This difference can be due to the structure of polyethylene (chains length, orientation, ageing, crystallinity …), thing which will be verified in chapter 5.0 because the rheological method used here to study the creep response of the unaged films only under different applied stresses in the two directions, which is the analog modeling , is a global phenomenological method. It doesn't give in any case an idea of the mechanism responsible of any response under loading.

3.4. Isometric curves

The stress-logarithmic time curves realized at room temperature at different deformations are reported in Fig.4.10. This curve not only relates the applied stress, the deformation reached and the result time of the creep tests, but also allows as determining the life time for each deformation.

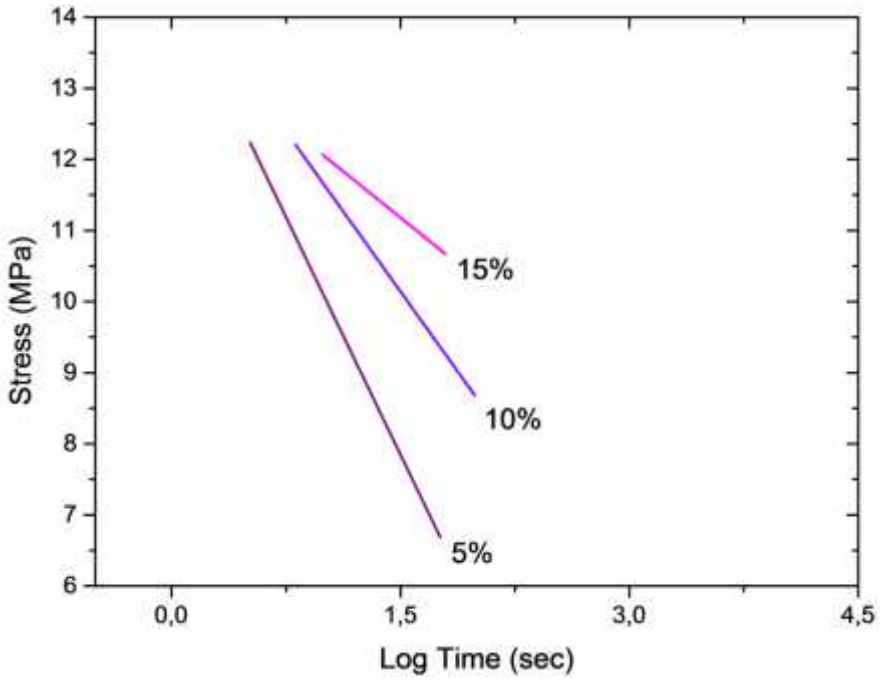

(a)

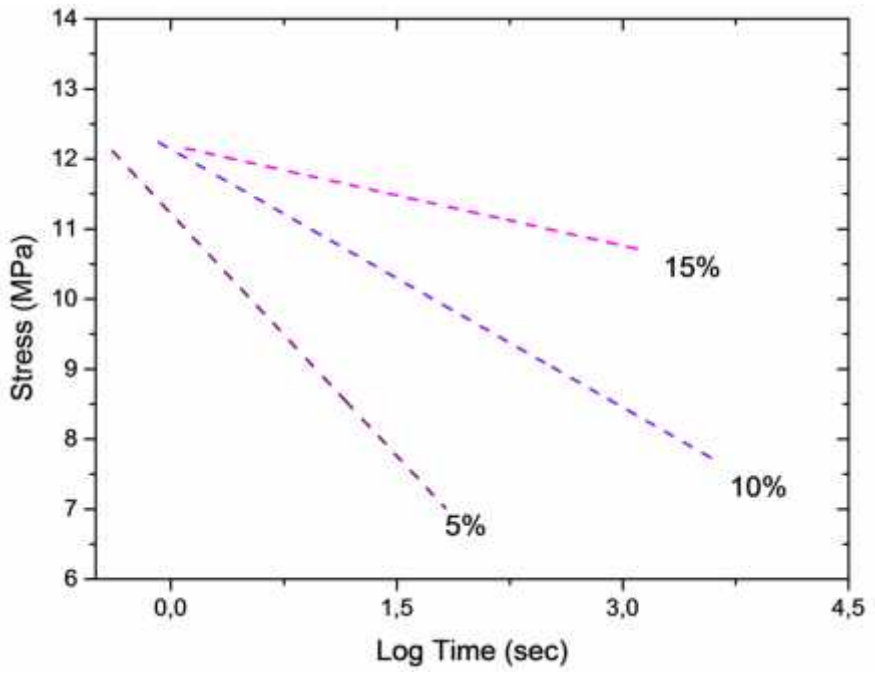

(b)

Fig.4.10: Isometric Curves stress-time of LDPE films deformed in the two main directions, (a) MD, (b) TD.

The PE curves are globally parallel in the evolution of σ function to log t and this, whatever the deformation direction. Moreover, it can be noticed that, for the MD, the life time decreases with increasing strain rate. In contrast, it increases with increasing strain rates for the TD.

3.5. Elastique portion

As mentioned earlier, elastic deformation of polymers (ε_e) in creep includes both immediate and delayed portions ε_1 and ε_2. The delayed strain (ε_2) is very low for the transvers direction (TD) deformation of the film (Fig.4.4.b). In Fig.4.11.a and 4.11.b are represented, the variation of the recovered elastic portion $E_e(t)$ (Eq.4.11) as a function of the creep time and for the MD and TD respectively.

$$E_e(t) = (\varepsilon_1 + \varepsilon_2)/\varepsilon \times 100 \qquad \text{Eq.4.11}$$

The variation of $E_e(t)$ for all applied stresses shows a rapid drop during the first 300 seconds of the creep test to show then an asymptotic trend. Practically 60% of the elastic portion E_e (300s) for the films with σ = 6.6 MPa and 7.6 MPa is transformed into an irreversible plastic

creep deformation for both directions. However The value of the E_e (300s), decreases significantly and progressively with increasing applied stresses.

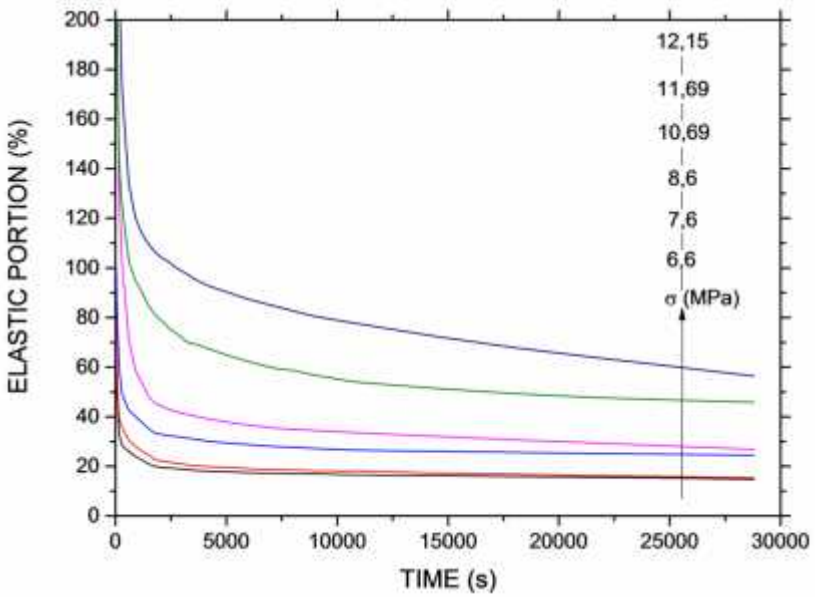

(a)

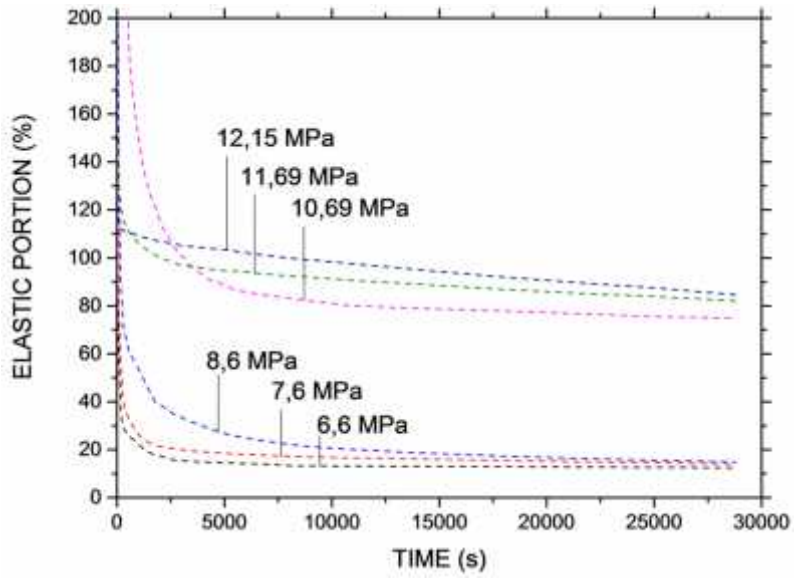

(b)

Fig.4.11: Elastic portion of the total strain as function of creep time for different applied stresses (a) MD, (b) TD.

Stricktly speeking, the presence of plastic creep deformation (component ε_4 of the total strain) does not allow using the term “linear viscoelasticity”, but at relatively low deformations (i.e: <100%), we can take this assumption as a first approximation for the prediction of creep behavior of polyethylene films.

4. Conclusion

The viscoelastic behavior of LDPE is strongly dependent of experimental conditions. Indeed, the creep-recovery tests showed that creep response is different in the two directions. During the loading phase; the curve shape is higher in the TD than MD. This difference can be explained by the fact that when the film is stretched in the TD, the chains in the amorphous phase being less oriented they make more time to reach their total tautness.

Also, the creep resistance and the different creep-recovery deformations ($\varepsilon_1, \varepsilon_2, \varepsilon_3, \varepsilon_a, \varepsilon_b, \varepsilon_c$) decrease with increasing applied stress.

The minimum strain rate increase with increasing applied stress, the presence of two slopes indicate the presence of two processes; one (process 1), with a comparatively large activation volume, predominates at low strain rates and the second process (process 2) with a smaller activation volume comes into operation at high strain rates so that the two processes are then acting together. However, the minimum strain rate ($\dot{\varepsilon}_{min}$) is greater in the TD.

The linear-non-linear viscoelastic transition for LDPE films, it is situated around 7.6 MPa.

- The life time of each deformation of the polyethylene films is determined from isocronic curves.
- The elastic portion decrease with increasing applied stress.
- The four parameters model is found to describe the creep behavior of LDPE films. The calculated instantaneous elastic deformation (E_1) is found to decrease from 149 for the smallest applied stress to 3.32 for the highest applied stress, the irrecoverable viscous flow (η_2) from 8.54E+11 to 3.27E+9, the recoverable retarded elastic deformation (E_3) from 79.6 to 2.36 and the viscosity (η_3) from 1768.98 to 9.59.

For all the experiments, the creep behavior of this film was controlled by the deformation of amorphous phase, more specifically the tie-chains. The dependence of the creep behavior on loading direction for the melt-extruded films is more or less controlled by the difference in the availability of the creep sites at the different orientations.

References

[1] L. E. Nielsen., The stress dependence of creep of polyethylenes., *J. Appl. Polym. Sci.*, 13, 1800 (1969).

[2] A. Cowking, Tensile creep and deformation mechanisms in oriented low-density polyethylene, J.Mat.Sci., 10,1751 (1975).

[3] P.G. Klein, D.W. Woods, and I.M. Ward, The effect of electron irradiation on the structure and mechanical properties of highly drawn polyethylene fibers., J. Polym. Sci., Part B: Polym. Phys., 25, 1359 (1987).

[4] Y. Ohta, H. Sugiyama, and H. Yasuda, The influence of short branches on the α, β and γ-relaxation processes of ultra-high strength polyethylene fibers., J. Polym. Sci., Part B: Polym. Phys., 32, 261 (1994).

[5] J. Rasburn, P.G. Klein, and I.M. Ward, The influence of short-chain branching on the creep behavior of oriented polyethylene, and its effect on the efficiency of crosslinking by electron irradiation., J. Polym. Sci., Part B: Polym. Phys., 32, 1329 (1994).

[6] H. Zhou and G.L. Wilkes, Creep behaviour of high density polyethylene films having well-defined morphologies of stacked lamellae with and without an observable row-nucleated fibril structure, Polymer, 39, 3597 (1998).

[7] Y.B. Unigovski, A.L. Bobovitch,E.M. Gutman,D Mogilansky., Effect of processing and density on morphology and creep behavior of linear low-density polyethylene., J.Polym Eng And Sci., 51, 1642 (2011).

[8] Pouyet, J. Element de visco_elasticit_e lin_eaire. T1.

[9] R.O.Ebewele, Polymer science and technology, 2000 by CRC Press LLC.

[10] U. Yilmazer., Effects of the processing conditions and blending with linear low-density polyethylene on the properties of low-density polyethylene films., Adv Polym Blends Alloys Technol (1992);3:132-44.

[11] C. G'sell, A. Dahoun, I.M. Hiver, C. Poinsot., Creep and yield behaviour of semi-crystalline polyethylene in uniaxial tension., J.Solid Mecand its App., 46, pp 75-82 (1996).

[12] J. A. Roetling, *Polymer*, 6,311 (1965).

[13] C. Bauwens-Crowet, J. C. Bauwens, and G. Hornès., Tensile yield-stress behavior of glassy polymers., *J. Polym. Sci.* 2,7,735 (1969).

[14] C.Devilliers., Dégradation chimique du PE et influence sur le comportement, l'endommagement et la rupture en fluage : Application à la durabilité d'une canalisation sous pression, Ph.D dissertation, Paris (France), 2012.

[15] Robert O. Ebewele., Polymer science and technology. 2000 by CRC Press LLC.

CHAPTER 5.0

AGEING EFFECTS ON THE CREEP-RECOVERY BEHAVIOR OF BLOWN EXTRUDED LOW DENSITY POLYETHYLENE FILM

Chapter 5.0 AGEING EFFECTS ON THE CREEP-RECOVERY BEHAVIOR OF BLOWN EXTRUDED LOW DENSITY POLYETHYLENE FILM

1. Introduction

The creep behavior of polyethylene has extensively been studied [1-7], but few studies have pointed on the ageing effect on the viscoelastic behavior. In thermoplastic polymers, the rate-controlling creep mechanism involves a cooperative motion of molecular chain segments with respect to each other. Indeed, ageing increases the crosslink density between the molecular chains, in amorphous phase which increase in turn the average molecular weight, provoking thus, the lowering of the extent and rate of the creep strain [5]. The effect of the branching density on the creep behavior is known to decrease the total creep strain at long-test time deformation while they increase the creep strain and the creep rate for the short-term creep [3-5]. It has also been shown that the creep rate is lowered by the methyl branch contents [4]. The creep behavior in polyethylene films is mainly controlled by the deformation of the amorphous phase, which is itself strongly affected, by the variation of the crystallinity and the tautness of the tie molecules [6].

In the present work, blown extruded polyethylene films have been weathered in severe climatic conditions in sub-Saharan facility characterized by an average temperature of 7.8°C in winter, 28.9 °C in summer (T_{max} = 45°C), a precipitation of 176 mm, an average wind speed of 17.2 km/h and sun radiation which can reach 1100 W/m^2. The changes undergone by the microstructure and their impact on the mechanical properties (i.e elastic and properties at break) have been checked for each ageing stage by spectroscopic analysis and tensile test, respectively. These types of tests and the description of the relation between the structure and the properties have already been widely described elsewhere [2, 8].

However, many works dealing with the effect of structure and morphology on the creep behavior of polyethylene films can be found in literature but seldom on ageing effects. In this work the effects of ageing on the mechanical properties and on the creep behavior of a LDPE film tested in the two main directions of the plane are studied. The goal of this work is to apply a long-term mechanical deformation mode, much more sensitive than tensile to the elementary microstructural changes.

In this work the effects of ageing on the mechanical properties and on creep behavior in the two main directions of the LDPE film plane are studied by applying a long-term mechanical deformation mode, much more sensitive than tensile to the elementary microstructural changes.

Indeed, creep-recovery which is another aspect of creep provides additional information on the structural changes undergone by the films via their impact on the viscoelastic properties.

The testing of the films in the two main directions highlights their anisotropic character. This can be useful to select the appropriate direction to place the film on the greenhouse to ensure a greater creep resistance and a longer service lifetime.

2. Experimental

Material: The LDPE utilized in this investigation is a commercial grade supplied by the Saudi basic industries corporation (SABIC) as "LDPE 2100 T N00W", (ρ_s= 0.92g/cm^3, MFI= 0.33g/ 10mn). This polymer is a neat grade exempt of stabilizing agents. Films were produced by blowing extrusion from the raw material in an Algerian industry (Sofiplast of Sétif). The drawing speed of the production line was fixed to 15 cm/s. The melt was extruded at about 175°C and blown in a continuous process characterized by a bubble diameter of 4.4 m and a wall thickness of 160 µm. It is known that the properties in the machine direction (MD) depend on the draw down ratio (DDR) and those in the transverse direction (TD) to the blow up ratio (BUR) [9].

Exposure: The exposition took place in Laghouat, Algeria (33° 48'N 2° 52'E) from December to august. The films are exposed on a metal support south oriented and inclined by 33° relative to the horizontal according to the standard NF51-165. A sampling was done bi-monthly, from the film zones distant from the contact points with the holding frame. This precaution was taken to avoid uncontrolled overheating of the material. The maximum of six months of exposure corresponds to the time at which the film became too brittle to resist to the wind strength.

Fourier transform infrared spectroscopy: FTIR spectroscopy was conducted on "Spectrum Two" maintained by Perkin Elmer to provide information of the functional groups present at the surface of the samples in the wavelength range 4000 cm^{-1} to 400 cm^{-1}. Scans were run at a resolution of 4 cm^{-1}. The specific absorption peaks were analyzed from the FTIR-spectra delivered by the equipment. For each peak the "optical density" (OD) was determined

following the usual definition as: OD = ln (I_0/I), were "I_0" is the reference infrared intensity corresponding to the baseline of the spectrum at the peak wave number and "I" is the minimum intensity at the base of the peak. The ATR-spectra obtained by analyzing the samples surfaces in contact with a Diamant crystal. Crystallinity of LDPE was determined using the method described by Zerbi et al [10]:

$$X\ \% = 1 - \frac{1 - \frac{I_a}{I_b}}{1 + \frac{1.233\, I_a}{I_b}} \times 100 \qquad (1)$$

Where I_a and I_b are the peaks area of the characteristic bands intensity at 1474-1464 cm^{-1} corresponding to the crystalline (1474 cm^{-1}) and the amorphous (1464 cm^{-1}) phases respectively. The constant 1.233 is the relation between these two (1474 cm^{-1} and 1464 cm^{-1}) for a completely crystalline polyethylene [11, 12].

Tensile tests: The stress-strain curves for all the samples were obtained by using an Roell zwik machine at room temperature (T=21°C, ± 1°C) at a nearly constant relative humidity (RH=50%, ± 5%). The test pieces were cut out of the original and the aged films. The dimensions of the rectangular test pieces were 70 mm × 10 mm, with a calibrated portion of length L0 = 40 mm, W0 = 10mm and thickness T0 = 0.16 mm. The results of the tensile test are presented in term of true stress, $\sigma = F(1 + \varepsilon)/A_0$, and true strain $\varepsilon(t) = \ln(L(t)/L_0)$. To optimize the duration of the test the strain rate was fixed at a low value to the yield point ($d\varepsilon/dt = 3 \times 10^{-4}\ s^{-1}$) (determination of the young modulus) and then stepped to a higher value ($d\varepsilon/dt = 3 \times 10^{-2}\ s^{-1}$) for the rest of the test until fracture occurred. To check the anisotropy of the film the test pieces were cut and tested in the two main directions corresponding to the machine direction (MD) and the transverse direction (TD).

Creep experiments: The creep test has been run on a creep tester developed in the laboratory of mechanic (Laghouat university) with rectangular specimens cut out of the original and aged film. The dimensions of the test pieces were 110mm, with a calibrated portion of length L_0 = 80mm, width W_0 = 10 mm, and thickness T_0 = 0.16 mm. All the tests were conducted at room temperature (T= 20°C ± 1°C, temperature very far above Tg = -110°C). The creep test was conducted by applying a constant stress of 7.6 MPa (i.e 1500 g) for duration of 8 hours. The recovery starts immediately after stress removal and for a period of 8 hours too. The load was prudently chosen in order to develop a stress below the yield stress measured by tensile test on the original film, because ageing affect mainly the amorphous phase.

The creep experiment has been carried out thanks to a camera which records the progression of markers on the surface of the sample. The monitored section of the test pieces (or effective length) is delimited by ink marks distant of 6 cm respectively. The mark in the middle of the sample is then centered with respect to the camera lens. These markers allow measuring the total deformation of the effective length.

The deformation between the two ends of the effective length of the test pieces are measured by means of several markers symmetrically distributed with respect to the middle of the specimen (d_0) and separated by 1 cm respectively. This precaution has been taken to verify that the deformation is homogeneous in the total effective length. A photograph is taken before starting creep (original state). After loading photographs are taken at regular interval. The whole is then processed by means of the Matlab software. The duration of the creep test (i.e. loading and unloading phase, 8 hours respectively) is limited by the most aged film samples (6 months).

The aim of these tests is to study the viscoelastic behavior of LDPE film. It is then necessary to know the yield strength of the film. For this, a tensile test on the virgin material, thereby to select a range of stresses for creep testing so that necking does not appear over time; hence study the creep in the amorphous phase.

3. Results

3.1.Infrared analysis

Exposure of polyethylene film to solar irradiation leads to an irremediable modification of the microstructure. The comparison of the IR spectra of the film samples picked up at regular intervals of time shows that some regions of the spectrum change with ageing. The most affected ones are those of the hydroperoxides (3300-3600 cm^{-1}), the carbonyls (1680-1780 cm^{-1}) and the double bonds (880-1100 cm^{-1}). The carbonyls absorption band (Fig.5.1.a) is certainly the most indicative of the extent of damages caused by oxidation to the macromolecular structure.

Its growing width and amplitude give a good insight on the relative concentration and the kind of the carbonyl species which develop through the ageing protocol [13, 14]. Of course, a cursory observation of this complex absorption band at the latest ageing stage allows seeing that it points drastically at 1712 cm^{-1} and there are many shoulders on its left side. It contains a variety of carbonyl species; among them one can quote the carboxylic acids (1712 cm^{-1}), the ketones (1718 cm^{-1}), the esters (1730-1740 cm^{-1}) [15-17], the peresters (1763 cm^{1}), the peracids (1785cm^{-1}) [16, 17] and the γ lactones (1788cm^{-1}) [18, 19] etc.…

Besides oxidation reactions, unsaturations also play a key role in the modification of the molecular structure affecting the mechanical response of the material under stress. During the first two months, it has been noticed a lowering of the vinylidenes (888 cm^{-1}) followed by an increase of the vinyl groups concentration (910 cm^{-1}) (Fig.5.1.b). Four months later, chain scission reactions which can be estimated, thanks to the vinyl groups (910 cm^{-1}) concentration since they appear subsequently to chain cleavage in the close vicinity of carbonyls via the well known Norrish type II process, become predominant compared to crosslinking reactions. As a result, the average molecular weight of the material decreases that should affect strongly the mechanical properties of the materials [2].

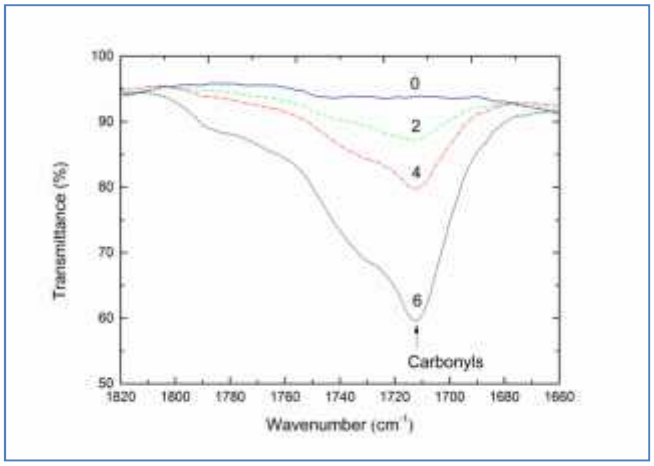

(a)

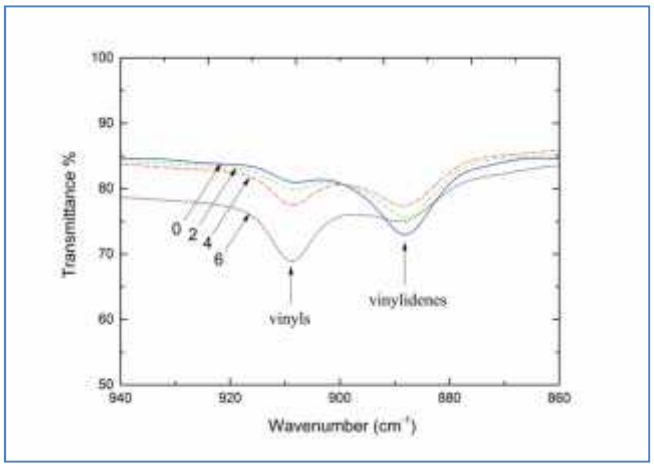

(b)

Figure.5.1: (a) Infra-red transmission spectra recorded from the LDPE 2100 T N00W films for various ageing stages (0, 2, 4, and 6 months): carbonyl stretching region. (b) Infra-red transmission spectra recorded from the LDPE 2100 T N00W films for various ageing stages (0, 2, 4, and 6 months): unsaturations stretching region.

3.2.Stress-strain behavior

The stress-strain curves for the unaged LDPE films are shown in Figure.5.2. As expected, these curves showed a distinct orientation dependence of the stress-strain behavior of these films in terms of modulus, yielding behavior, strain hardening, and breaking. These differences in mechanical properties have been correlated to unique structural changes at respective deformation directions in a detailed investigation on the deformation process of the LDPE films has been carried out and has been studied in detail in chapter 3.0. Here, only those features that are related to the creep study are restarted.

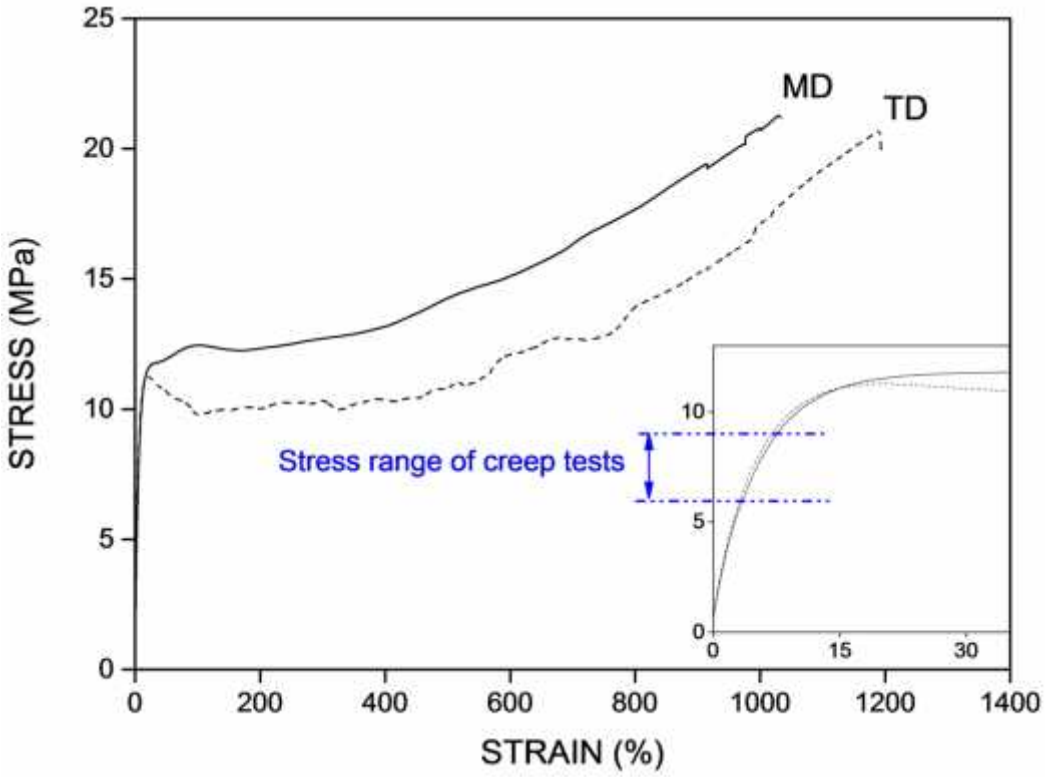

Fig.5.2: Stress-strain curves for LDPE films at the designated two orientations.

For the MD stretch, the stress-strain curve looks more typical for unoriented semi-crystalline polymers with a spherulitic morphology, with yielding (at 28% by the well-defined local maximum in the stress-strain curve), cold drawing, strain hardening and failure. For the TD stretch, yielding took place at smaller strain (20%) than MD stretch and is associated with the formation of a sharp neck with boundaries perpendicular to the stretching direction. Following yielding, the samples displayed extensive cold drawing by the expansion of the neck along the samples' length ended by strain hardening and failure. Also noticed are the uneven features of the stress-strain curves.

Furthermore, the stress-strain curve displayed an elastic domain in the stress range bellow 10 MPa and in the strain range bellow13%. The load was prudently chosen in order to develop the stress below the yield stress measured by tensile test on the original film (neither very long nor quick), because ageing affect mainly the amorphous phase.

3.3.Cree-recovery behavior

The creep-recovery curves for the unaged and two aged months films under different stresses and at both directions (MD and TD) are presented in Fig.5.3.a and 5.3.b, in which the creep-recovery strain is plotted against time. For these curves, the solid lines represent experimental data points for the MD, and the dashed lines represent those for the TD. At each orientation, a higher stress resulted in a larger initial creep strain and a larger creep rate. Now for each orientation, the aged month resulted in a lower creep strain and a lower creep rate. However, the creep resistance of the material under the stress of 8.6 MPa decreases instantaneously at a very small time (100s) to reach higher deformations (12.5 %) and expands until 19% for MD and 44% for TD, in the end of loading phase. Neither this stress is interesting for creep study since the material enter in plastic deformation range, nor that of 6.6 MPa since it is too small and take a long time to creep. For this reason the stress 7.6 MPa is the optimal choice to develop the creep in the elastic domain.

Data related to the creep rate, for unaged and two-aged months aged films at two directions are shown in Figure 5.4.a and 5.4.b, where creep rate is plotted against the creep strain. The results show a logical trend where the plateau creep rate is achieved by the material for each individual creep experiment. Additionally, the minimum strain rate decreases with ageing whatever the applied stress.

Figure 5.5.a and 5.5.b represent the evolution of the minimum strain rate vs stress for unaged and 2 months-aged PE and for the two directions. The strain rate sensitivity coefficients (defined in section 4.3.1) are listed in Table.5.1. It can be seen that slope tends is parallel, and the breaking slope points; activation volume (V), remain the same with ageing.

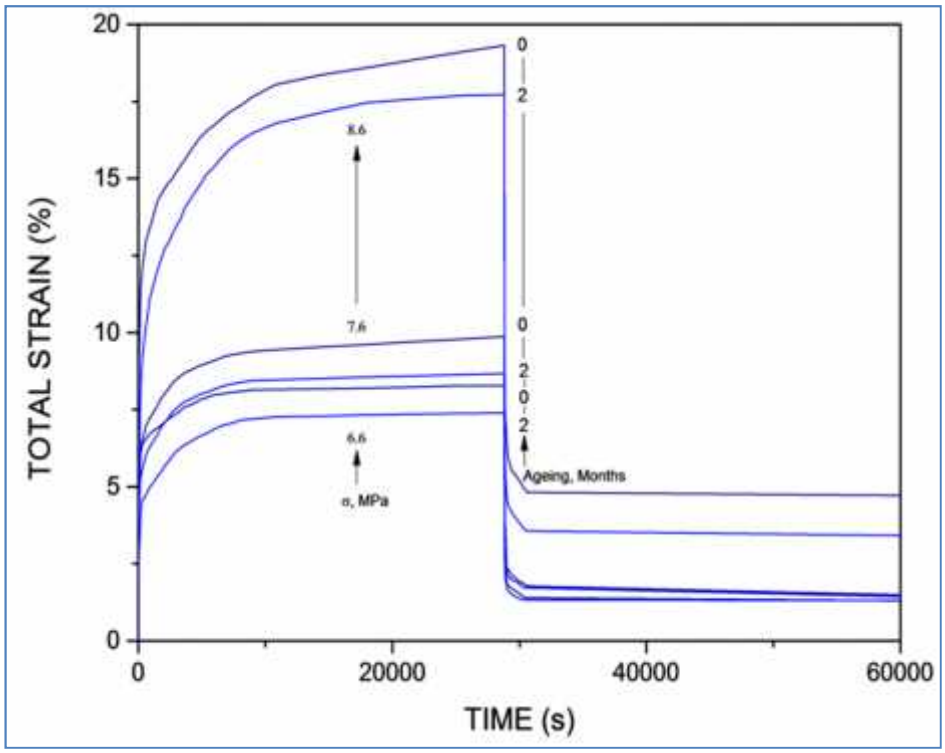

(a)

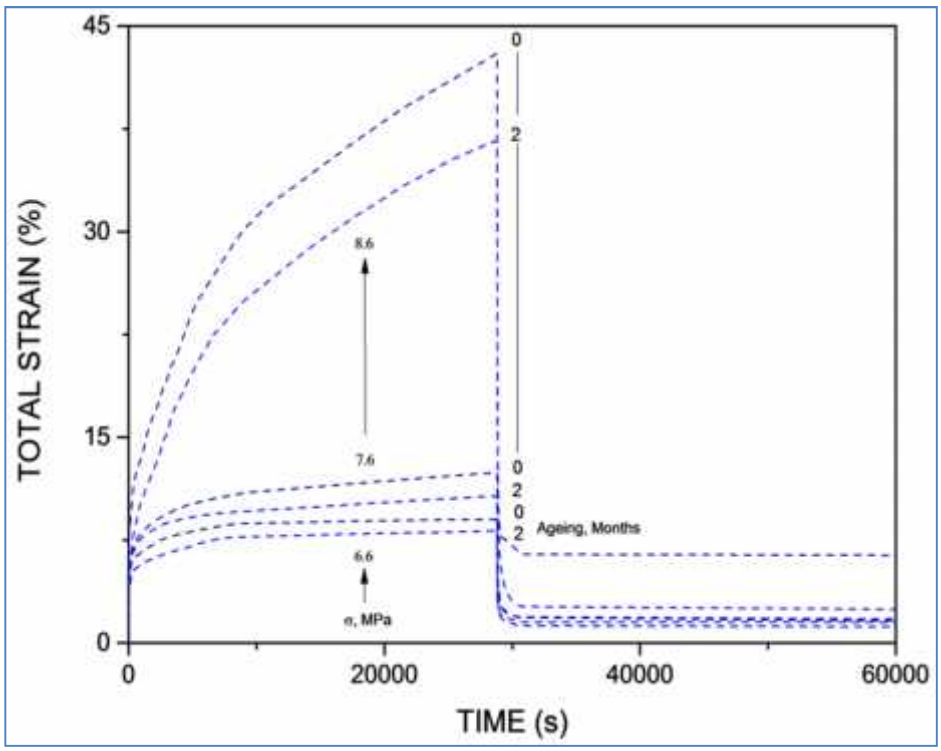

(b)

Fig.5.3: Two months aged LDPE 2100T at different applied stresses (6.6MPa, 7.6MPa and 8.6 MPa) at two directions (a) machine direction (MD), (b) transverse direction (TD).

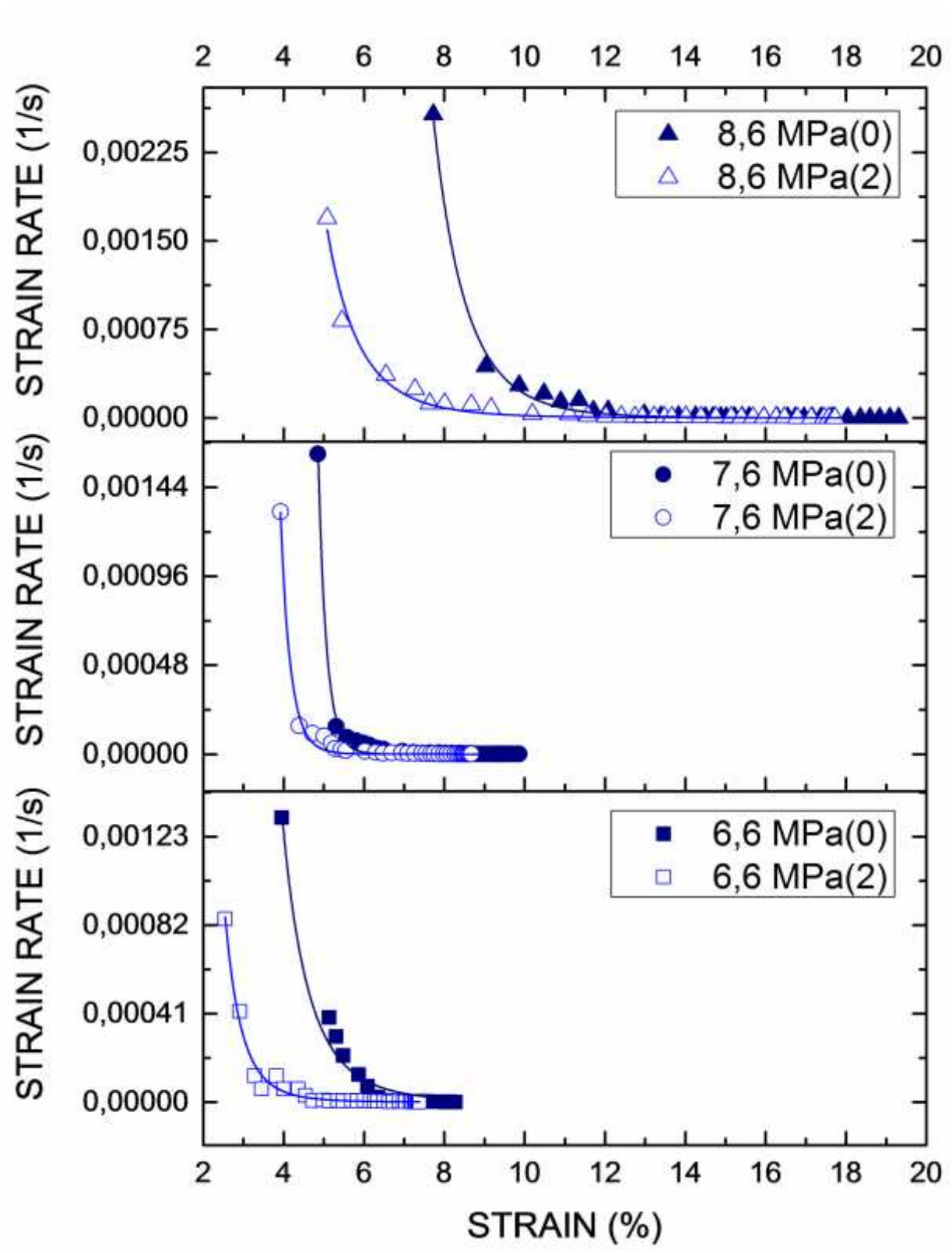
STRAIN RATE (1/s)
STRAIN RATE (1/s)
STRAIN RATE (1/s)
STRAIN (%)
8,6 MPa(0)
8,6 MPa(2)
7,6 MPa(0)
7,6 MPa(2)
6,6 MPa(0)
6,6 MPa(2)
0,00225
0,00150
0,00075
0,00000
0,00144
0,00096
0,00048
0,00000
0,00123
0,00082
0,00041
0,00000
2
4
6
8
10
12
14
16
18
20

(a)

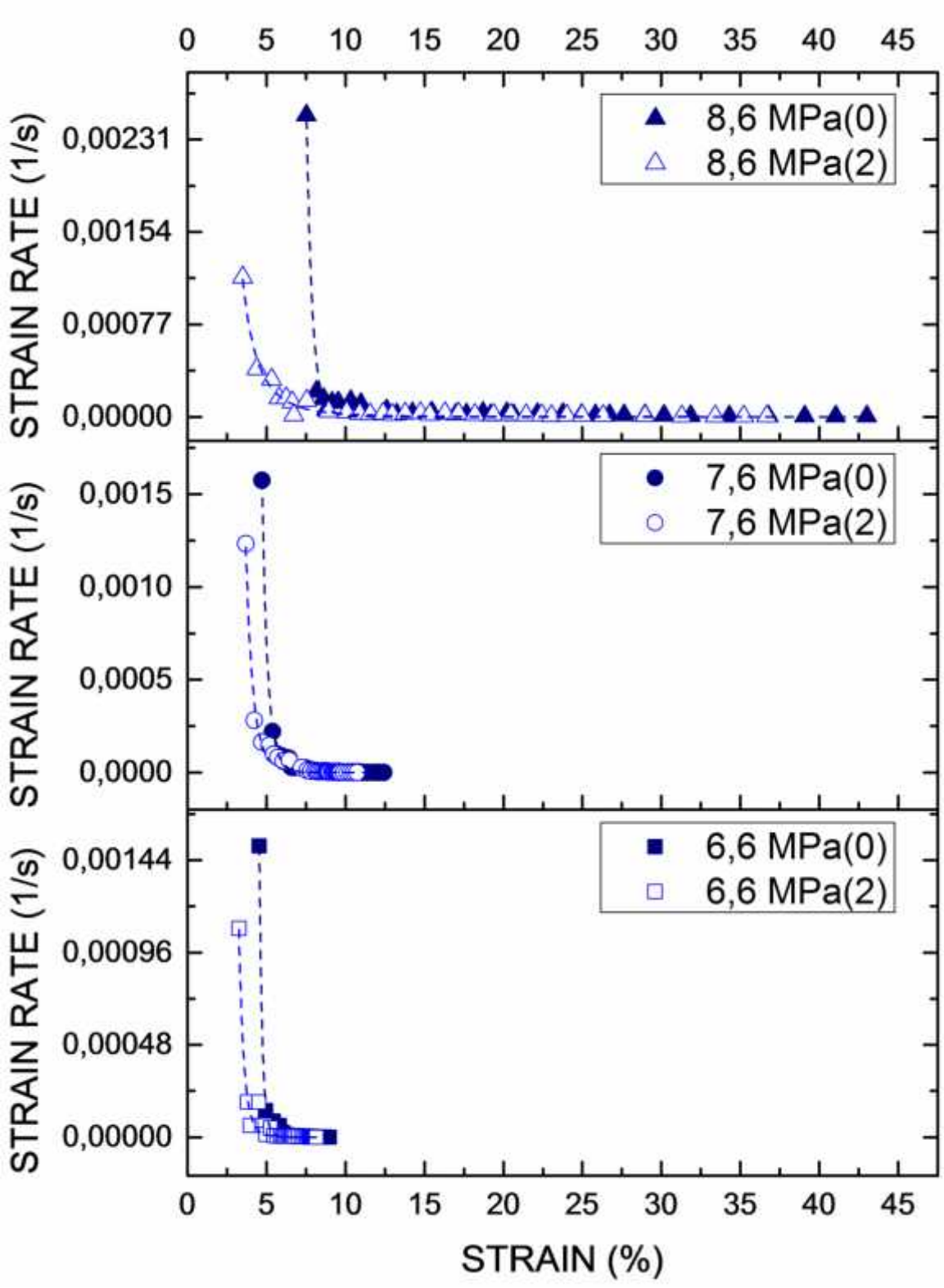

(b)

Fig.5.4: Evolution of strain rate vs. strain for unaged and two-aged months films (a) Machine direction (MD), (b) Transverse direction (TD).

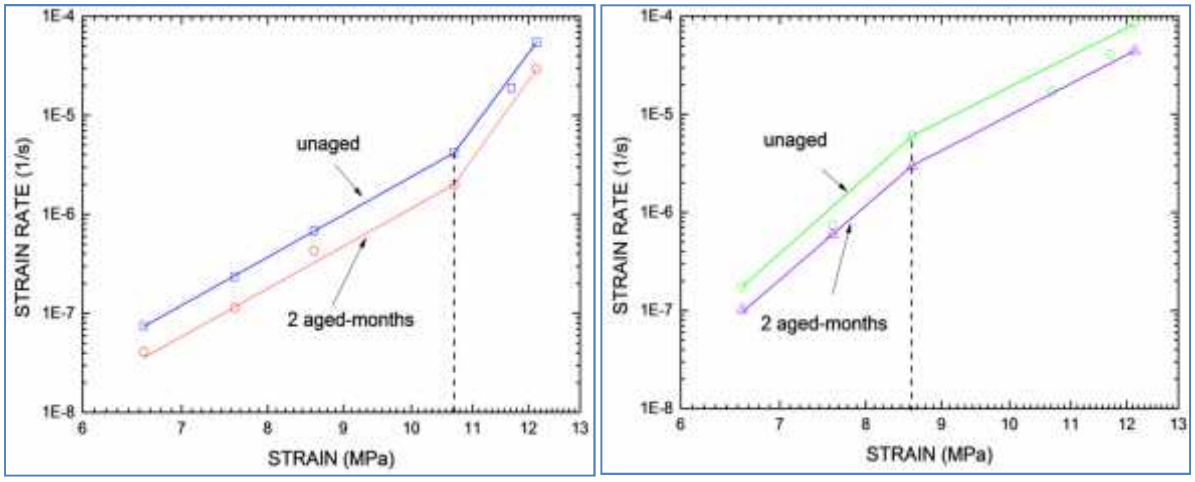

(a) (b)

Fig.5.5: Evolution of the minimum strain rate function to the nominal applied stress for unaged and 2 months-aged PE; (a): MD, (b): TD.

Furthermore, it has been observed that n_1 decreases with ageing while n_2 increases for both directions. However, the activation volume (V) is not sensitive to ageing since it remains stable. On the other hand, for an applied tress, the minimum strain rate decrease with ageing (Fig.5.5), this means that an aged PE where present higher crystallinity is stiffer than PE with low crystallinity. Knowing that an increase in the ageing state is synonymous for us, to a more severe oxidation, it is concluded that the PE stiffens during ageing. The chemical aging therefore tends to make the material more viscous.

Our curiosity led us to search if the LDPE films, behaves in the same way or not with advanced exposure time for both directions. It is with this aim that the tests at relative low stresses (7.6 MPa) and advanced exposure time were realized. The stress was prudently chosen below the activation volume (V) of TD creep.

Table.5.1: Values of strain rate sensitivity coefficients, ¦ 1, ¦ 2, for the unaged and two-months aged LDPE films investigated.

Ageing (months)	Orientation	Strain rate sensitivity coefficients	
		n_1	n_2
0	MD	8.37	20.04
	TD	13.39	7.59
2	MD	8.35	20.97
	TD	13.01	7.8

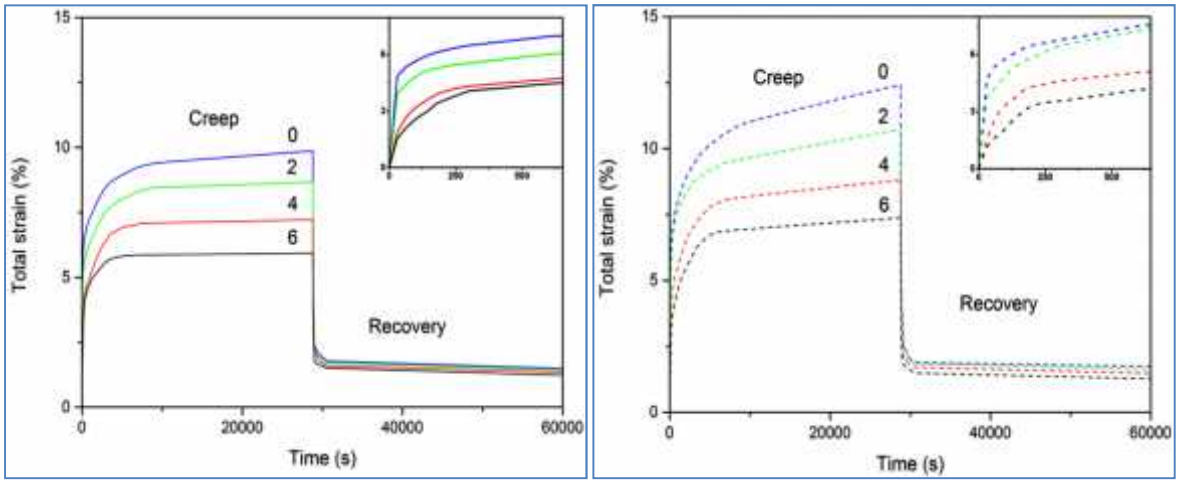

(a) (b)

Fig.5.6: Ageing effect on the creep-recovery behavior of the LDPE 2100T for different exposure time (0, 2, 4, 6) at two directions (a) machine direction (MD), (b) transverse direction (TD).

The creep-recovery curves of the test pieces for both directions and for the different ageing stages are represented in Fig.5.6.a and 5.6.b.

a) Creep behavior (Loading phase)

The analysis of the mechanical properties of the original samples shows that the value of the immediate elastic deformation (ε_1) is slightly greater in the MD than in the TD, per contra, the delayed elastic deformation ε_2 and the viscous flow (ε_3), this time, are lower in the MD (Table.5.2).

Table.5.2: Ageing effects on the different deformations identified in the creep-recovery curves of LDPE for the two main directions (a) MD, (b) TD.

Ageing (Months)	**Orientation**	$\varepsilon_1(\%)$	$\varepsilon_2(\%)$	$\varepsilon_3(\%)$	$\varepsilon_a(\%)$	$\varepsilon_b(\%)$	$\varepsilon_c(\%)$
0	MD	4.86	4.32	0.69	4.80	3.57	1.49
	TD	4.79	5.49	2.14	4.78	5.90	1.74
2	MD	3.92	4.31	0.45	3.90	3.38	1.39
	TD	4.37	4.81	1.55	4.36	4.74	1.62
	MD	3.40	3.62	0.20	2.93	2.94	1.35

4	TD	3.23	4.64	0.93	2.96	4.38	1.47
	MD	2.81	3.05	0.07	2.58	2.13	1.22
6	TD	2.43	4.29	0.66	2.34	3.76	1.28

With ageing, the different deformations values (ε_1, ε_2, ε_3) decrease in both directions. The ε_3 values in the MD are much lower than in TD; however the rate of lowering is almost the same for the two directions.

Fig.5.7.a and Fig.5.7.b represent the variation of strain rate ($\dot{\varepsilon}$) for the two directions and the different ageing stages. The main advantage of this type of representation is that it makes easier to determine the stationary stage corresponding to a minimum creep strain rate ($\dot{\varepsilon}_{min}$). It appears that the value of the strain rate is higher in the TD than in the MD for all the ageing times. In such curves it is possible to distinguish the different creep domains such as the primary creep; where the creep rate decreases progressively until reaching a minimum value ($\dot{\varepsilon}_{min}$), and the secondary creep; where the creep rate remains constant. It is observed that with ageing, the minimum strain rate ($\dot{\varepsilon}_{min}$) value of both directions decreases and the material reaches earlier this domain, however it remains always greater in the TD.

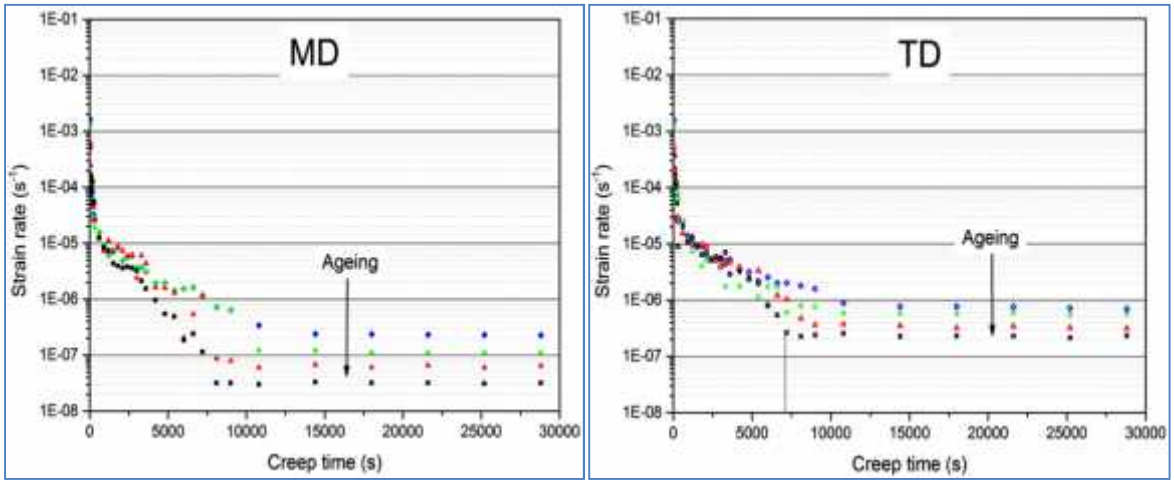

(a) (b)

Fig.5.7: Strain rates versus creep time of unaged and weathered LDPE in two directions a) MD, b) TD.

The variations of the viscous flow "ε_3" for the two directions versus the optical density (OD) of the vinyl groups is reported in Fig.5.8.a.

The results show the same trend for the two directions, since the viscous flow "ε_3" decreases with the increase of the OD of vinyl groups. However, the TD values are higher

than that of the MD. As mentioned before (§3.1); the appearance and the growth of the vinyl groups absorption band is a good indicator of the short chain segments formation coming from chain scission reactions and contributing to the increase of the crystallinity via a chemo-crystallisation process. Elsewhere, others of us have demonstrated by NMR that shorter branches of butyl and methyl lengths appear with ageing. [2]. Indeed, Rasburn and Ward have verified that the strain rate of the different creep domains lowers with the increasing of short chain branching concentration, consequently the creep resistance increases as a whole [7]. As a matter of fact, both effects occur in the studied material (i.e. the increase of the short chain branches and crystallinity), also the creep-recovery curves display an overall lowering of the strain rate, an increasing creep resistance and an earlier reaching of the secondary creep. The chemo-crystallization process leads either to the thickening of the existing crystalline lamellae or the nucleation of new crystallites reducing thereby the amorphous region that support the deformation; and thus makes the material stiffer [8]. Also, the deformation requires more energy. The reduction of the length of branching tends to increase the cohesion of the chain backbones (by secondary bonds) reducing thereby their slippage [5]; these both effects act in increasing the overall resistance to creep [6].

The representation of the viscous flow as a function of the optical density of vinylidene groups for the different ageing stages is reported in Fig.5.8.b.

The viscous flow decreases with the consumption of the vinylidene, however the values in TD are higher than in the MD. For both directions it appears that it exists an almost linear relationship between the viscous flow and the vinylidene consumption, this reveals the importance of the crosslinking effects on this rheological greatness. Indeed, the formation of crosslinking via the reaction of these double bonds reduces dramatically the polymer chains slippage.

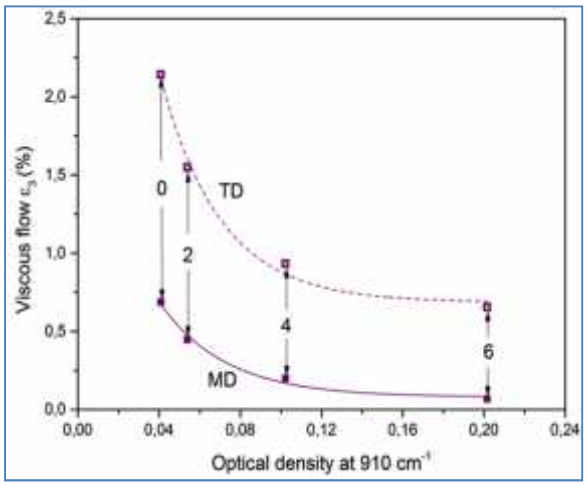

Fig.5.8.a: Strain rates versus optical density of vinyl (910 cm^{-1}).

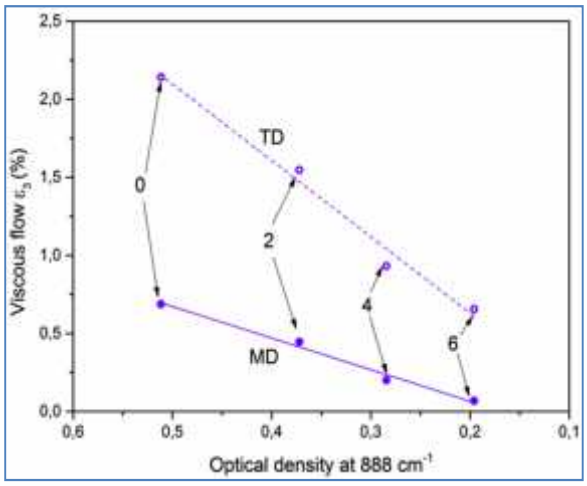

Fig.5.8.b: Viscous flow (ε_3) versus the inverted scale of the optical density (OD) of vinylidene (888cm^{-1}). (OD)

Others have demonstrated that highly cross-linked polymers do not show the viscous flow ε_3, and this is true to a very good approximation for highly crystalline polymers as well [20].

b) Recovery behavior (Unloading phase)

The recovery of the films for both directions is never complete, in all the cases the tested samples do not return to their original length resulting in a permanent deformation ε_c during loading.

Table.5.1 and Fig.5.6, show that the longer the creep time, and more the chains are oriented, the lower are the instantaneous elastic recovery (ε_a) and delayed recoveries (ε_b, ε_c). Chains orientation seems to play a key role in the recovery, since the material elongation is greater and easier in the TD than in the MD. Indeed, as suggested above the initial deformation ε_1 is mainly due to the unrolling of the molecular chains in the amorphous phase, then, this is followed by their progressive disentanglement, for a longer loading time. The chain alignment becomes slightly more perfect and the chains become closer to each other, allowing the creation of secondary bonds, these last ones oppose to the complete recovery of the polymer chains to their initial state after unloading [21].

In Fig.5.9.a and 5.9.b are represented, the variation of the recovered elastic portion $E_e(t)$ (Eq.2) as a function of the creep time and for the MD and TD respectively.

The variation of $E_e(t)$ for all the different ageing stages shows a rapid drop during the first 300 seconds of the creep test to show then an asymptotic trend. Practically 60% of the elastic portion $E_e(300s)$ for the unaged films is transformed into an irreversible plastic creep

deformation for both directions. The value of the Ee (300s), decreases significantly and progressively with ageing (~ 55%, 50% and 40% for the aged samples of 2, 4 and 6 months respectively).

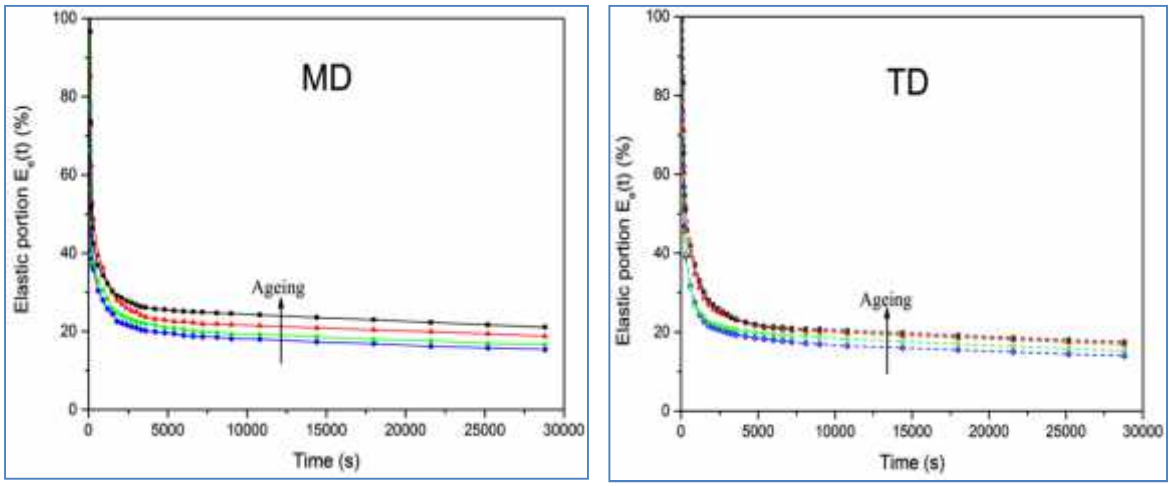

(a) (b)

Fig.5.9: Elastic portion $E_e(t)$ of the total strain $\varepsilon(t)$ as function of the creep time for different exposure times: (a) MD and (b) TD.

The reduction of $E_e(t)$ is a consequence of the effects described above which encompass cross-linking, chain scissions and the reduction of the chains branching length. The combination of these effects is also responsible of the decrease for both directions of each of the instantaneous elastic (ε_a), the delayed elastic (ε_b) and the final recovery (ε_c) (Table.5.1).

4. Conclusion

The aim of this chapter was to determine the ageing effect on the creep behavior of LDPE. It was important to dispose unaged and weathered samples to realize the appropriate mechanical tests.

First, we studied the behavior of LDPE for uniaxial solicitation. Samples were tested on tensile tests for both directions to determine the creep range loads, the samples were then subjected to creep tests. Creep tests allowed highlighting a stiffening of PE during ageing. Indeed, the comparison between the unaged and aged samples shows an increase in the creep resistance. This is explained by:

- A decrease in minimum creep rate, also in strain rate sensitivity coefficients of Norton low n_1 for low stresses. However strain rate sensitivity coefficients n_2 increases for high stresses for both directions.
- The activation volume (V) is not sensitive to ageing since it remains stable.

A thorough study has been investigated for advanced ageing stages, since the results obtained for two-aged samples differ from the unaged ones, this is absolutely due to the microstructural and morphological changes undergone by the material.

During the loading phase; the curve shape is higher in the TD than MD. This difference can be explained by the fact that when the film is stretched in the TD, the chains in the amorphous phase being less oriented they make more time to reach their total tautness.

In first the time of ageing, the lowering of the creep curves in both directions, and therefore the decrease of ε_1, ε_3, is probably due to crosslinking reactions. Also, it has been found a close relationship between the viscous flow and the vinylidene groups, these last ones have thus revealed the effect of crosslinking on the viscoelastic properties can be due to crosslinking in the beginning and to chain scissions for longer ageing time. The viscous character of the material is strongly lowered by the two last chemical reactions, but also by crystallinity.

Creep rate is a good indicator of the effects of the structural changes on the ability of the material to deform. With ageing and for both directions the material reaches earlier the secondary creep domain, this domain begins when $\dot{\varepsilon}_{min}$ is reached. It could be still noticed that $\dot{\varepsilon}_{min}$ for the TD is higher than in MD, this difference can be related to the molecular orientation which is mainly connected to the capability of chain unrolling and slippage. The lowering of the branch lengths with ageing increases the cohesiveness of the main chains (by formation of macromolecular secondary bonds) which acts also negatively on the creep rate.

Recovery has revealed a very fast drop of the elastic portion occuring in reason of the degradation process. The instantaneous (ε_a) and the final recoveries (ε_b , ε_c), diminish with increasing exposure time supporting the findings of creep.

It can be concluded that creep-recovery test on LDPE films is very efficient in the recognition of the extent of structural damages caused by ageing on their viscous-elastic behavior.

References

[1] Tidjani, A., Comparison of formation of oxidation products during photo-oxidation of linear low density polyethylene under different natural and accelerated weathering conditions., Polym. Degrad. Stab. 2000, 68, 465.

[2] Chabira, S. F.; Sebaa, M.; G'sell, C., Influence of climatic ageing on the mechanical properties and the microstructure of Low-Density Polyethylene films., J. Appl. Polym. Sci. 2008, 110, 2516.

[3] Nielsen, L. E., The stress dependence of creep of polyethylenes, J. Appl. Polym. Sci. 1969, 13, 1800.

[4] Cowking, A., Tensile creep and deformation mechanisms in oriented low-density polyethylene., J. Mater. Sci. 1975, 10, 1751.

[5] P.G. Klein, D.W. Woods, and I.M. Ward, The effect of electron irradiation on the structure and mechanical properties of highly drawn polyethylene fibers., J. Polym. Sci., Part B: Polym. Phys., 25, 1359 (1987).

[6] Y. Ohta, H. Sugiyama, and H. Yasuda, The influence of short branches on the α, β and γ-relaxation processes of ultra-high strength polyethylene fibers., J. Polym. Sci., Part B: Polym. Phys., 32, 261 (1994).

[7] J. Rasburn, P.G. Klein, and I.M. Ward, The influence of short-chain branching on the creep behavior of oriented polyethylene, and its effect on the efficiency of crosslinking by electron irradiation., J. Polym. Sci., Part B: Polym. Phys., 32, 1329 (1994).

[8] Chabira, S. F.; Sebaa, M.; Huchon, R.; De Jeso, B. The changing anisotropy character of weathered low-density polyethylene films recognized by quasi-static and ultrasonic mechanical testing, J. Polym. Degrad. Stab. 2006, 91, 1887.

[9] Yilmazer, U., Effects of the processing conditions and blending with linear low-density polyethylene on the properties of low-density polyethylene films., J. Appl. Polym. Sci. 1991, 42, 2379.

[10] Guo, J. J.; Yan, H.; Bao, H. B.; Wang, X. M.; Hu, Z. D.; Yang, J. J. Spectrosc. Spect. Anal. 2015, 35, 1520.

[11] Lin, L.; Argon, A. S., Structure and plastic deformation of polyethylene., J. Mater. Sci. 1994, 29, 294.

[12] Meijer, H. E. H.; Govaert, L. E., Mechanical performance of polymer systems: The relation between structure and properties ., Prog. Polym. Sci. 2005, 30, 915.

[13] Ebewele, R. O. Polymer Science and Technology; CRC Press: Boca Raton, New York, 2010; Chapter 14, p 369.

[14] Sebaa, M.; Servens, C.; Pouyet, J., Natural and artificial weathering of low-density polyethylene (LDPE): Calorimetric analysis., J. Appl. Polym. Sci. 1993, 47, 1897.

[15] Murray, K. A.; Kennedy, J. E.; McEvoy, B.; Vrain, O.; Ryan, D.; Higginbotham, C. L., The effects of high energy electron beam irradiation on the thermal and structural properties of low density polyethylene., J. Radiat. Phys. Chem. 2012, 81, 962.

[16] Wojtala, A.; Czaja, K.; Sudol, M.; Semeniuk, I., Weathering of low-density polyethylene grafted with itaconic acid in laboratory tests., J. Appl. Polym. Sci. 2012, 124, 1634.

[17] Barcelo, D. In Molecular Characterization and Analysis of Polymers; Chalmers, J. M.; Meier, R. J., Eds.; Elsevier: New York, 2008; Vol. 53, Chapter 10, p 387.

[18] Salvalaggio, M.; Bagatin, R.; Fornaroli, M.; Fanutti, S.; Palmery, S.; Battistel., Multi-component analysis of low-density polyethylene oxidative degradation., E. Polym. Degrad. Stab. 2006, 91, 2775.

[19] Yagoubi, W.; Abdelhafidi, A.; Sebaa, M.; Chabira, S. F., Identification of carbonyl species of weathered LDPE films by curve fitting and derivative analysis of IR spectra., Polym. Test. J. 2015, 44, 37.

[20] Unigovski, Y. B.; Bobovitch, A. L.; Gutman, E. M.; Mogilansky, D., Effect of processing and density on morphology and creep behavior of linear low-density polyethylene., Polym. Eng. Sci. 2011, 51, 1642.
[21] G'sell, C.; Dahoun, A.; Hiver, J. M.; Poinsot, C. IUTAM Symposium on Micromechanics of Plasticity and Damage of Multiphase Materials; Pineau, A.; Zaoui, A., Eds.; Springer: The Netherlands, 1996; Vol. 46, Chapter 10, p 75.

CHAPTER 6.0

SUMMARY AND FUTURE WORK

Chapter 6.0 SUMMARY AND FUTURE WORK

6.1. Summary

Contributive studies have been carried out in this work to highlight the effect of ageing on the relationship between LDPE film structure and its mechanical behavior. The films used were naturally weathered for a period of six months and the sampling was done bimonthly. The material morphology strongly affected by orientation acquired during processing offers an advantageous opportunity to investigate the anisotropic character of the film checked by mechanical tests at different angles of the film plane with respect to the main directions [machine direction (MD) and blowing direction (TD)]. Also, the plans deformation and lateral contraction measurements on the pristine and aged samples allowed a better understanding of films deformation and their lateral contraction and upwards then to Poisson's ratio calculation. The lamellar morphology has provided an ideal investigation field to study the ageing effects on crystalline lamellar thickness and distribution. The main objective was thus to better understand the orientation effect on the viscoelastic behavior and also to try understanding the molecular motion processes that govern the particular mechanical behavior of creep-recovery. This technique has been revealed very sensitive towards the very slight changes of the viscoelastic properties induced by ageing. The present study involves many aspects of multidisciplinary fields which include:

1. Morphological analysis of low density polyethylene films influenced by ageing.
2. Orientation dependence of mechanical properties for blown extruded low density polyethylene film.
3. Creep-recovery behavior and loading effect on the pristine blown extruded low density polyethylene film.
4. Ageing effects on the creep-recovery behavior of blown extruded low density polyethylene film.

Many new insights were obtained with regard to each individual subject and the obtained information is believed to better enhance the understanding on the creep-recovery behavior for this semicrystalline polymer before and after degradation as well. To summarize, the following accomplishments have been made in this dissertation:

1. In the structural and morphological study (chapter 2.0), the dramatic structural and morphological changes have been highlighted by different techniques namely; XRD, DSC, and AFM. It was shown that the outdoor exposure leads to a complex photochemical mechanism provokes an increase in crystalline concentration either the lamellar thickness or by nucleating new crystallite via a chemo-crystallization process. Furthermore, this study also confirms that XRD and DSC are reliable tools in terms of determining the crystallinity. Therefore, it is concluded that the use of DSC to calculate lamellar thickness and its distribution is particularly suitable. These results corroborate with those of AFM which demonstrate that the surface aspect of the film changes significantly with natural exposure. Indeed, the roughness and the height valley increase in reason of the increase of the surface crystalline zones. This result supports the hypothesis that the material degradation follows a gradient of physicochemical defects from the surface to the core through the film thickness. Surprisingly, it has been found that the peaks-spacing and R_{rms} which logically progress inversely, followed an evolution that obeys to linear mathematical relationships. However, the AFM couldn't be useful to the calculation of the lamellar thickness since this method is limited to the analysis of surface texture only.
2. In the stress-strain deformation study (chapter 3.0), polyethylene film deformation under controlled deformation rates investigation is achieved. It was shown that relative elongation and true strain are strongly dependent on the deformation angles, highlighting then the anisotropic character of the material. Specifically, the true strain is greater in the 45° stretch followed by 90° then 0°. Furthermore, planes delimited by the marks remain uniform during the whole deformation meaning that the film plans undergoes parallel deformation. The lateral contraction is significant in the 45° stretch comparing to two other orientations. However, the material stretched in 0° and 90° approximately shrink with the same rates. Furthermore, the true strain and lateral contraction of aged samples decrease reflecting the microstructural alteration of the material. The Poisson's ratio was determined and it is estimated to be 0, 33. This value is close to that of the literature. In another hand, several relationships between the microscopic deformation mechanisms and the induced morphological changes and macroscopic tensile properties have been clearly demonstrated. Stretching parallel to the MD results in lamellar separation, followed by break-up of the crystalline lamellae via chain slip. Stretching perpendicular to the MD causes the crystalline lamellae to break-up or rupture by chain pull-out. With ageing, the properties at the break

decrease indicating the loss of ductile character of the material. Furthermore, the effect of ageing and crystallinity degree for a given strain rate, and the influence of the strain rate for a given ageing degree have been demonstrated.

3. The creep study carried out in this dissertation (chapter 4.0) represents one of the few systematic investigations yet undertaken to address the critical role that tie-chains plays in the creep deformation process. It has been found that during the loading phase, the creep deformation which mainly controlled by the amorphous phase is higher in the TD than MD. It has been concluded that the tautness of tie chains is an important structural features that influence the creep resistance. From another hand, the creep resistance and the different creep-recovery deformations ($\varepsilon_1, \varepsilon_2, \varepsilon_3, \varepsilon_a, \varepsilon_b, \varepsilon_c$) decrease with increasing applied stress, so the minimum strain rate increases. However, the minimum strain rate ($\dot{\varepsilon}_{min}$) is greater in the TD. The linear-non-linear viscoelastic transition and lifetime of each deformation of the polyethylene films is determined from isometric and isochrone curves. The recovered elastic portion decreased with increasing applied stress. Furthermore, the four parameters model have been calculated from the real creep-recovery behavior of PE at different stresses.
4. Ageing by natural weathering effects on the creep-recovery behavior was investigated in this dissertation (chapter 5.0) is one of the seldom undertaken research subjects. The microstructural and morphological changes revealed by FTIR which result from competition between crosslinking and chain scission reactions affect adversely the mechanical properties (tensile tests) leading to a global material stiffening. Also, it has been found a close relationship between the viscous flow and the vinylidene groups, these last ones have thus revealed the effect of crosslinking on the viscoelastic properties. This is due to crosslinking in the beginning and to chain scissions for longer ageing time. The viscous character of the material is strongly lowered by the two last chemical reactions, but also by crystallinity. The minimum strain rate ($\dot{\varepsilon}_{min}$) higher in the TD than MD, is a good indicator of the effects of the structural changes on the ability of the material to deform, this difference is related to the molecular orientation which is mainly connected to the capability of chain unrolling and slippage. With ageing the lowering of the branch lengths increases the cohesiveness of the main chains (by formation of macromolecular secondary bonds) which acts also negatively on the creep rate. Recovery has revealed a very fast drop of the elastic portion occurring in reason of the degradation process. The instantaneous (ε_a) and the

final recoveries (ε_b ,ε_c), diminish with increasing exposure time supporting the findings of creep.

6.1. Future work

Due to the complex relationship between the creep-aging under investigation, it remains still questions left open for further efforts. In light of these, some considerations for potential recommended studies are listed below:

- Creep-recovery behavior and mechanical deterioration of stabilized polyethylene greenhouses covering under arid conditions.

- Modeling of the creep-recovery behavior of LDPE films.